High-dimensional dependence modelling using Bayesian networks for the degradation of civil infrastructures and other applications

Alex Kosgodagan

UNIVERSITE BRETAGNE LOIRE

IMT Atlantique
Bretagne-Pays de la Loire
École Mines-Télécom

Thèse de Doctorat

Alex KOSGODAGAN - DALLA TORRE

Mémoire présenté en vue de l'obtention du
grade de Docteur de l'École nationale supérieure Mines-Télécom Atlantique Bretagne Pays de la Loire
sous le sceau de l'Université Bretagne Loire

École doctorale : Sciences et technologies de l'information et mathématiques

Discipline : Mathématiques appliquées et applications des mathématiques, section CNU 26
Unité de recherche : Laboratoire des Sciences du Numérique de Nantes (LS2N)

Soutenue le 26 juin 2017
Thèse n° : 2017IMTA0020

High-dimensional dependence modelling using Bayesian networks

for the degradation of civil infrastructures and other applications

JURY

Président :	**M. Christophe BÉRENGUER**, Professeur des Universités, Grenoble INP
Rapporteurs :	**M. Roger COOKE**, Professor Emeritus, Resources for the Future **M. Laurent BOUILLAUT**, Chargé de Recherche – HDR, IFSTTAR
Examinateurs :	**M. Philippe LERAY**, Professeur des Universités, Polytech Nantes **M. Laurent TRUFFET**, Maître assistant – HDR, IMT Atlantique **M. Wim COURAGE**, Senior Researcher, Structural Reliability, TNO
Invité :	**M. Thomas G. YEUNG**, Maître Assistant, IMT Atlantique
Directeur de thèse :	**M. Bruno CASTANIER**, Professeur des Universités, Université d'Angers
Co-directeur de thèse :	**M. Oswaldo MORALES-NÁPOLES**, Assistant Professor, TU Delft

Acknowledgement

First of all, I would like to deeply thank all my supervisors B. Castanier, O. Morales-Napoles and T. G. Yeung, for their support, insight and the way each contributed to (hopefully) shape me as a young and autonomous researcher throughout this three-year journey as well as for their invaluable advice and encouragement. I am very grateful for the many opportunities they gave me to attend scientific conferences and for introducing me to their research groups. Special thanks goes to W. Courage for his kindness and commitment taking a significant part in my supervision as well.

Second of all, I want to thank both my Dutch and French colleagues many of whom became good friends throughout the past years. Starting with the Dutch side, thank you Wiebke, George and Dominik for the time we spent as young PhD together sharing Oswaldo as supervisor. Then, the "TNOers", thank you Nadieh, Johan, Laura, Adrii, Jos, Siska, Tineke, Yvonne and many others I am probably forgetting. From the French side, thank you Axel, Juliette, Quentin, Fabrice, Yuan and his chinese folks, Gilles, Guillaume, Naly, Laurent, Chams, Olivier, Dominique, Fabien, Hélène, Isabelle and Anita for integrating me with kindness into the team. Also, a thank you to the people I enjoyed sharing my office with, Alan, Lori, Rui, Agri and Iwan.

Besides the friends I made along the way, those whom I share so many great memories with and being around for a very long time now, I would like to thank you Pop, Louis, Eloi, Kevin, Julie L., Camille B., Julie M., Camille F., Hélène, Caroline, Jerome, Alexis, Etienne,...

Last but not least, I would like to thank my family who showed a constant loving support and always had faith in me. I want to thank my uncles Pietro and Ruggero, my aunt Palma, my brother Sébastien and my wonderful mom.

Contents

Chapter 1

Résumé

Contents

1.1 Introduction

Dans les domaines de la fiabilité et de la sûreté structurelle, l'exemple du réseau routier hollandais met en avant la complexité d'une part, et la nécessité d'autre part, de pouvoir modéliser les dynamiques d'un tel réseau. En effet, cet enchevêtrement de voies ne possède pas moins de 3200 kilomètres de routes référencées dont 2200 kilomètres d'entres elles font partie du réseau autoroutier. Au sein de ce réseau de transport, on compte approximativement 3000 ouvrages d'art. Dans ce contexte, l'objectif majeur pour les gestionnaires est de maintenir le réseau à un niveau satisfaisant des critères de sécurité et de confort. Toutefois, les facteurs rendant la tâche ardue de gérer un si vaste réseau sont multiples. Concernant la fiabilité des ponts routiers, ceux-ci incluent pêle-mêle, des innovations dans leur design et leur construction, l'évolution du trafic routier

conduisant à des dynamiques changeantes au niveau du poids auxquelles les ponts sont soumis, les changements climatiques, etc. Une observation générale sur laquelle cette thèse s'appuie est que ces facteurs exhibent de l'aléa.

L'émergence d'approches purement probabilistes se réfèrent souvent aux travaux de Abdel-Hameed [1975] où un processus gamma à pour la première fois été employé pour modéliser l'usure d'un composant. Depuis, une myriade de modèles s'appuyant partiellement ou totalement sur des méthodes probabilistes ont été développés.

Les travaux présentés dans cette thèse ont pour objectif de modéliser des problèmes de dégradation d'infrastructures en grandes dimensions dans un cadre probabiliste. Les réseaux Bayésiens (RB) répondent à ces critères. Ils proposent une compréhension intuitive des relations entre les nœuds du graphes au travers de dépendances (in)conditionnelles. La littérature existante dénote une attractivité grandissante quant à l'utilisation des RB en fiabilité [Weber et al., 2012]. Par ailleurs, les RB se basent sur la version graphique de la propriété de Markov s'exprimant par les relations de dépendances conditionnelles. À l'instar des RB, les processus de Markov ont acquis une légitimité dans leur utilisation en fiabilité et sûreté structurelle pour les ouvrages d'art [Kallen, 2007].

Plus formellement, un RB est un *graphe orienté acyclique* fournissant une représentation compacte d'une distribution de probabilité d'un ensemble de variables aléatoires $(X_1, ..., X_n)$ sous la forme de distributions conditionnelles. En utilisant des notions

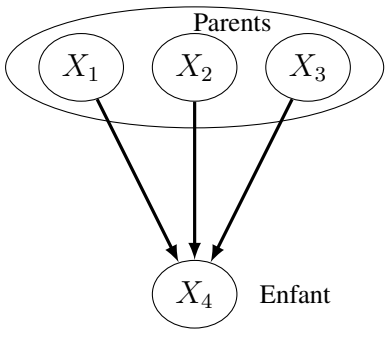

Figure 1.1 – A Bayesian Network on 4 variables

basiques de probabilité, à savoir la formule des probabilités totales, la densité jointe de quatre variables aléatoires peut s'écrire

$$f(x_1, x_2, x_3, x_4) = f(x_1) \prod_{i=2}^{4} f(x_i|x_1...x_{i-1}) \tag{1.1}$$

Les prédécesseurs directs d'un nœud X_i sont appelés *parents* et l'ensemble de tous les parents de X_i s'écrit $Pa(X_i)$. À chaque variable aléatoire est associée une probabilité conditionnelle de cette variable sachant ses parents, $f_{X_i|X_{Pa(X_i)}}, i = 1, ..., 4$. L'équation (1.1) appliquée au RB représenté en Fig. 1.1 peut ainsi être simplifiée grâce aux propriétés de dépendance conditionnelles supposées par les RB :

$$f(x_1, x_2, ..., x_n) = \prod_{i=1}^{4} f(x_i|x_{Pa(i)}) \tag{1.2}$$

Il existe plusieurs classes de RB. Selon la classe considérée, la paramétrisation d'un RB diffère. Nous nous sommes concentrés dans ces travaux en particulier sur deux d'entre elles. La première est la classe de RB dynamique discrète [Dagum et al., 1992, Murphy, 2002] où les relations de dépendance s'expriment par des probabilités conditionnelles classiques. La dimension dynamique intervient en termes de transitions temporelles entre chaque nœud. Cependant, pour cette classe la quantification du RB croît de manière exponentielle ayant pour paramètres le degré [1] de chaque nœud ainsi que leur nombre d'états. Il est toutefois utile de mentionner que cette complexité peut être atténuée en générant de manière systématique les probabilités conditionnelles concernant les relations temporelles nœud-à-nœud.

La seconde classe de RB est la classe des RB *non-paramétrique* (RBNP) [Kurowicka and Cooke, 2005]. À titre comparatif, les RBNP peuvent comprendre aussi bien des variables discrètes, continues et même un mélange continu-discret. Cependant, la

1. Le degré d'un nœud étant le nombre d'arrêtes incidentes qu'il possède

plus grande différence réside dans l'expression de la dépendance probabiliste. Celle-ci se traduit par des corrélations conditionnelles de rang et copules conditionnelles bivariées associées à chaque arrête. Les copules ne nécessitant souvent que très peu de paramètres, e.g., un seul paramètre pour la copule Gaussienne, les RBNP se révèlent être peu couteux. Toutefois, les RBNP se limitent à une utilisation statique. En effet, aucune caractéristique temporel n'a été étudiée mis à part de manière marginale dans les travaux de Morales-Napoles and Steenbergen [2014]. Une partie des travaux de cette thèse s'attache donc à construire un cadre dynamique dans lequel les RBNP s'inscrivent.

En pratique, la paramétrisation est effectuée à l'aide de données. Les jugements d'experts peuvent toutefois également être employés si les données sont insuffisantes ou de qualité ne permettant pas de les exploiter. Dans cette thèse, nous explorons un scénario nécessitant de paramétrer un RB discret dynamique et pour lequel les données disponibles sont insuffisantes. Nous employons la méthode de Cooke afin de combler ce déficit [Cooke, 1991]. Comme nous l'avons précédemment évoqué, la quantification d'un RB dynamique est très couteuse et il serait par conséquent impossible d'avoir recours aux jugements d'experts afin de résoudre ce problème. Le choix d'utiliser un RBNP est d'autant plus renforcé qu'il est de plus en plus courant d'obtenir des données de corrélations conditionnelles de rang auprès d'experts [Werner et al., 2017].

En complément de leur qualité à traduire et organiser des problèmes hautement dimensionnels, les RB possèdent également un autre avantage communément appelé *inférence* ou *update Bayésien*. Concrètement, l'inférence consiste à calculer la distribution de certains nœuds pour lesquels aucune information n'est connue sachant la valeur d'autres nœuds du RB. L'inférence peut être effectuée aussi bien de "haut en bas" (diagnostique) que de "bas en haut" (prédiction). Cette propagation d'information s'effectue encore une fois de manière différente selon que l'on traite les RB dynamiques ou les RBNP. D'un côté, l'inférence pour les RB dynamiques exige la résolution d'intégrales multidimensionnelles dont la valeur croit exponentiellement [Pearl, 1988]. D'un autre

côté, les RBNP permettent d'accomplir l'update Bayésien de manière analytique tant que la copule Gaussienne est supposée. Si la loi jointe est donnée par une autre copule, le RBNP est discrétisé et le problème d'inférence retombe dans le cadre discret.

1.2 Résumé des travaux

Le Chapitre 3 [2] développe un modèle de prédictions de fissurations d'acier dues au phénomène de fatigue pour des ouvrages d'arts autoroutiers. L'objectif est d'exploiter des données provenant d'un système installé à un point sensible du pont. Ceci permet de formuler des prédictions pour les autres points du pont ne bénéficiant pas de données. Le modèle requiert deux composantes sous-jacentes afin d'évaluer la durée de vie restante du pont. Premièrement, le mécanisme de *fracturation élastique linéaire* ainsi que le type de fissuration pouvant apparaitre sont présentés en Section 3.2. Deuxièmement, la Section 3.3 décrit le cadre de dépendance probabiliste où un réseau Bayésien non-paramétrique est proposé. Le RBNP a pour but d'exploiter les corrélations entre les variables régissant le modèle à travers les différents points sensibles du pont ayant des caractéristiques identiques. Le but est de tirer parti de ces corrélations afin de propager les informations venant du système de monitoring vers les sections n'étant pas monitorées.

Le cadre proposé par le RBNP nous permet par la suite d'effectuer des analyses de sensibilité sur l'ensemble des variables du modèle en Section 3.4. Les incertitudes autour des prédictions de fissurations sont réduites en conditionnant par échantillonnage Monte Carlo et en ne conservant que les simulations correspondant aux données de monitoring. En conséquence, nous avons pu mettre en évidence des différences d'inférence significatives concernant les variables régissant le modèle.

Le Chapitre 4 [3] présente l'analyse des données d'experts obtenues par la méthode de

2. Ce Chapitre est extrait de l'article de Attema et al. [2016].
3. Ce chapitre est basé sur l'article de Kosgodagan et al. [2016]

Cooke afin de partiellement paramétrer le modèle introduit au Chapitre 5. Le Chapitre débute en présentant dans ses grandes lignes le modèle de dégradation, qui est encore un problème de fissuration d'acier, en Section 4.2. La Section 4.3 énonce la méthodologie de Cooke et définit les deux métriques permettant de classer les experts, i.e., les mesures de calibration et d'information. Ces métriques sont calculées à partir de variables de calibration qui sont elle-mêmes construites à partir de données existantes relatives à des mesures de fissuration présentés en Section 4.3.1. Les résultats de la performance des experts sont présentées en Section 4.3.2 avançant, d'un côté, les scores médiocres de calibration obtenus pour chaque expert. Ceci étant probablement dû au faible nombre d'experts (3). D'autre part, la valeur combinée du score de calibration est très satisfaisante. Ce même score est substantiellement amélioré après que des tests de robustesse sont effectués et décrit en Section 4.3.3. Les observations majeures de jugement d'experts sont en premier lieu une grande incertitude exprimée dans l'évaluation de probabilités. Deuxièmement, la pertinence des variables de calibration est abordée, notamment par rapport aux variables nécessitant de paramétrer le modèle. Ces remarques sont énumérées et discutées en Section 4.3.4.

Le Chapitre 5 [4] introduit le modèle intitulé réseau Bayésien dynamique co-varié (RBDC). L'objectif est de modéliser la dégradation d'un réseau d'ouvrages d'art dans scénario où les données de détérioration sont limitées. Le modèle de dégradation est présenté en Section 5.2 où un processus de Markov à temps discret est proposé pour décrire la détérioration de chaque élément constituant le réseau. La Section 5.2.1 détaille l'insertion de co-variables dans les probabilités de transitions qui rendent ces transitions dynamiques. Dans le but de connecter les éléments du réseau, le RBDC est présenté en Section 5.2.2 où les ensembles des graphes et des probabilités conditionnelles sont donnés explicitement. Le modèle ainsi construit décrit un réseau Bayésien dynamique à deux dimensions, où la seconde dimension est exprimée par la relation en-

4. Ce chapitre est basé sur l'article Kosgodagan et al. [2017]

tre co-variables. Une méthodologie est proposée en Section 5.2.3 afin d'étudier la sensibilité du RBDC lorsque l'on effectue l'inférence. Cette méthodologie est motivée par la possible explosion combinatoire du réseau, qui plus est par l'ajout de cette seconde dimension. Deux configurations d'inférence sont proposées qui visent à être représentatives de l'ensemble des combinaisons existantes

La paramétrisation du modèle est ensuite discutée en Section 5.3. Nous rappelons que les résultats de jugement d'experts décrit au Chapitre 4 sont implémentés afin de quantifier à la fois des probabilités de transitions du processus de Markov, ainsi que probabilités conditionnelles requises par le RBDC. La Section 5.3.1 rappelle brièvement la méthode de Cooke et ses objectifs. En Section 5.3.2, les développements permettant la quantification des probabilités de transitions sont exhibés au travers de temps moyen de premier passage. La Section 5.4 présente le cas d'un problème de détérioration pour un réseau d'ouvrages d'art où le mécanisme latent de dégradation considéré consiste en l'apparition de fissurations se propageant dans le tablier due à la fatigue. Le RBDC est choisi comme méthodologie dans ce contexte où la structure de dépendance et le choix des co-variables sont décrit en Section 5.4.1. Les co-variables choisies représentent la densité du trafic et la sollicitation en poids induit par le trafic sur l'ouvrage d'art, étant les principales causes endogènes du mécanisme de fatigue. Les données de terrain permettant de quantifier ces deux co-variables sont discutées en Section 5.4.2. Les résultats de sortie du jugement d'experts sont combinés avec ces mesures de trafic et de poids afin d'obtenir in fine les matrices de transitions Markoviennes et de temps moyen de premier passage, ainsi que les courbes de probabilités de survie des ponts. Ces résultats sont décrit en Section 5.4.3.

La Section 5.5 illustre différentes expérimentations utilisant les métriques de sensibilité afin d'étudier la manière dont le RBDC réagit. Nous avons d'abord observé que l'insertion cumulative d'information domine au détriment d'une configuration où l'insertion est individuellement réalisée au cours du temps. Par ailleurs, la sensibilité

de l'information décroît en temps, quelque soit la manière dont l'information a été introduite (cumulative ou bien individuelle). Par conséquent, il serait privilégié d'adopter une surveillance du réseau accrue à des périodes précoces.

Le Chapitre 6 traite de la démonstration théorique qu'un processus de Markov d'ordre k peut être représenté comme un RB non-paramétrique dynamique. Une définition formelle du RBNP est tout d'abord formulée en Section 6.2. Les conditions nécessaires et suffisantes afin de caractériser la partie probabiliste d'un RBNP sont données. Il s'agit des distributions marginales associées à chaque nœud, l'ensemble des copules conditionnelles bivariées et l'ensemble des corrélations conditionnelles de rang associées à chaque arrête du graphe.

Les copules conditionnelles sont présentées en Section 6.3 s'inscrivant spécifiquement dans le cadre du processus Markovien d'ordre k. Le concept de la copule temporelle est présenté, i.e., la copule extraite de n'importe quel processus stochastique à deux pas de temps différents. Des explications concernant la relation entre copules et probabilités conditionnelles sont également indiquées. Nous fournissons de manière explicite la relation entre la mesure d'auto-corrélation pour un processus stochastique et la formulation de corrélations conditionnelles de rang.

Le corps de la Section 6.4 développe la preuve de la représentation d'un processus Markovien d'ordre k comme RBNP dynamique. Le théorème que nous énonçons s'appuie sur les travaux de Joe [1996] concernant les constructions de copules bivariées (*pair-copula constructions*), mais aussi sur les travaux récents Bauer and Czado [2016] sur la formulation de la loi jointe d'un RBNP en termes de copules conditionnelles bivariées. Une procédure résumant étape par étape les éléments clés du théorème est fournie en fin de Section.

La Section 6.5 exhibe la factorisation de distributions marginales multidimensionnelles pour des ensembles de nœuds. L'idée étant d'étudier l'expression analytique des distributions conditionnelles apparaissant dans l'expression des copules conditionnelles

bivariées. Deux cas sont traités. Le premier aborde celui où aucune paire de nœuds de l'ensemble de conditionnement n'a une longueur supérieure à l'ordre k du processus de Markov. La longueur ici représente la différence ordinale entre chaque nœud. Le second cas traite la configuration complémentaire. Cette séparation en deux cas provient de la capacité à séparer les ensembles de nœuds en utilisant la propriété de k-dépendance conditionnelle de Markov. Deux lemmes sont présentés subséquemment et résument ces découvertes. L'algorithme implémentant les deux lemmes est également décrit. Sa complexité est abordée et nous conjecturons qu'il performe mieux que celui de Bauer and Czado [2016]. Enfin, nous illustrons notre approche globale au travers d'un exemple centré autour du mouvement Brownien.

1.3 Conclusion

Cette thèse s'est attelée à étudier des problèmes de dégradation, notamment celui du mécanisme de fissuration due à la fatigue, en grandes dimensions à travers les réseaux Bayésiens. L'approche globale prônée dans ce manuscrit possède deux composantes complémentaires en ce sens qu'elle fait appel à des outils à la fois probabilistes et statistiques. La raison ayant motivé ce choix est double. Tout d'abord, les systèmes se sont complexifiés au cours des dernières décennies et la part d'incertain relative à la fiabilité et la sûreté s'est accrue en conséquence. De plus, l'identification et la quantification de leur causes, possédant souvent de l'incertain aussi, apparaissent de plus en plus difficile. Deuxièmement, l'accessibilité grandissante de grands ensembles de données tendraient à se diriger vers des méthodes statistiques. Nous avons mis en lumière que les RB se révèlent être une approche versatile au sein de laquelle les angles probabilistes et statistiques s'entrelacent. Leur efficacité dans le domaine de la modélisation de dégradation pour des ouvrages d'arts a été testée et validée dans les Chapitres 3, 4 et 5. Bien qu'aucune application orientée à la fiabilité n'ait été présentée dans le Chapitre 6, nous

pouvons affirmer que l'approche développée est dans la lignée des chapitres précédant concernant des considérations de détérioration et leur efficience. Un argument immédiat serait que quelque soit la classe de RB considérée, la propriété de Markov symbolisée par la dépendance conditionnelle a été, et continue d'être une approche attractive dans des problématiques de détériorations structurelles.

De manière globale, le mécanisme de fatigue de l'acier provoquant un risque de fissuration nous a conduit à explorer deux classes de RB ayant des représentations différentes de dépendance. Ce mécanisme peut être décrit comme problème à grandes dimensions et les RB se sont avérés être une méthode adaptée pour y répondre. D'un côté, lorsque la modélisation Markovienne est adéquate dans le cadre de dégradation structurelle, les RB dynamiques sont apparus efficaces. En dépit de la possible explosion combinatoire en termes de quantification, la dépendance traduite par les probabilités conditionnelles peut être évaluée de manière systématique, à moins de supposer, par exemple, des contraintes d'inhomogénéité.

La capacité des deux classes de RB à gérer ou non des distributions continues, discrètes ou bien mixtes est également un aspect primordial. Théoriquement, il est presque toujours possible de discrétiser des variables continues. Cependant, cela se révèle en général couteux en informations perdues et en temps de calcul durant l'étape de la modélisation. Les RBNP ont prouvé leur efficacité en premier lieu pour répondre à cet objectif. La dépendance probabiliste s'exprime à travers des copules conditionnelles bivariées ainsi que des corrélations conditionnelles de rang. Brièvement abordée au Chapitre 3, ces deux caractéristiques de dépendance permettent de capturer une grande variété de schémas de dépendances, e.g., des effets de queues, des localisations spécifiques des masses dans les distributions, etc. Cette dernière caractéristique est particulièrement intéressante lorsque la fiabilité structurelle exhibe des dépendances très changeante au travers d'un vaste réseau. A ce tire, nous avons montré au Chapitre 6 que les dépendances au sein d'un RBNP peuvent également être gérées de manière

dynamique. Cependant, les composantes de dépendance ainsi que les distributions marginales sont calculées à partir du processus de Markov qui les suppose implicitement.

Chapter 2

Introduction

Contents

2.1 Context & motivation

The late prolific mathematician Paul Erdős had been (and still is) famous for the number that bears his name, the so-called Erdős number. This number provides the "collaborative distance" between the Hungarian mathematician and anyone else, as measured by authorship of mathematical papers. Erdős explored and significantly contributed to mathematics as he is credited with more than 1500 publications in various mathematical branches. Amongst others was the graph theory that gave birth to the Erdős number.

The study of graphs, or networks, can be traced back to the work of Euler in 1736

and the well-known Königsberg Bridge Problem. We do not develop on the problem but the interested reader may refer to Newman et al. [2011] for a detailed explanation of the problem. Graphs have experienced a growing popularity since then and lead to the foundation of a sound theory [Harary, 1994, Gross et al., 2013]. Domains in which graphs have been successfully applied are numerous from physics and computer science to biology and the social sciences. Researchers quickly realized that networks allow a great variety of ways to represent complex problems, and that there is much to be learned by studying them.

In the civil engineering field, the Dutch national road network consists of around 3200 kilometres of roads, of which 2200 kilometres are highways. Within this network, there are approximately 3200 bridges. In this setting, the key objective of decision makers to keep the network in a satisfactory level can prove challenging. There can be various factors which make civil infrastructure management a hard task. For bridge reliability, these include the changes in construction design, the dynamics of loading induced by traffic density, the impact of the weather, and more specifically meteorological catastrophes, etc. However, all these factors exhibit uncertainty that is important to account for.

Traditionally, deterministic physics-based models are put forward in literature to describe degradation mechanisms. They attempt to describe the deterioration process from a physical point of view, e.g. differential equations that govern the evolution of a phenomenon. For example, the Paris law can be used for modelling the growth of cracks in steel plates. The description of very complex relationships, however, make these models intractable as these relationships are often not easy to identify or quantify. Probabilistic dependence is able to achieve this, moreover, the ability to incorporate randomness is enticing.

The emergence of pure probabilistic approaches in the reliability field often cites the seminal work of Abdel-Hameed [1975] where a gamma process was first used to model

the wear of a device. Since then, a myriad of probabilistic models have been developed.

The research presented in this thesis aims at modelling high dimensional deterioration problems within a probabilistic framework. Bayesian networks (BN) comply very well with the requirements cited above. They offer an intuitive understanding of (un)conditional dependencies and a comprehensive visual representation. Models that rely on BN in the area of reliability and risk-analysis are numerous [Weber et al., 2012]. Moreover, BN feature a Markov-based framework expressed through the conditional independence statements. Markov processes have proven to be particularly suitable in deterioration modelling for civil infrastructures [Kallen, 2007]. Nevertheless, little attention has been given to multiple correlated Markov processes in reliability different than through simple correlation as has been done traditionally. Moreover, such a naive approach should have complex and inefficient parametrization characteristics.

Bayesian networks offer the possibility to tackle the high dimensionality component in a consistent, continuous and, possibly, generic manner. Their attractiveness partly comes from the causal reasoning one can perform. We can count at least four classes of Bayesian networks in the literature

1. discrete (static) BN [Pearl, 1988] where dependence is handled through classic discrete conditional probability
2. discrete dynamic BN [Dagum et al., 1992, Murphy, 2002] which are similar to their static counterpart but add a time-varying layer
3. continuous Gaussian BN [Shachter and Kenley, 1989] where the joint distribution is assumed to be Gaussian as well as any sub-vector of marginal distribution
4. *non-parametric* or *pair-copula* BN (NPBN) [Kurowicka and Cooke, 2005]. This class of BN is the most recent and was developed to relax the restrictive Gaussian assumption of Gaussian BN and where dependence is handled through copulae and rank correlation

The importance of flexibility in terms of dependence for the last class of BN has be-

come very enticing over the past decade [Hanea et al., 2015]. However, no theoretical development incorporating a structured dynamic aspect has been investigated thus far. In this thesis, we first investigate a way to extend the dynamic BN to account for another dimension that could be represented by space.

Parametrization for Bayesian networks differs from class to class. For the discrete, static or discrete, dynamic class, the quantification can quickly become tremendously demanding. For each source vertex, i.e., parentless vertices, we associate marginal distributions, and for any child vertex a conditional probability is associated. The conditional distribution is as large as the number of parents the child node has. This number is usually referred to as the degree of the vertex which can be interpreted through a dimensional aspect where one parent means one dimension. For discrete, dynamic BN, this burden can be mitigated by generating in a systematic fashion the conditional probabilities for the time connection between vertices.

Compared to their discrete counterpart, NPBN can handle both discrete (in an ordinal scale) and continuous variables. However,what sets them apart is the formulation of probabilistic dependence which further significantly reduces the quantification task. In fact, dependence is expressed through (conditional) bivariate copulae and (conditional) rank correlations. Copulae often feature a few parameters to estimate, e.g., the Clayton copula has one parameter, Gaussian has one parameter, etc. Rank correlations are assigned to each of the edges. Altogether, even for very complex and large NPBN, the quantification together with the dependence and distribution freedom make NPBN very attractive for high-dimension modelling.

In practice, parametrization is often performed with data but can also be done through expert judgment if data is insufficient or of poor quality. This thesis explores a scenario where data is missing. Cooke's method for eliciting expert opinion is used and should be encouraged whenever limited data is available [Cooke, 1991]. As previously mentioned, quantifying a discrete BN can be a tremendous task and so it would be for experts

also. The Bayesian network model limits the use of expert judgment for too complex structures due to the increased elicitation burden. By complex we understand both the degree [1] of each of the nodes as well as the number of states per node. By consequence, models can either be simplified to make quantification possible or another type of BN could be chosen, for instance, NPBN.

Nonetheless, throughout the last decade the flow of collected data has kept growing, which has given rise to "Big data", analytics and machine learning. Aside from the quantification task, measurements may then be used to perform inference. One can calculate the distributions of unobserved vertices, given the values of the observed ones. If the reasoning is done "bottom-up" (in terms of the reasoning logics and the directionality of arcs), the BN is used for diagnosis, whereas if it is done "top-down", the BN serves for prediction. Inference is performed differently in both classes of BN that are considered in this thesis. For the discrete, dynamic BN, inference can become very challenging in terms of computational demand, especially when the structure is very large which is often the case when using dynamic BN. In fact, it is known to be exponentially increasing [Pearl, 1988].On the other hand, non-parametric BN offer the possibility to perform analytical updating whenever the joint distribution is given by a Gaussian copula. If the joint distribution is given by another copula than the Gaussian, then because of computational advantages a discretization is recommended and inference is performed accordingly.

Returning to the bridge degradation modelling case, a network of such elements is comprised of underlying factors such as traffic that interact between each other. Thus, it is natural to account for dependencies. Moreover, these factors can be deterministic or random, hence a probabilistic methodology may be a logical choice. Another desirable characteristic is the capacity to efficiently insert available evidence. By "efficiently" we mean the computational demand. This would dynamically update degradation estimates

1. the degree of a node is the number of edges incident to it

from one part of the network to the others in addition to future decision plans.

This thesis contributes to the existing literature through the following. Chapter 3 demonstrates the efficiency of NPBN for a highly dimensional crack growth prediction problem. This problem includes no less than twenty random variables governing the physical mechanism for which the NPBN is used to link them. For each of these variables, the NPBN adds a spatial component translated by more than 300 additional variables reaching an order of thousands of random variables. Even in this very complex context, the NPBN shows an acceptable behaviour in terms of computational efficiency. This computational characteristic also extends to inference which propagates data coming from a monitoring system so that it eventually helps reduce the uncertainty of crack growth prediction.

Chapter 4 highlights the benefit of using Cooke's method for eliciting expert opinions in order to partly parametrize the model. Chapter 5 highlights similar advantage as those in Chapter 3, but considers a dynamic BN. We introduce a model that extends this class of BN by adding a dimension that could be useful to incorporate a spatial component. This dimension serves to represent a network-scale bridge degradation. For a potentially very large network of bridges, the proposal proves could be efficient at dynamically describing the stochastic evolution of each asset as well as measuring the impact of information at both the local and network levels.

Lastly, Chapter 6 focuses on a theoretical proof linking Markov processes to NPBN. More precisely, we show that any Markov process possesses a dynamic NPBN representation. This specification provides a new angle from which one could build up a Markov-based model where dependence considerations are of primary interest. The NPBN metrics translate these considerations through copulae and rank correlation. Inference is also addressed as we provide the necessary and sufficient conditions to perform analytical conditioning that reduce to the solubility of integral form.

Since Bayesian networks lean on both graph and probability theory, it is useful to

introduce them in this Chapter. We also benefit from the introduction of graph theoretical terminology and preliminaries on probabilities to consistently use them throughout this thesis.

2.2 Bayesian networks

In this Section, the basic principles of Bayesian Networks are explained. Leaning on both graph and probability theory, we start by providing the essential elements related to graphs. Comprehensive introduction to Bayesian networks can be found in Lauritzen [1996], Cowell et al. [1999] and Hanea et al. [2015]. The research carried out in this thesis presents both practical and theoretical developments for essentially two different classes of Bayesian networks, known as discrete, dynamic BN and non-parametric BN. However, it should be noted that the following principles hold regardless of the class we consider.

2.2.1 Preliminaries on graphs

Let $V \neq \emptyset$ be a finite set and let $E := \{(v, w) \in V \times V : v \neq w\}$ Then $\mathcal{G} = (V, E)$ denotes a *graph* with vertex set V and edge set E. $\mathcal{G}$ is said to contain an *undirected* edge if there exists $v, w \in V$ such that $(v, w) \in E$ and $(w, v) \in E$. Conversely, we say that V contains a *directed* edge if there exists $v, w \in V$ such that $(v, w) \in E$ and $(w, v) \notin E$. A graph containing only undirected edges is called an *undirected graph* and, likewise, a graph containing at least one directed edge is called a *directed graph*. The *degree* of a vertex is the number of edges incident with it. A *path* of length n from a to b is a sequence $a = a_1, ..., a_n = b$ of distinct vertices such that $(a_{i-1}, a_i) \in E$, for every $i = 1, ..., n$. A path from a_1 to a_n is called *directed* if at least one of the connecting edges is directed. We term a path from a to b a *cycle* if $a = b$. In particular, a directed path from a to b is termed a *directed cycle* if $a = b$. A graph without directed

cycles is known as a *chain graph* (CG). A CG containing at least one directed edge is called a *directed acyclic graph* (DAG). We define the *adjacency* set of a vertex $v \in V$ as $ad(v) := \{w \in V : (v, w) \in E \text{ or } (w, v) \in E\}$. If $w \notin ad(v)$, we say that v and w are *non-adjacent*.

Let $\mathcal{G} = (V, E)$ be a DAG. Since all edges of $\mathcal{G}$ are directed, we can speak of paths instead of directed paths. For $v \in V$, we let

$$
\begin{aligned}
pa(v) &:= \{w \in V : \mathcal{G} \text{ contains } (w, v)\} && \text{(parents of } v\text{)} \\
an(v) &:= \{w \in V : \mathcal{G} \text{ contains a path from } w \text{ to } v\} && \text{(ancestors of } v\text{)} \\
de(v) &:= \{w \in V : \mathcal{G} \text{ contains a path from } v \text{ to } w\} && \text{(descendants of } v\text{)} \\
fa(v) &:= pa(v) \cup \{v\} && \text{(family of } v\text{)} \\
nd(v) &:= V \setminus (\{v\} \cup de(v)) && \text{(non-descendants of } v\text{)}
\end{aligned}
$$

A set $I \subseteq V$ is called *ancestral* if $pa(v) \subseteq I$ for any $v \in I$. The smallest ancestral set containing I is denoted by $An(I)$. As is readily verified, $An(I) = I \cup \{\cup_{v \in I} an(v)\}$. A bijection $B : \{1, ..., |V|\} \to V, i \mapsto v_i$ satisfying $i < j$ whenever $\mathcal{G}$ contains (v_i, v_j) for some $i, j \in \{1, ..., |V|\}$ is called a *well-ordering* of $\mathcal{G}$. Note that in a well-ordered DAG the set $\{v_1, .., v_k\}$ is ancestral for all $k \in \{1, ..., |V|\}$.

2.2.2 Directional separation and conditional independence

Directional separation (D-separation) is a criterion of directed graphs for deciding whether a set of variables is independent of another set, given a third set. The idea is to associate "dependence" with "connectedness" (i.e., the existence of a connecting path) and "independence" with "unconnected-ness" or separation. Pearl [1988] was the first to investigate the D-separation criterion to relate this graphical feature to probabilistic conditional independence. From the graphical representation only, one can determine conditional independencies.

Let $\boldsymbol{X} = \{X_1, ..., X_{n_1}\}$, $\boldsymbol{Y} = \{Y_1, ..., Y_{n_2}\}$ and $\boldsymbol{Z} = \{Z_1, ..., Z_{n_3}\}$ be pair-wise

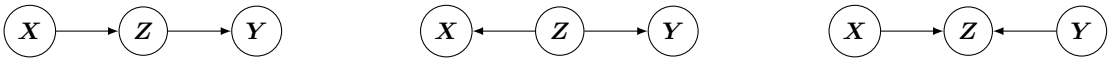

(a) Serial linking (b) Diverging linking (c) Converging linking

Figure 2.1 – D-separation configurations

disjoint sets of vertices, i.e. $\boldsymbol{X}, \boldsymbol{Y}, \boldsymbol{Z} \subseteq V$, with n_1, n_2, n_3 integers. A path from $\boldsymbol{X}$ to $\boldsymbol{Y}$ is a path from a vertex $X_i \in \boldsymbol{X}$ to a vertex $Y_j \in \boldsymbol{Y}, i \in \{1, ..., n_1\}, j \in \{1, ..., n_2\}$. We say that $\boldsymbol{Z}$ *separates* $\boldsymbol{X}$ from $\boldsymbol{Y}$ in $\mathcal{G}$, and write $\boldsymbol{X} \perp \boldsymbol{Y} | \boldsymbol{Z}$, if every path from $\boldsymbol{X}$ to $\boldsymbol{Y}$ contains a vertex in $\boldsymbol{Z}$. In particular, we write $\boldsymbol{X} \perp \boldsymbol{Y} | \emptyset$ or simply $\boldsymbol{X} \perp \boldsymbol{Y}$ if there exists no path between $\boldsymbol{X}$ and $\boldsymbol{Y}$. There can be three graphical configurations where the D-separation criterion can be examined. Fig 2.1 illustrates these three cases where:

1. The structure in Fig. 2.1(a) shows that if $\boldsymbol{Z}$ is not given it is clear that $\boldsymbol{Y}$ is depending on $\boldsymbol{X}$ (through $\boldsymbol{Z}$). However if $\boldsymbol{Z}$ is given, it is clear that $\boldsymbol{X}$ is not influencing $\boldsymbol{Y}$ any more. Only $\boldsymbol{Z}$ is influencing $\boldsymbol{X}$, but $\boldsymbol{Z}$ is not depending on $\boldsymbol{X}$ anymore. $\boldsymbol{X}$ and $\boldsymbol{Y}$ are D-separated by $\boldsymbol{Z}$.
2. The conditional independence characteristics of graph in Fig. 2.1(b) are similar to those of Fig. 2.1(a)
3. The suggested structure in Fig. 2.1(c) is slightly counter-intuitive. If $\boldsymbol{Z}$ isn't given, $\boldsymbol{X}$ and $\boldsymbol{Y}$ are D-separated and because of that independent. If $\boldsymbol{Z}$ is given, then this will influence $pa(\boldsymbol{Z})$ depending on the quantification of their dependencies. The remark is that if any of $\boldsymbol{Z}$ its children are given, this will (eventually) reflect on $\boldsymbol{Z}$ and because of that possibly make $\boldsymbol{X}$ and $\boldsymbol{Y}$ conditionally dependent. So altogether $\boldsymbol{X}$ and $\boldsymbol{Y}$ are D-separated if and only if no information is given about $\boldsymbol{Z}$ and all its descendants.

We are now able to establish the connection between the the graphical property of D-separation and conditional independence.

Let again $\mathcal{G} = (V, E)$ be a DAG on $d = |V|$ vertices. Let $\boldsymbol{X}$ be an $\mathbb{R}^d$-valued random variable. For any $I \subseteq V$, we write $\boldsymbol{X}_I := (X_v)_{v \in I}$. If $I = \{v\}$ for some

$v \in V$, we write X_v. Furthermore, we write $\boldsymbol{X}_I \perp \boldsymbol{X}_J | \boldsymbol{X}_K$ whenever $\boldsymbol{X}_I$ and $\boldsymbol{X}_J$ are *conditionally independent* given $\boldsymbol{X}_K$ for pairwise disjoint sets $I, J, K \subseteq V$. Then, conditional independence can be expressed through the D-separation property as

$$X_v \perp \boldsymbol{X}_{nd(v)\setminus pa(v)} | \boldsymbol{X}_{pa(v)} \qquad \text{for all } v \in V \tag{2.1}$$

Since $ad(v) \cap (nd(v) \setminus pa(v)) = \emptyset$ for every $v \in V$, it can be easily seen that the conditional independence restrictions obtained from eq. (2.1) correspond to missing edges in $\mathcal{G}$. A probability measure satisfying eq. (2.1) is simply called $\mathcal{G}$-Markovian.

A Bayesian network or (directed) graphical model based on a DAG $\mathcal{G}$ is a family of $\mathcal{G}$-Markovian probability measures. It provides a compact representation of high dimensional uncertainty distribution over a set of variables $\boldsymbol{X} = \{X_1, ..., X_d\}$ and encodes the probability density or mass function on $\boldsymbol{X}$ by specifying a set of conditional independence statements in a form of an acyclic directed graph and a set of probability functions. The joint density $f_{\boldsymbol{X}}$ thus has the following factorization

$$f_{\boldsymbol{X}}(\boldsymbol{x}) = \prod_{v \in V} f_{X_v | \boldsymbol{X}_{pa(v)}}(x_v | \boldsymbol{x}_{pa(v)}) \quad \text{for all } \boldsymbol{x} = (x_1, ..., x_d) \in \mathbb{R}^d \tag{2.2}$$

2.3 Outline of the thesis

As a general overview, the first three Chapters discuss degradation models previously put forth while the last Chapter provides the theoretical validation that any k-th order Markov process possesses a dynamic NPBN representation.

In Chapter 3, a model is developed to assess prediction of fatigue cracking for a highway steel bridge. The objective is to exploit the output of a monitoring system placed at a certain sensitive spot on the structure to make predictions for non-monitored locations. The model requires two underlying components to assess the remaining lifetime of the bridge. First, in Section 3.2, the type of cracks considered as being a serious threat to

traffic safety are introduced, i.e. transverse cross section cracks and two types of longitudinal cross-section cracks. Also, the physics-based cracking mechanism known as *linear elastic fracturing* is discussed.

Second, Section 3.3 depicts the dependence framework where a non-parametric Bayesian network is constructed. The NPBN is meant to exploit correlations between the governing random variables of the model across different locations over the bridge. The goal is to make use of this characteristic to propagate information coming from monitored sections into non-monitored parts.

The NPBN framework subsequently allows carrying out sensitivity tests as well as root cause analyses in Section 3.4. Sample-based conditioning is performed through Monte Carlo simulations. By keeping only those simulations corresponding to the monitoring results, it helps reduce the uncertainty of the crack predictions and evidences significant differences between conditional and unconditional distributions of the model governing variables. This Chapter is based on the published paper Attema et al. [2016].

Chapter 4 outlines the structured expert judgment analysis carried out to assess inputs for the model presented in Chapter 5. The Chapter starts with a summarized description of the probabilistic model in Section 4.2 where the need of Cooke's classical method to fill in the missing data is incentivized.

Section 4.3 details Cooke's methodology and defines the two metrics for ranking the experts, i.e., calibration and information. These metrics are computed using seed variables that are formulated using real-world data on fatigue cracking presented in Section 4.3.1. Results of the experts' performances are shown in Section 4.3.2 highlighting, on the one hand, the poor calibration score per expert that may be due to the small number of experts (3). On the other hand, the satisfactory value of the same score for the combined opinion can be notably mentioned. The experts' performance is even improved after robustness analysis is executed in Section 4.3.3. The main observations are first on great uncertainty results for the assessment of probability estimates. Second, the

relevancy of the seed variables is raised with respect to the variables of interest. These remarks are finally discussed in Section 4.3.4. This Chapter is based on the published article Kosgodagan et al. [2016].

Chapter 5 introduces the so-called covariate, dynamic Bayesian network (covariate-DBN) model. The objective is to model the degradation for a network of "similarly classified" assets under very limited data where attention is drawn to the modelling of a large-scale network. The deterioration framework is explained in Section 5.2 where a discrete-time Markov stochastic process is used to model the degradation for each of the elements constituting the network. Section 5.2.1 details that compared to the classic Markov transition probabilities, we also incorporate so-called covariates so that they dynamically influence these transitions. In order to connect the elements the covariate dynamic Bayesian network is specified in Section 5.2.2 where the sufficient and necessary probabilistic and graph parts are explicitly exhibited. The constructed model thus formulates a two-dimension, dynamic BN where the second dimension is expressed through the covariate connection. Subsequently, a methodology to investigate inference sensitivity is proposed in Section 5.2.3. Since the network can grow in size very quickly across the two dimensions, inference combinations quickly become intractable as well. This motivates the development of a sensitivity metric where two representative inference configurations are examined.

Next, the parametrization of the model is discussed in Section 5.3. Recall that the expert judgment outcome of Chapter 4 is used both to calibrate the transition probabilities of the Markov chains as well as some required conditional probabilities stemming from the Bayesian network framework. Section 5.3.1 briefly recalls the objective of Cooke's method. In Section 5.3.2, emphasis is made on the mathematical development for calibrating both the transition probabilities through expected first passage time and those conditional probabilities. Discussion on the complexity of the model's parametrization is addressed too. The choice of assuming classes of assets significantly decreases the

number of inputs to estimate as this number would grow across this second dimension.

Section 5.4 presents the case of deterioration for a network of bridges where the underlying physical deteriorating process considered is fatigue crack growth in the bridge deck plate. The covariate-DBN methodology previously developed is used from which the dependence structure together with choice of the set of covariates is exhibited in Section 5.4.1. The covariates are chosen to be traffic density and loading, as they are known to be the main driving factors for motorway fatigue degradation. Data for these covariates is available and introduced in Section 5.4.2. The output of the expert judgment is used and combined with field data so that the Markov transition matrices, the expected first passage time matrices and degradation curves are obtained. These are shown in Section 5.4.3.

In Section 5.5, various experiments are presented showing the sensitivity of the proposed model for the network-scale extension using the methodology presented in Section 5.2.3. It was observed first that cumulative inserted pieces of information dominate over individual piece of information. Second, the sensitivity of the inserted information decreases in time so that pieces of evidence inserted at early epochs should be preferred over later ones. This Chapter is based on Kosgodagan et al. [2017].

Chapter 6 treats the theoretical proof that any k-th order Markov process can be represented as a dynamic non-parametric Bayesian network. A formal definition of NPBN is first provided in Section 6.2. The necessary and sufficient condition to specify the probabilistic part of any NPBN are given : the marginal distributions associated to each vertex, and the set of all conditional pair-copula and conditional rank correlation associated to each of the edges.

The metrics mentioned in Section 6.2 are presented in Section 6.3 in the k-th order Markov process context. The concept of the so-called time-copula is introduced, i.e., the copula of any two different time-steps one can extract from a stochastic process. Details on relationship between copulae and conditional probabilities are provided. Next,

we make explicit the relation between autocorrelation for any stochastic process to the formulation of conditional rank correlation.

The body of Section 6.4 stands for the central part of the Chapter where the proof of the k-th order Markov process as a dynamic NPBN is exhibited. The theorem that we develop first relies on the findings of Joe [1996] on pair-copula constructions, and second on the recent derivations of Bauer and Czado [2016] to express the joint density for an NPBN. A summarized procedure is provided at the end of the Section for guidance.

Section 6.5 provides the derivation for the marginal distribution of sets of vertices. The motivation is to investigate the analytical expressions of conditional distributions which are required in the pair-copula formulation. Two cases are addressed. One that deals with sets of vertices where there are no pair of vertices whose length is less than the order k of the Markov process. By the length we mean the difference of the respective value of each vertex. The second case copes with sets of vertices possessing at least one pair of vertices whose length is great than or equal to the order k. This case separation is due to the conditional independence that split vertices whose length is great than k. Two corresponding lemmas are formulated and algorithm is presented as well. The computational complexity of the algorithm is discussed and how it performs better to that of Bauer and Czado [2016]. We finally illustrate our findings through an example focused on Brownian motion.

Lastly, Chapter 7 gathers up the conclusions of each Chapter and presents some perspectives.

The pieces of work carried out in this thesis were half supported by the TNO program "Enabling Technologies-Models" under the project GrAphical MEthods for Systems Risk and Reliability (GAMES2R). This program mainly aims at establishing a generic set of probabilistic models and methods, for application mainly in modelling systems risk and reliability. The other half comes from a fellowship of the French Ministry of

Industry.

Chapter 3

Non-parametric Bayesian network to assess crack growth prediction for steel bridges [1]

Contents

3.1 Introduction

Fatigue cracking is one of the main degradation mechanisms of steel bridges. It is the result of fluctuating stresses caused by the crossing of heavy vehicles. Especially welded

1. This Chapter is based on Attema et al. [2016]

details in the deck structure are vulnerable to fatigue cracking [Maljaars et al., 2012] because these details are directly loaded by passing wheels and because of the stress concentrations, initial notches and high residual stresses that are specific to welded deck structures. Some critical welded details occur multiple times in a bridge deck, so that cracks can basically occur everywhere in the deck. On the other hand distribution of loads to adjacent parts of the structure is often possible if a detail is weakened as a result of a fatigue crack. The latter implies that critical crack lengths —- i.e. crack lengths at which failure can be assumed —- are typically long (in the order of 400 mm or longer) and that crack growth rates of large cracks are typically low as compared to fatigue tests on single details. For these reasons monitoring systems aimed at identifying fatigue cracks can be used to guarantee the safety of the bridge.

Although the costs of monitoring vary from bridge to bridge, it can be said that monitoring systems are in general expensive, especially if a large surface such as a bridge deck needs to be covered. Installation costs form a large portion of the total costs. According to Issa et al. [2005] the installation time of a complete measurement system for bridges can potentially consume over 75% of the total testing time. Installation labour costs can approach well over 25% of the total system cost. But also maintenance costs and costs of data processing can be significant. For this reason, this research considers a system that monitors a small part of the bridge deck and uses the output of the system in order to provide an assessment of the general condition of the non-monitored part of the bridge deck.

The output provided by the monitoring system is used to probabilistically predict the remaining life of the structure. Apart from the output of the monitoring system (observations), this prediction requires two underlying models required for the assessment of the remaining lifetime of the bridge. The two models used in the assessment are:

1. a physical fracture mechanics model to evaluate the crack growth rate,
2. a non-parametric Bayesian network to update the crack growth and end-of-life

prediction of the non-monitored part of the bridge deck based on the observations of the monitored part

Previous research has been devoted to incorporating monitoring data in the fatigue life prediction. For example, Deng et al. [2014], Liu et al. [2010] have considered monitoring of stress ranges and number of cycles. In other cases, the results of fatigue crack inspections has been used in order to assess the remaining life, e.g. Boutet et al. [2013], Toft et al. [2014]. Research in which the observations regarding crack size monitoring are considered and used for prediction of the remaining resistance or life span is less common in the literature. One of the main differences between inspections and monitoring from the point of view of the models required, is that monitoring systems usually only cover a part of the structure. Hence models that use the information obtained from the monitored part of a structure in the assessment of the non-monitored part are required. This is achieved here through the use of a non-parametric Bayesian network.

The choice of the class of non-parametric Bayesian network comes essentially from their ability to handle continuous distribution in more natural and efficient way than their discrete counterpart. As we may see, the majority of the variables governing the model have continuous distributions. Second, inference in discrete BN is known to be very computationally demanding, especially when continuous distributions may sometimes have to be discretized into hundreds of states. In the NPBN framework, inference can be analytically and thus almost instantaneously achieved if the normal copula is assumed. Otherwise, this can rapidly be done with approximation algorithms [Hanea et al., 2015] however, without losing the modelling advantage.

The chapter is organized as follows. Section 3.2 introduces the considered types of crack as well as the set of (random) variables governing the model. Section 3.3 presents the dependence model through the NPBN used to quantify the complete dependence structure of the random variables governing the model. Section 3.4 shows how to apply

the monitoring results in order to make predictions about the non-monitored details. Last, conclusions are summarized and discussed in section 3.5.

3.2 Description of the detail

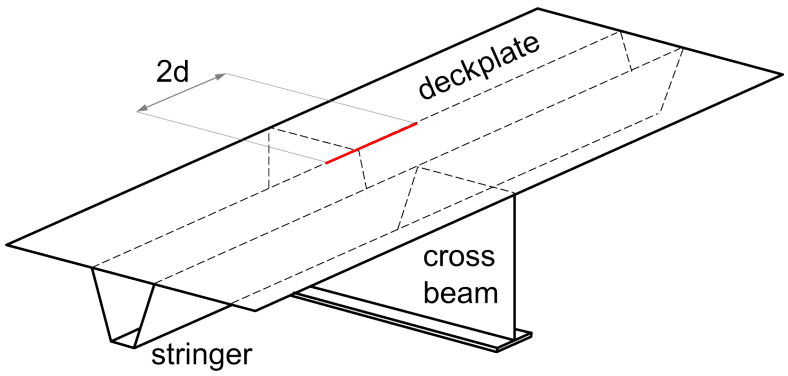

(a) 3d view of the detail

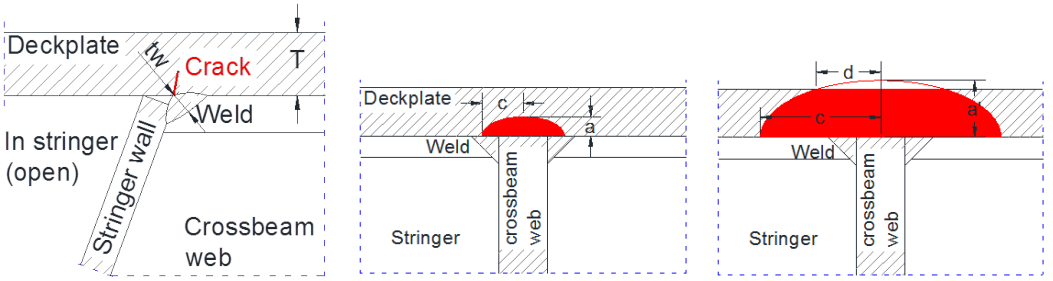

(b) Transverse cross-section (c) Longitudinal cross-section with surface crack (d) Longitudinal cross-section with through-surface crack

Figure 3.1 – Crack of concern

The main focus is a type of crack that is observed in orthotropic steel bridge decks. The crack starts from the root of the weld between a trapezoidal stringer and the deck plate -– usually at the junction with a crossbeam — and subsequently grows along the weld line (Figure 3.1). This type of detail occurs multiple times in a bridge deck. Per crossbeam the number of heavily loaded details — i.e. details directly below the wheel tracks — is approximately equal to 6. Depending on the span of the bridge, the total

number of heavily loaded details varies between 10 and 100.

Figure 3.1 displays the type of crack considered here. The crack shapes considered are a semi-elliptical surface crack and a through-thickness crack, indicated in Figures 3.1(c) and 3.1(d), respectively. If not repaired, a surface crack will grow and form a through-thickness crack after a certain number of cycles. The dimensions of the surface crack are indicated with depth a and semi-length c. Those of the through-thickness crack are the semi-length on the bottom side c, the semi-width on the top side d and the effective height a, see Figure 3.1.

The type of crack in Figure 3.1 is considered as being a serious threat to the traffic safety, because a wheel load rolling on one side of the crack may cause a level difference between the two parts of the deck plate separated by the crack, implying that the vehicle is uncontrollable. In addition, it is difficult to detect the type of crack because it is covered by the surface finish on the top side and by the stringer on the bottom side. Moreover, the type of crack is observed in many existing bridges in various countries.

Variables 1–4 in Table 3.1 provide the relevant geometric dimensions of the detail, here a_0 and c_0 are the initial defect dimension at the weld root prior to fatigue loading. Because a_0 and c_0 are correlated, a distribution is provided for the ratio between a_0 and c_0. For each variable, the distribution function is provided together with the average, μ, and the coefficient of variation, V. Moreover, a dependence structure between the various locations of this type of detail in one bridge is imposed. This dependence structure exists since these different details are exposed to similar conditions and it is quantified by the rank correlation, r, between variables in different sections of the bridge. In particular, these are the correlations between variables in the monitored and non-monitored sections of the bridge. All the variables in Table 3.1 are based on those presented in Maljaars and Vrouwenvelder [2014] where a fracture mechanics model of a different detail in the same type of orthotropic deck structure is provided. However, some modifications accounting for the specific detail and models are considered here.

Because we concentrate mainly on the Bayesian network modelling, we skip the part explaining the physics-based model, i.e. the linear elastic fracture mechanics (LEFM). However the reader is referred to Attema et al. [2016] for the complete clarification.

3.3 Dependence model

The crack growth model using LEFM outputs the crack growth development for one detail of the bridge. As explained earlier, a bridge may contain hundreds of these heavily loaded details. Correlation between variables in different sections of the bridge has to be taken into account which can stem from various reasons, e.g. same welding procedure, similar loading condition, etc. The goal is to make use of this characteristic in order to propagate information coming from monitored sections into non-monitored parts. The rank correlations, r, of the random variables between different locations of the detail of Section 3.2 are given in Table 3.1. These correlations were quantified by field data, using previous literature and expert opinion (as provided in Maljaars and Vrouwenvelder [2014]). The aim is at quantifying the complete dependence structure of the random variables. In order to achieve this, a non-parametric Bayesian network (NPBN) is used. From this Bayesian network, the variables in Table 3.1, used in the crack growth model underlying every detail in a bridge, are sampled.

The set of random variables determining the crack growth development in the monitored location is displayed in Table 3.1. It is assumed that these variables are independent of each other. Moreover, one set of these variables for the crack growth development is present in every other detail on the bridge in the non-monitored section. These variables are correlated with each other. The dependence structure of each variable in different parts of the bridge is described with an NPBN. The monitored section is the most vulnerable section of the bridge due to the fact that the dynamic amplification factor for this location differs from the one in the other locations.

Table 3.1 – Model variables

i	X_i	Variable	Units	Distribution	μ	V	r
1	T	Deck plate thickness	mm	uniform	12	0.03	0
2	t_w	Weld throat	mm	uniform	5	0.03	0.3
3	a_0	Initial crack depth	mm	lognormal	0.15	0.66	0
4	a_0/c_0	Initial aspect ratio	-	lognormal	0.62	0.40	0
5	R	stress intensity ratio	-	normal	0.5	0.2	0.6
6	K_{1C}	fracture thoughness	N/mm$^{3/2}$	lognormal	6325	0.25	0
7	ΔK_0	crack growth threshold at R=0	N/mm$^{3/2}$	lognormal	243	0.4	0.95
8	A	crack growth parameter	N,mm	lognormal	$2 \cdot 10^{-13}$	0.6	0.85
9	m	crack growth exponent	-	deterministic	3	-	-
10	p	curvature parameter	-	lognormal	0.7	0.25	0.7
11	SCF	stress concentration factor at the crossbeam web	-	lognormal	2.1	0.1	0.8
12	l_{sc}	extension length of stress concentration	mm	lognormal	80	0.2	0.8
13	c_f	semi crack length of a critical crack	mm	lognormal	250	0.25	0
14	s_{fy}	annual trend factor on axle loads	-	normal	0.002	0.1	1
15	n_{fy}	annual trend factor on number of vehicles	-	normal	0.011	0.2	1
16	n_{tmax}	max. annual number of heavy vehicles on slow lane	-	normal	$2.5 \cdot 10^6$	0.15	1
17	n_{axle}	average number of axles per heavy vehicle	-	lognormal	4	0.15	1
18	δ_{ex}	dynamic amplification factor near expansion joint	-	normal	1.2	0.2	0
19	δ_{pl}	dynamic amplification factor away from expansion joint	-	normal	1	0.05	0.7
20	C_{unc}	uncertainty factor	-	lognormal	1	0.17	0.85

Figure 3.2 displays both the typical dependence structure (Figure 3.2(a)) of these variables and one sampled non-monitored location (Figure 3.2(b)). As an example,

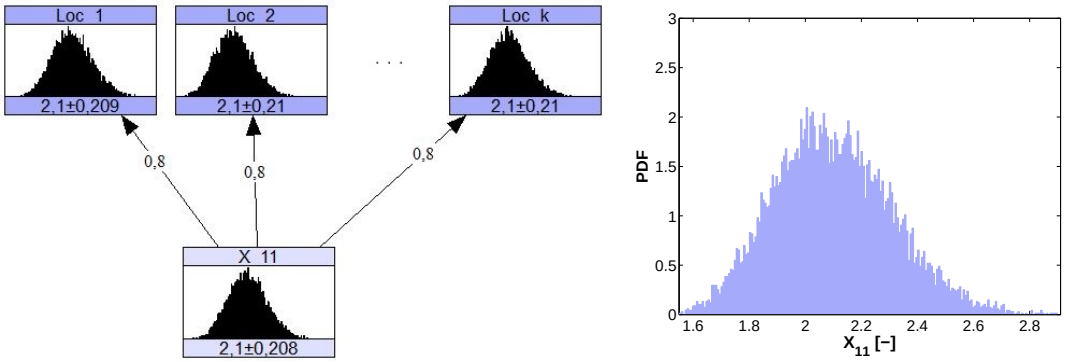

(a) Unconditional dependence structure of X_{11}

(b) Samples of one location that agree with monitoring

Figure 3.2 – Typical dependence structure for one monitored location together with k others non monitored locations (a) and one sample of one location complying with monitoring (b)

variable 11 from Table 3.1 is shown, i.e. the stress concentration factor at the crossbeam web. The histograms represent the unconditional distributions both for the monitored (parent) and for the non-monitored (children) locations elsewhere in the bridge. The mean and standard deviation are displayed below the corresponding histogram. The arcs connecting the nodes are also displayed in Figure 3.2(a) and the numbers .8 represent the rank correlation between the monitored and non-monitored locations. The probability density function (PDF) illustrated in Figure 3.2(b) represents one of the k sampled non-monitored locations and is obtained by Monte-Carlo simulations where only those samples that agree with monitoring data are selected.

Both the dependence structure and sampled non-monitored locations for all other variables listed in Table 3.1 are built in the same way as Figure 3.2. In this way, a k-dimensional distribution for each variable has been obtained, and consequently, a multidimensional distribution represented by sets of BNs similar to the one is shown in Figure 3.2(a). It is important to mention that other dependence configurations have been explored and discarded. The alternative configurations include, for example, a complete graph (all variables connected to each other, so that correlations are also considered

between all non-monitored locations for each variable), however, no significant difference in the output of the model was observed with respect to the simpler configuration displayed in Figure 3.2(a).

3.4 Sample-based conditioning for the monitored section

Let us consider a (fictitious) bridge with construction year 1991 and with a total number of 492 heavily loaded details of type described in Section 3.2 (Figure 3.1). The LEFM model describes the crack growth development of a crack in one such a detail. Monte-Carlo simulations are used to sample the variables of Table 3.1 for both the monitored and non-monitored details. The difference between these locations is the location of the detail; the monitored detail is located close to the expansion joint, experiencing a higher dynamic load (variable 18) than the non-monitored details away from the expansion joint (variable 19).

Apart from the higher dynamic load in the monitored detail of the bridge, the same model is used to predict the crack growth development in the non-monitored details. The Monte-Carlo sampling also takes into account the dependence structure imposed by the Bayesian network. In other words, each sample is drawn from a multivariate distribution giving values for all the variables of Table 3.1 and for all the modelled details of the bridge, taking into account the correlations between the different locations.

To reduce the uncertainty of the model, a crack monitoring system is installed near the detail close to the expansion joint with the objective of updating believes regarding crack growth of this detail. Let us assume that a crack is first detected in 2013, i.e. 22 years after construction of the bridge. The depth, a, of this first detected crack is estimated between 3 and 6 mm. This monitoring result is now used to interfere in the BNs. As stated, inference in NPBN may be exact under the normal copula assumption.

In the case of the present application, however, the crack size resulting from the monitoring system is output instead of input for the model, and hence, exact inference is not possible. Instead, sample-based conditioning is performed by selecting only those Monte-Carlo simulations that agree with the monitoring results. Out of a total of 10^5 Monte-Carlo simulations, 2716 Monte-Carlo samples had a crack depth, a, between 3 and 6 mm in 2013. A selection of these conditioned samples is indicated in black in Figure 3.3 for the monitored section. Figure 3.3 reveals that the extra information coming from the monitoring system significantly decreases the variability of the outcomes and thereby increases the accuracy of the crack growth predictions.

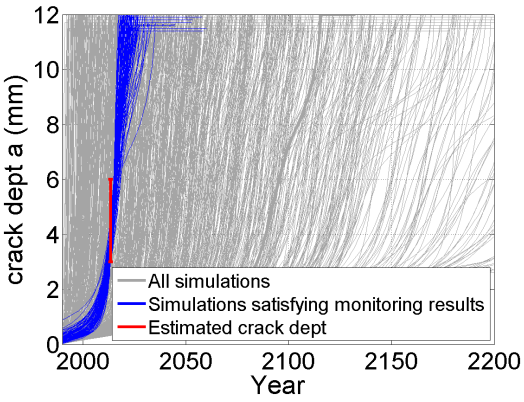

Figure 3.3 – Crack growth development for monitored detail conditioned on the monitoring results

The variables of Table 3.1 can be conditioned on the monitoring results by selecting the values for the variables of the Monte-Carlo simulations complying with the monitoring results. This enables us to obtain a first root cause analysis and find out which variables have a significant influence in the current use-case. An example of the sample-based conditioning for variable 11 is presented in Figure 3.2(b). Other variables in the monitored and non-monitored sections of the bridge are conditioned similarly.

For these specific variables, sample-based conditioning shows different amplitude in terms of sensitivity. While it was explored that for the majority of them the posterior dis-

tribution remains practically unchanged (e.g. variable 11 of Figure 3.2), a few, namely variables 5 (stress intensity ratio) and 7 (crack growth threshold at R = 0) prove to be relatively sensible with respect to conditioning. For variable 7, the conditional and unconditional distributions are displayed in Figure 3.4. Here, it is observed that the probability distribution for the difference between the unconditional distribution and the distribution obtained after conditioning on the monitoring results. Quantitatively for variable 7, this is translated by the following: for the unconditional case, its average equals 243N/mm$^{3/2}$ and its standard deviation equals 97.2N/mm$^{3/2}$, whereas for the conditional case, the average equals 189.34N/mm$^{3/2}$ and standard deviation 61.55N/mm$^{3/2}$.

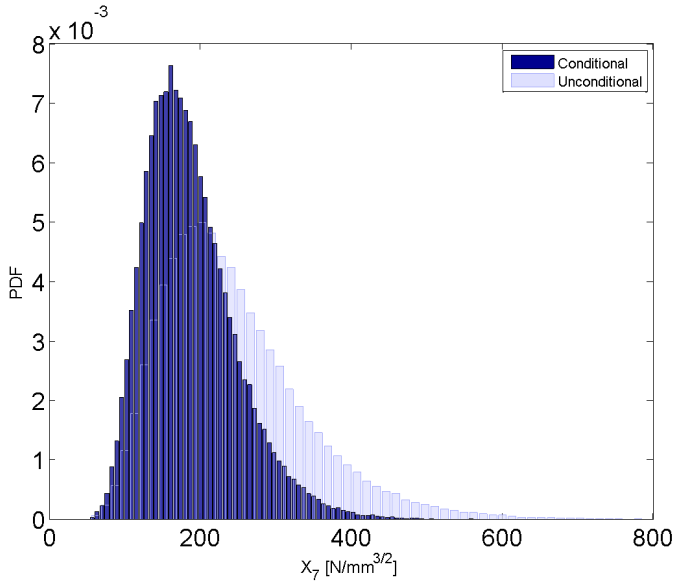

Figure 3.4 – Prior and posterior distribution of variable 7 (crack growth threshold at $R = 0$).

3.5 Conclusion

A crack growth model for cracks in welded details of the orthotropic deck structure of steel bridges has been developed. The type of crack considered can be a serious threat to bridge reliability and timely maintenance is crucial. Crack growth predictions can therefore be very useful in determining maintenance intervals for which traffic safety can be guaranteed without performing unnecessary maintenance. Monte-Carlo simulation has been used to predict the 5, 50 and 95% quantiles of the crack growth developments of cracks in a specific bridge.

In order to reduce some of the associated uncertainties, a monitoring system for detecting fatigue crack activity has been installed. Sample-based conditioning on the Monte- Carlo simulation was then used in order to obtain a new conditioned failure year distribution. This conditioned failure year distribution shows less variation (with a span of approximately 20 years) and enables us to give a more accurate crack growth prediction.

Monitoring a complete bridge is expensive and might be unnecessary because crack growth developments in different sections of the bridge are correlated. A Bayesian network was used to describe the dependence structure between the different details of the bridge and the monitored section which is, because of the presence of the expansion joint, the heaviest loaded section of the bridge. Through the same approach, a new conditioned failure year distribution is obtained not only for the monitored detail, but also for other details of the bridge. The updated, more accurate prediction of the failure year of the details considered causes a reduction of unnecessary maintenance and helps preventing unplanned closure of the bridge due to ad hoc repairs.

In summary, the following conclusions can be derived:

— Installing a monitoring system significantly decreases the uncertainty of the crack growth prediction.

— The BN makes it possible to apply the monitoring results in order to make more

accurate predictions about the non-monitored details.

— The BN also enables a root cause analysis, and indeed, it was discovered that the crack growth threshold and the stress intensity ratio are the variables with most influence in the crack growth model.

— The combination of the crack growth model and monitoring system provides therefore valuable information about the degradation of the bridge.

Future research would profit from monitoring other sections of the bridge while taking advantage of the dependence model proposed for the non-monitored section of the bridge. The Bayesian network can be used to incorporate knowledge on every detail of the bridge, each time updating the crack growth predictions. The current model constitutes a first step towards this goal.

The next steps constitute further calibration of distributions and correlations between parameters using field measurements and information from fatigue tests. In addition, further validation of the outcomes of the model by comparing it to reported cracks in actual bridges is suggested.

Chapter 4

Expert judgment in life-cycle degradation and maintenance modelling for steel bridges

Contents

This chapter presents the seminal work of the model presented in chapter 5 which addresses large-scale degradation issue. In particular, the model assumes hypothetical types of assets ought to be representative for a whole stock and, by consequence, for

which data does not exist. As mentioned in chapter 3, expert judgment is sometimes required when data is not available, missing or of poor or dubious quality. An expert judgment workshop was thus organized to partially calibrate the model using Cooke's method from which various analyses were accordingly executed.

4.1 Introduction

Ensuring a satisfactory level of safety and driving comfort are generally the primary objectives for motorway bridge managers. Throughout a bridge service life, numerous maintenance type of interventions need to be performed to keep the structure above such levels. If a newly constructed bridge is considered to be in a perfect condition and the degradation phenomenon assumes a monotonic decreasing-shape function, a bridge's condition can then be described as a function in time bouncing up and down between these two phases. A schematic illustration of these cycles is proposed in Fig. 4.1 where two different maintenance plans are implemented. One strategy typically proposes a corrective-and-rehabilitation option for maintaining the bridge (solid line) while the other one's purpose is to extend its service lifetime by coupling preventive and corrective maintenance decisions postponing a full renovation to the latest (dashed line). Substantial financial investments are initiated in order to perform these repairs and costs are typically non-linear especially when considering a full rehabilitation compared to preventive or corrective actions. These are generally considered the three principal maintenance categories available to decision makers. In Fig. 4.1 the areas separated by the dotted line labelled *Preventive maintenance level* divides preventive (area above) and corrective (below) maintenance options. When the bridge degradation function hits the solid line *Minimum acceptable level* it necessarily entails a repair. Hence a well-timed maintenance strategy aims to save money without jeopardizing safety and functionality.

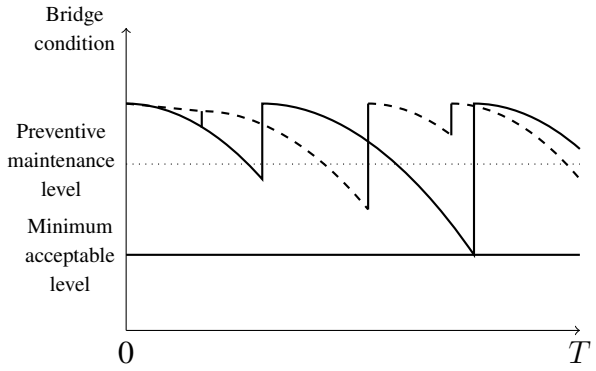

Figure 4.1 – Schematic representation of bridge degradation and maintenance cycles

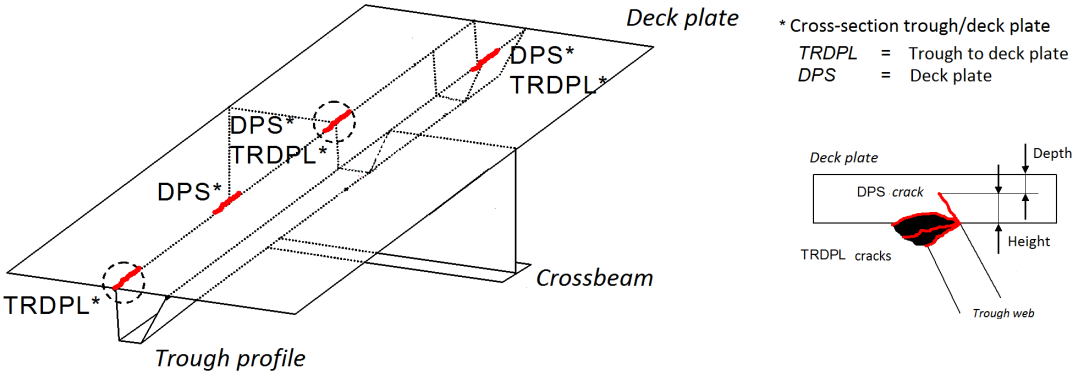

Figure 4.2 – Three-dimensional view of the bridge considered cracks' location (left); longitudinal cross-section with 'trough to deck plate' (TRDPL) crack location (right);.

Degradation modelling is of utter importance in such a context as future maintenance plans are determined based upon the shape (slope and monotonicity) of the degradation curve. Both deterministic and stochastic models have been widely surveyed to assess deterioration mechanism in the bridge reliability field Morcous and Hatami [2011]. In practice, a significant number of countries have integrated a so-called bridge management system (BMS) that opts for a discrete-time stochastic Markov process (or chain) as standard support tool to describe the degradation behaviour in time Mirzaei et al. [2014]. The goal of this system is also to bring forward knowledge at a network scale.

Indeed optimizing locally at the single bridge scale may not comply with the network-scale optimization requirements, for instance if personnel and equipment available are limited. However information per bridge does not necessarily facilitate the choice for decision makers because dealing with sometimes hundreds of elements makes it difficult to prioritize. Hence a full probabilistic degradation model is sought encompassing both the Markov framework and the network level case.

The deterioration phase is governed here by a combination of a Markov chain embedded in a Bayesian network that provides in a compact way probabilistic information to a bridge inventory. We draw much attention in the way both of these tools are quantified. In fact, the objective is to construct a network of bridges whose structure resembles that of the Dutch bridge network. In particular, motorway orthotropic steel deck bridges are of central attention. To properly quantify our model we use the classical, or Cooke's, method for structured expert judgement Cooke [1991]. It is frequently used when field data is missing, difficult to obtain or of poor quality. In this case, variables that are needed to be assessed refer to degradation inputs for moveable and fixed types of steel bridges through transition durations between consecutive deterioration states.

The remainder of the chapter is presented as follows. Section 4.2 introduces the main concepts of the the degradation model. Section 4.3 starts with the introduction of the classical method and brings forward the choice of the calibration variables constructed from existing data on fatigue cracks. Results are then presented together with a subsequent discussion. The chapter ends with section 4.4 by drawing conclusions and presenting some perspectives.

4.2 Degradation modelling for orthotropic steel bridges

As we want to represent a network of steel bridges whose purpose is to resemble as accurately as possible that of the Dutch motorway steel bridges network, two classes of

steel bridge are considered: fixed and moveable. They do not refer to specific existing bridges but describe more conventionally each type of fixed and moveable steel bridges through various characteristics (key geometry aspects, type and thickness of overlay, deck plate thickness, and so on). Fatigue cracking is generally considered as the main phenomenon driving degradation for orthotropic steel bridges. It results from fluctuating stresses caused by the crossing of heavy vehicles. Typically, loading and traffic characteristics are key quantities when studying fatigue mechanism in this context. The nature of these two variables is reasonably assumed to be random Morales-Napoles and Steenbergen [2014]. Specifically we are looking at cracks located in the deck plate and in 'trough to deck plate' parts as suggested in Fig. 4.2. Their number together with their size are crucial parameters to monitor. The condition of a bridge is then broken down into several states featuring characteristics on various degrees of severity on crack size, location and number. These states subsequently stand for the state space S of a Markov chain $\{M_t, t \geq 0\}$. The latter describes probabilistically the evolution of a bridge's condition in time. It is assumed that a bridge can either stay in the same state or move to its next worst state at the next time step given its current condition state, thus $p_{i,i}, p_{i,i+1} > 0$ where $p_{i,j} = P(M_{t+1} = j | M_t = i)$ with $i, j \in S$. One of the goals is to quantify the $p_{i,j}$'s through expert elicitation as detailed in section 4.3. To then address the network-scale maintenance problem the Markov chain $\{M_t\}$ acts as time sequenced nodes in a dynamic Bayesian network (DBN).

A Bayesian network (BN) is a directed acyclic graph (DAG) whose nodes represent random variables and whose arcs designate probabilistic dependencies between nodes. Most of the applications use discrete BNs where marginal distributions are specified for the nodes with no parents, and conditional probability tables for child nodes. A BN encodes in a compact way the probability density or mass function on a set of variables by specifying a set of conditional independence statements in the directed acyclic graphs associated with a set of conditional probability functions. More specifically, a

BN consists of a qualitative part, the DAG structure, and a quantitative part, the set of conditional probability distributions. A full characterization of a BN lies entirely in these two parts. The graphical property called *directional separation* (abbreviated as *d-separation*) asserts conditional independence statements. This attribute covers three different possible layouts for which variables can be d-separated. The attractiveness of BNs comes thus partly from the ability to model high dimensional probability distributions in a relatively intuitive visual way. In addition, knowledge, on a state of a variable for instance, can be inserted and propagated throughout the graph. This way, the marginal distributions of other nodes for which evidence is not available are updated accordingly using algorithms developed for this purpose Jordan [1999]. This mechanism is called *probabilistic inference*. Readers are referred to Pearl [1988] for a full mathematical treatment on BNs and foundations therein.

It is often sought in reliability modelling the need to describe dynamically, in the sense of time-indexed, the evolution of degradation as opposed to the static or stationary case. A special type of BN called dynamic BN (DBN) deals with domains containing recurring networks that evolve over time. This is particularly desirable when stochastic processes are involved Straub [2009]. The complete DBN model is presented in Fig. 4.3. Nodes $T_t^{(k)}$ and $L_t^{(k)}$ denote respectively traffic and loading variables where superscript (k) refers to the bridge number. At each time slice, the structure suggests that load depends on traffic and the degradation process $\{M_t\}$ depends on the load in turn. We assume that this sequential connexion is a reasonable way to first describe that explanatory variables $T_t^{(k)}$ and $L_t^{(k)}$ impact degradation in this manner. Second traffic quantities link consecutively every traffic node proper to each bridge so that the network is set up.

Various methods have been tested to quantify Markov chain's transition probabilities using field data, however since we are constructing general classes of bridges we do not possess such material at hand. Additionally, BN's conditional probabilities have to be

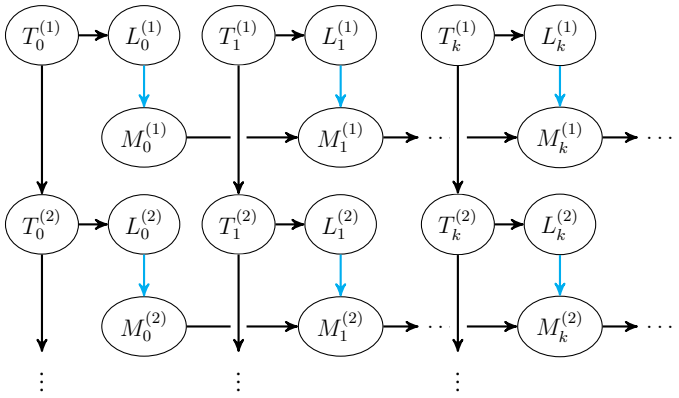

Figure 4.3 – The DBN structure for the network of bridges

assessed as well. In practice, again, collected data generally provides the sufficient quantification material to feed the BN with. In the absence of it, expert judgment is applied to fill it out. The light blue arrows in Fig 4.3 correspond to the links for which missing conditional probabilities are quantified by expert opinions. For the remainder of the conditional distributions, field measurements are used to quantify $T_t^{(k)}$ and $L_t^{(k)}$ where each can have three condition states, *High, Medium* and *Low*, and *Heavy, Normal* and *Light*, respectively.

Since the distance between degradation condition state in state space S is not necessarily constant and, in addition, assumption is made on the distance pattern (whether it is linear or not), we narrow down the number of states to four, $S = \{1, 2, 3, 4\}$. Indeed, the number of probabilities of transition to elicit for the Markov chain as well as the conditional probabilities for the DBN is a direct consequence of the size of S; the larger it gets the more tedious it is for experts. On this basis, experts answered a total of 24 questions of interest detailed in Table 4.1. We mention that items for Question 2 (V13 to V24) were not directly elicited in this way. Rather, out of a sample of size N, experts are asked to give a proportion of it.

Table 4.1 – Variable of interest elicited as part of the expert opinion workshop aiming to quantify probabilistic inputs for the degradation of motorway orthotropic steel bridges.

Question 1	Expected duration (in years) to transition between the following condition states		
• under a normal load for a moveable bridge		• under a heavy load for a moveable bridge	
V1	$1 \rightarrow 2$	V7	$1 \rightarrow 2$
V2	$2 \rightarrow 3$	V8	$2 \rightarrow 3$
V3	$3 \rightarrow 4$	V9	$3 \rightarrow 4$
a fixed bridge		a fixed bridge	
V4	$1 \rightarrow 2$	V10	$1 \rightarrow 2$
V5	$2 \rightarrow 3$	V11	$2 \rightarrow 3$
V6	$3 \rightarrow 4$	V12	$3 \rightarrow 4$

Question 2	Prob. of transitioning to next worse state conditional on load and state at previous time step for		
• a moveable bridge		• a fixed bridge	
V13	$P(M_t = 2 \mid M_{t-1} = 1, L_t = Normal)$	V19	$P(M_t = 2 \mid M_{t-1} = 1, L_t = Normal)$
V14	$P(M_t = 3 \mid M_{t-1} = 2, L_t = Normal)$	V20	$P(M_t = 3 \mid M_{t-1} = 2, L_t = Normal)$
V15	$P(M_t = 4 \mid M_{t-1} = 3, L_t = Normal)$	V21	$P(M_t = 4 \mid M_{t-1} = 3, L_t = Normal)$
V16	$P(M_t = 2 \mid M_{t-1} = 1, L_t = Heavy)$	V22	$P(M_t = 2 \mid M_{t-1} = 1, L_t = Heavy)$
V17	$P(M_t = 3 \mid M_{t-1} = 2, L_t = Heavy)$	V23	$P(M_t = 3 \mid M_{t-1} = 2, L_t = Heavy)$
V18	$P(M_t = 4 \mid M_{t-1} = 3, L_t = Heavy)$	V24	$P(M_t = 4 \mid M_{t-1} = 3, L_t = Heavy)$

4.3 Structured Expert Judgment

Eliciting data from expert's opinion using Cooke's method is a growing popular way tested and applied in numerous fields Cooke and Goossens [2008]. The goal of applying structured expert judgment fosters rational consensus as opposed to political consensus. Opinions are combined via different possible weighted averaging schemes, where the weights are based on performance measures. The classical model is extensively formalized in Cooke [1991]. The main procedure and objectives are ²duced below.

A group of experts are asked to assess their uncertainty of continuous quantities for which the realizations are known post hoc. These variables are chosen to resemble the quantities of interest, and/or to draw on the sort of expertise which is required for the assessment of the variables of interest. They are called *calibration* or *seed* variables. Experts then provide their uncertainty estimates through pre-chosen quantiles (usually

the $5^{th}, 50^{th}$ and 95^{th}). Note that variables of interest are assessed in a similar way. Concisely, *calibration* measures the degree to which experts are statistically accurate with respect to estimates provided for the seed questions. In turn, *information* measures the degree to which experts' uncertainty estimates are concentrated relative to a background measure (uniform or log-uniform generally). "Good expertise" corresponds to good calibration (typically greater than 0.05) and high information.

More precisely, assume from expert $e = 1, ..., E$, each provide their uncertainty estimates through the $5^{th}, 50^{th}$ and 95^{th} quantiles on items (or calibration variables) $i = 1, ..., N$. For each item, experts divide their belief range into four inter-quantile intervals, for which the corresponding probabilities of occurrence are: $p_1 = 0.05$ for a realization value less or equal than the 5^{th}, $p_2 = 0.45$ for a realization value in the inter-quantile range $(5^{th}, 50^{th}]$, $p_2 = 0.45$ for a realization value in the inter-quantile range $(50^{th}, 95^{th}]$ and $p_4 = 0.05$ for a realization value strictly greater than the 95^{th} percentile. Empirically we thus get for each expert $e = 1, ..., E$ the probability of the relative frequency that realizations fall in the inter-quantile bins (0.05,0.45,0.45,0.05) denoted by the vector $\mathbf{s}(e) = (s_1(e), ..., s_4(e))$. The calibration score is given by

$$C(e) = 1 - \chi^2_n(2NI(\mathbf{s}(e), \mathbf{p})) \tag{4.1}$$

where $I(\mathbf{s}(e), \mathbf{p}) = \sum_{i=1}^{4} s_i(e) \ln\left(\frac{s_i(e)}{p_i}\right)$ and χ^2_n is the Chi-square distribution with n degrees of freedom. On the other hand the information score is computed per expert as

$$I(e) = \sum_{i=1}^{N} f_{e,i} \ln\left(\frac{f_{e,i}}{g_i}\right) \tag{4.2}$$

where $f_{e,i}$ and g_i are the expert e's density and the background measure on item i respectively.

Subsequently, scores are combined to form weights. These weights are constructed to be a strictly proper scoring rule in an appropriate asymptotic sense, that is, experts

Table 4.2 – Seed variables elicited as part of the expert opinion workshop aiming to quantify probabilistic inputs for the degradation of motorway orthotropic steel bridges.

Item ID	Measurement technique	Location of crack	Year 1^{st} measurement	Crack length 1^{st} (mm)	Year 2^{nd} measurement	Crack length 2^{nd} (mm)
S1	Crack-PEC	DPS	2008	200	2009	**360**
S2	Crack-PEC	DPS	2008	250	2009	**350**
S3	Crack-PEC	DPS	2006	100	2009	**1040**
S4	Crack-PEC	DPS	2006	200	2009	**500**
S5	Crack-PEC	DPS	2006	300	2009	**350**
S6	UT	DPS	2009	30	2010	**50**
S7	UT	DPS	2009	80	2010	**90**
S8	UT	DPS	2009	100	2010	**100**
S9	UT	DPS	2009	550	2010	**590**
S10	VO	TRDPL	2008	100	2009	**250**
S11	VO	TRDPL	2008	100	2010	**250**
S12	Crack-PEC	DPS	2010	400	2011	**500**

receive their maximal expected long-run weight by stating their true belief. Important to mention that statistical accuracy dominates informativeness, in other words poor calibration cannot be compensated by high information. Calibration and information constitute the essential metrics to weight the experts in view to combine their opinions. The weighted combined uncertainty distribution is called the *decision maker* (DM) in the sense of linear pooling. The DM is thus a weighted linear pool of experts' individual weight. Consider the following weighting score for expert e

$$w_\alpha(e) = \mathbf{1}_\alpha(C(e)) \times C(e) \times I(e) \tag{4.3}$$

where $\mathbf{1}_\alpha(x) = 0$ if $x < \alpha$ and $\mathbf{1}_\alpha(x) = 1$ otherwise. This weighting score is referred to as *global* weighted score (GL) and complies with the above mentioned scoring rule criterion. Let $\text{DM}_\alpha(i)$ be the result of linear pooling for seed item i with weights

proportional to (4.3):

$$\mathrm{DM}_\alpha(i) = \sum_{e=1,\ldots,E} w_\alpha(e) f_{e,i} \Big/ \sum_{e=1,\ldots,E} w_\alpha(e) \tag{4.4}$$

Moreover, α can be chosen so as to maximize the DM combined score, we then speak of optimized DM. It must be mentioned that other weighting scores are available to the analyst. For the *equal weight* (EQ) score every expert receives the same weight, it is the usual arithmetic weighted average. Then for the *item weight* score (IT), calibration and information are computed per item as opposed to the global weight score where it is used an average information scores. Note that the optimized DM only applies to GL and IT DMs. Recall that the goal of the proposed DM is to reach rational consensus.

4.3.1 Data on fatigue cracking

To come up with the seed questions, we exploited data coming from crack measurements performed at the Tacitus bridge. The latter is a steel box girder cable stayed bridge located in the Dutch province of Gelderland. These measurements were performed using three different techniques, namely Crack Pulsed Eddy Current, further denoted as Crack-PEC, Ultrasonic Testing (UT) and visual observation (VO). A detailed explanation of each technique can be found in Jong [2007]. Next, the measurements were carried out at various spots on the bridge, essentially located at the deck plate (DPS) when preforming Crack-PEC and UT techniques and at the *trough to deck plate* (TRDPL) spot for the VO measurements (see Fig. 4.2 for details). These inspections were done between 30 to 35 years after the bridge was in service. The questions then used combinations of the above variables so that experts were asked to assess crack lengths. The seed variables are listed in Table 4.2 where each row reads as follows:
"A crack was detected by the measurement technique *to be* crack length 1^{st} *(mm) in* Year 1^{st} measurement*, what would be its length (mm) in* Year 2^{nd} measurement *using*

the same measurement technique ?"

The realization of each question refers to the last column *Crack length* 2^{nd}. The expertise calls on experts' reasoning, experience and ability to quantify own uncertainty on how a crack develops between two crack length records. This way, a total number of 12 seed variables were obtained and elicited from the expert panel. The $5^{th}, 50^{th}$ and 95^{th} percentiles of estimates of each expert for these 12 seed questions are presented in Fig. 4.4 including the DMs assessments as well as the realization (vertical red line). Together with the variables of interest, we end up having 36 items that need to be assessed.

4.3.2 Results

For the elicitation, the pool of experts consists of $E = \{1, 2, 3\}$ whose field of expertise is in the steel bridge management and reliability community, including various type of inspections and decision-making more generally.

Table 4.3 – Results of the performance assessment for 3 experts and three different decision makers (DMs) were compared: the equal weight DM, the global weight DM, and item weight DM.

Expert ID	Calibration	Relative information		Normalized weight without DM		Normalized weight with DM		
		Total	Realization	Global	Equal	Global	Equal	Item
Exp. 1	2.7E-4	2.42	0.52	0.17	1/3	7.9E-4	8.5E-4	6.3E-4
Exp. 2	9.8E-5	1.79	1.21	0.15	1/3	6.8E-4	7.3E-4	5.4E-4
Exp. 3	6E-4	0.84	0.91	0.68	1/3	3.1E-3	3.4E-3	2.5E-3
Equal weight	0.446	0.445	0.36				0.995	
Global weight	0.446	0.23	0.39			0.995		
Item weight	0.446	1.093	0.49					0.996

After answering the 12 seed questions and the 24 variables of interest, the estimates are processed in the EXCALIBUR software Cooke and Solomatine [1992]. Calibration and relative information scores together with experts' weight according to the different

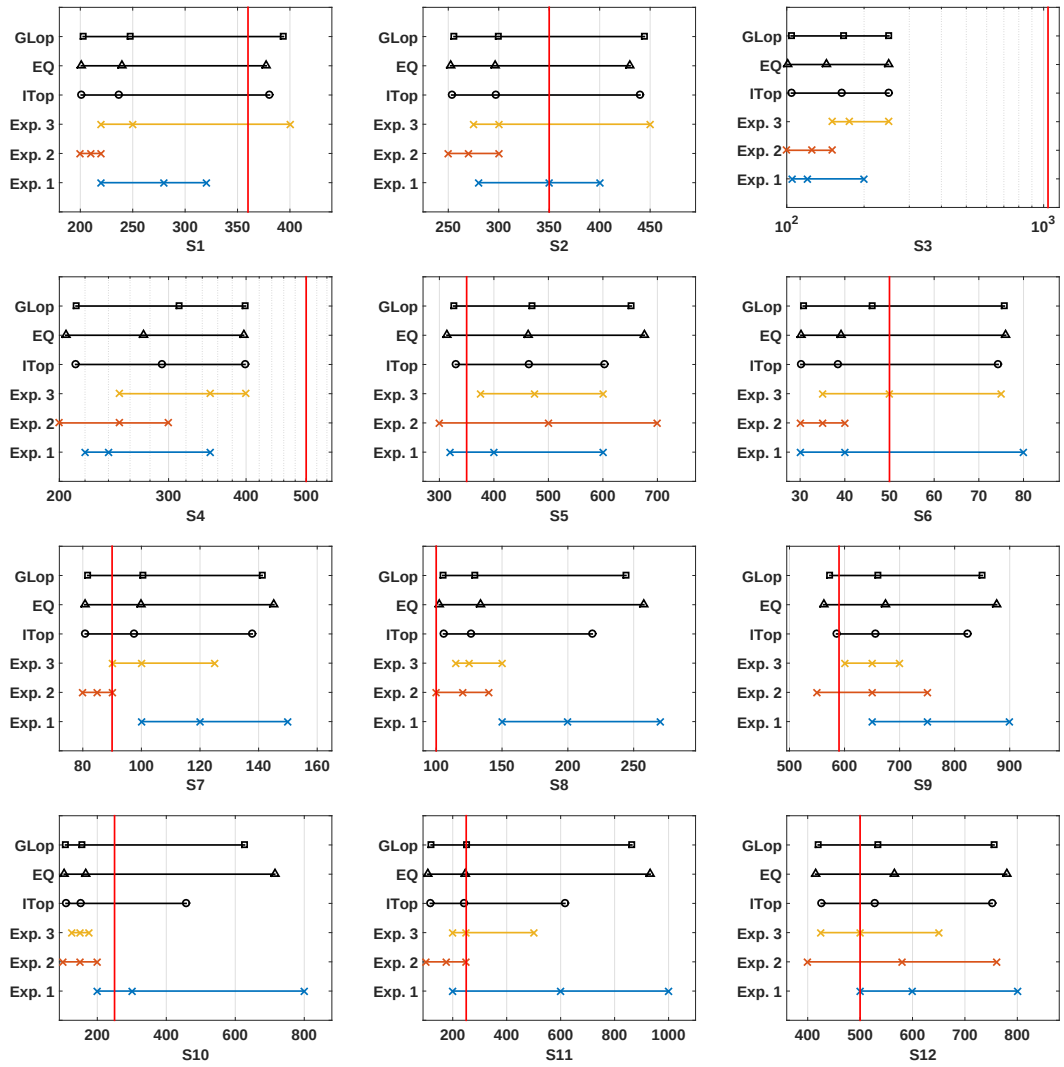

Figure 4.4 – Distributions for the 12 seed variables as represented by their 5th, 50th and 95th percentiles for 3 experts and combined distributions derived from the item weight optimized DM (Itop), the equal weight DM (EQ) and the global weight optimized DM (GLop). The vertical red line in each plot shows the true value for the seed variable.

DMs (GL, EQ and IT) are presented in Table 4.3. Among the three experts' calibration score, none of them exceeds the cut-off level (0.05) as the greatest calibration value is obtained by expert 3 (6E-4). Theoretically, a panel in which one or more experts' calibration score is greater than this threshold means that all the other experts are attributed a zero weight. Regarding the three different DMs, they all have the same score (0.446) which desirably proves to be significantly larger than individual calibrations. As for relative information, both sub-columns ('Total' and 'Realization') refer to information scores computed with respect to all the items and only the seed variables respectively. Interesting to notice that expert 1 was quite informative regarding the overall questionnaire (2.42) but much less when looking at only the seed variables (0.52). The same observation applies to expert 2 (1.79 and 1.21 respectively) with a lesser difference than for expert 1. Expert 3 shows consistently a very similar degree of information between all the variables (0.84) and the seed variables (0.91). For the DMs, information naturally decreases between 'Total' and 'Realization' while IT DM gets the highest score in both (1.093 and 0.49). Experts commented unanimously that were more comfortable in eliciting seed question compared to the variables of interest. Though it is interesting to observe that informativeness is greater when looking at the overall score than when focusing only the seed variables. In terms of weight attribution, the columns 'Normalized Weights' (with and without DM) are used in determining the DM. For 'Normalized Weights without DM' only GL and EQ DMs are computed since the weights used for the IT DM vary from item to item. Expectedly, expert 3 gets the biggest weight (0.68) for the GL DM while expert 1 (0.17) and 2 (0.15) contributions are low. When accounting for the DM, for all three schemes the DM gets almost the whole weight (0.99) whereas all three experts contribute marginally (< 0.003).

4.3.3 Robustness tests

Part of the post hoc analysis of the results includes robustness tests to estimate how stable the combined DMs outcomes are to (sets of) experts or calibration items. For instance item-wise, one calibration question is removed at a time and the DMs scores are re-computed. The similar procedure can be done expert-wise. Typically in our case, all three experts missed to capture within their $[5^{th}, 95^{th}]$ quantile range the realization for S3 and S4 (see Table 4.2) as they all underestimated it. This is illustrated in Fig. 4.4 where the chosen abscissa scale is logarithmic due the fact that the realization is located too far away on the right from each of the experts' distribution. In other words, the latter fell in their upper inter quantile range, i.e. above the 95^{th} percentile. As a comparison, the results of the performance assessments before and after performing the robustness tests are displayed in Table 4.4. By removing only S3, the DMs' calibration score improves substantially by a factor almost as large as 2 having again all three the same value (0.852). Similar to the general case, IT DM outperforms the other decision makers having the highest information score (1.021) by a factor greater than 2 compared to EQ DM (0.41) and by 5 to GL DM(0.19). We mention that robustness test on experts was performed too but did not lead to any improvement. This is likely due to the small size of the panel (3 experts).

The combined distributions for the variables of interest taking into account the outcome on the robustness test are given in Fig. 4.5. The uncertainty intervals are narrower for the item weight DM, than for the other DMs. In spite of this, rather large uncertainties are expressed especially for variable V1, V4, V6, V7 and V10 for question 1 and for V14, V15, V18, V20, V21, V24. Specifically for V1, it reads that there is 0.9 probability that under a normal solicited load a moveable bridge would take between 3.09 and 49.45 years to transition between states 1 and 2, with a median equal to 21.62 years. We also observe that items regarding transition from state 1 to 2 (V1, V4, V7 and V10) show a great uncertainty interval compared to the other transitions asked to

Table 4.4 – Results of the performance assessment for 3 experts and three different decision makers (DMs) before (left table) and after (right table) robustness tests

Expert ID	Calibration	Relative Information		Calibration	Relative Information	
		Total	Realization		Total	Realization
Exp. 1	2.7E-4	2.42	0.52	1.0E-3	2.42	0.35
Exp. 2	9.8E-5	1.79	1.21	8.3E-4	1.77	1.09
Exp. 3	6E-4	0.84	0.91	2.4E-3	0.80	0.80
Equal weight	0.446	0.445	0.36	0.825	0.410	0.244
Global weight	0.446	0.23	0.39	0.825	0.191	0.300
Item weight	0.446	1.093	0.49	0.825	1.021	0.431

experts no matter the type of bridge nor its loading configuration. Similarly, V15 and V21 possess a larger uncertainty interval and have in common to address the exact same question that only differs in the type of bridge considered.

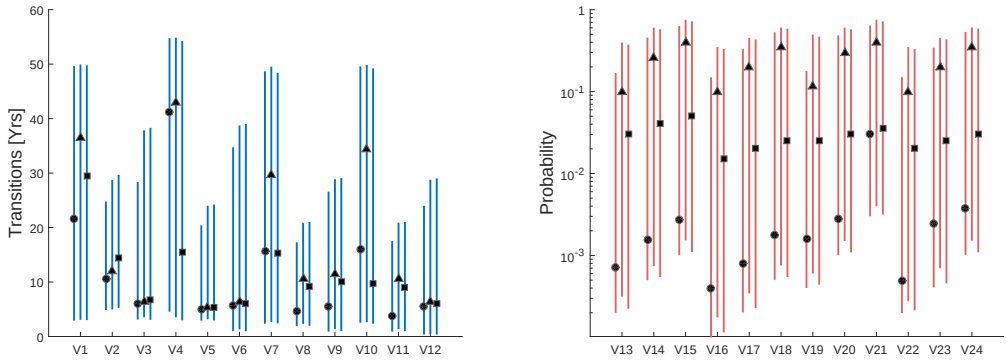

Figure 4.5 – The decision maker's distribution estimate of question 1 (left) and question 2 (right) from table 4.1, expressed by the 5^{th} and 95^{th} percentiles through the segments lower and upper tips respectively, and the 50^{th} by the related symbol for the item weight (○), the global weight (△) and the equal weight (□).

4.3.4 Discussion

Remarks coming from experts were partly related to the usage of the method as well as the degradation modelling approach in this context. Narrowing down fatigue cracking only to the deck plate and the trough-to-deck-plate locations was indeed addressed by the pool of experts.

A successful implementation of Cooke's method lies on a large extent on finding suitable seed variables. As mentioned, those should in principle resemble as much as possible variables of interest. Indeed experts' performance on the seed variables should be judged indicative for their performance on the variables of interest. In our case, the link refers to cracking condition and development for the seed variables. In terms of the variables of interest, this type of knowledge was integrated to bridge condition as quantitative thresholds separating the different states (Question 1) and further extended to conditional probabilistic assessments (Question 2). Undoubtedly, the latter turned out to be challenging as many experts argued. However, the way conditional probabilities were assessed through proportions out of a sample mitigated the risk of getting zeros or ones in the estimates.

It is worth mentioning that the expert pool number here limits to three which claims to be rather small compared to surveys using Cooke's method Cooke and Goossens [2008] where the number of experts usually ranges from 4 to 45. A larger panel of experts should likely enrich current results by bringing together additional experts' knowledge to the current combined DMs. Concretely, it could also entail having one or more experts whose calibration score is greater than the cut-off level (0.05).

The combined distributions for the variables of interest obtained under the item weight DM can readily be used to provide the input parameters for the degradation model, since this DM obtained the highest performance before and after performing robustness tests.

4.4 Conclusions & perspectives

The research presented here proposed a structured expert judgment method to quantify a degradation model composed of a combination of a Bayesian network and a Markov chain. The use of the classical method to combine opinion was elaborated to fulfill two objectives. First to explore the usefulness of applying the well-established classical method of expert judgment elicitation to the field of steel bridge reliability and maintenance. In fact, the ambition of this study is to provide insights in this particular domain via uncertainty assessments. In that sense, this can possibly highlight the limited knowledge as well as attempting to give another viewpoint that current practice has. Furthermore, although substantial material is available in various fields including in the domain of infrastructure reliability using the classical method, no records were found for this particular class of structures. Second, in either a little- or no-data scenario, the probabilistic framework provided by Cooke's method complies with first objective. Though in this regard, addressing the quantification problem demonstrates a rather great uncertainty interval proving how challenging this task still is, especially when using discrete BNs whose requirements through probabilistic assessments can be very demanding.

The exploitation of the expert judgment outcome is carried out in Chapter 5 where the complete degradation model is introduced. As a perspective, a more extended model could address the possibility of jumping by more than one state when deteriorating, hence allowing for transitions probabilities $p_{1,3}, p_{1,4},$, etc., or even considering maintenance actions entailing for instance $p_{i,j}$ with $i > j$, to be non-null. An undesirable consequence though would be a larger number of items to add to the current elicitation.

Chapter 5

A two-dimension dynamic Bayesian network for large-scale degradation modelling with an application to a bridges network

Contents

This Chapter introduces a two-dimension dynamic Bayesian network further denoted as *covariate-DBN*. Prediction and stochastic modelling of degradation is still the main concern and in line with the previous chapters. However, switching from single- to multiple-asset perspective is the main difference in this chapter. A glimpse of the main body of the model was given in chapter 4. The introduction of the "second" dimension through covariates aims to facilitate the fleet- or network-scale problem when considering a stock of assets. Recall that calibration of the model is performed via the combination of field measurements and the expert elicitation presented in chapter 4.

5.1 Introduction

Little attention has been drawn to fleet- or network-scale degradation problems. More specifically, in the ground transportation infrastructure field, a few recent papers treat bridge networks [Frangopol and Bocchini, 2012]. As one would expect, when considering systems on a much larger scale, the number of variables and uncertainties increases significantly as compared to looking only locally at individual assets. The former approach does not further facilitate cost-efficient strategies in terms of future maintenance plans at a larger scale. This has become even more desirable with the growing use of continuous monitoring that asset managers may use to either update the current knowledge of a system or formulate predictions on various key indicators. In the reliability field many different type of assets are continuously and efficiently monitored (e.g., roads, buildings, bridges, etc.), however it is often cost-prohibitive and not vital to

place a monitoring installation at each individual asset. By consequence, collected data varies in size and informativeness from asset to asset so that much effort is often given to identifying the most relevant and sensitive elements.

Particularly for deterioration modelling, uncertainty surrounding the degradation process is highly present from environmental conditions, material properties, etc. Markov-based models are now widely accepted as suitable stochastic processes especially in the bridge degradation modelling domain [Mirzaei et al., 2014]. It is common practice to exploit inspection data on various parts of an asset to model both the component-level and the overall condition through Markov processes. The main task in Markov-based models reduces almost exclusively to the assessment of the transition probabilities. Several general methodologies have been developed to using condition ratings data as well as those specific to bridges [Jiang et al., 1988, Madanat et al., 1997, Micevski et al., 2002, Reale and O'Connor, 2012, Mašović and Hajdin, 2013]. In the case where condition ratings are not available, synthetic condition states can be sampled from assumed prior distributions or degradation models. In particular, in Riveros and Arredondo [2014], condition state values are randomly generated to represent a range of condition states at each ten-year interval using Weibull distribution and a Latin hypercube simulation. However the degradation pattern comes from knowledge of the specific area of concern or is somewhat assumed a priori like in Kobayashi et al. [2010] where a hazard exponential model is used to derive the Markov transition probabilities. While almost the entire literature encourages the use of either the two methodologies mentioned, there is a scarcity of models investigating the case where very limited field data are to be used.

The objective here is to model the degradation for a network of "similarly classified" assets under very limited data. It is denoted "similarly classified" assets as those state evolutions are highly correlated. A new methodology is proposed to parametrize the transition probabilities of a Markov chain of a particular asset. In absence of the aforementioned data, or where data is very limited, it is proposed a method to quantify

the mean duration of the first passage time between degradation conditions to derive the transition probabilities through a simple linear equation. The expected durations of transitions are elicited by means of the classical Cooke's method [Cooke, 1991] for combining expert opinions. This provides a procedure that fully quantifies in a probabilistic way durations of transition. Furthermore, Cooke's method also allows us to provide a distribution-free method in order to obtain the transition probabilities. To our knowledge, this is the first application of Cooke's method to parametrize a Markov chain.

Information on underlying mechanisms (covariates) interacting with one another may be available for some of the most relevant elements. Their role is twofold: (1) they serve as factors impacting degradation upon which the Markov process depends and (2) to generate a coherent probabilistic framework to address dependency among assets in the network-scale problem. Multi-dimensional (e.g., spatial) dependencies that may exist in the network elements are conveyed through these covariates. The new methodology proposed here extends the classic framework of dynamic Bayesian networks (DBNs) by providing an approach to model the state of a large-scale set of assets in a consistent manner without necessary data for the standard parametrization approaches. The extended DBN, which is termed a *covariate-DBN*, also allows the propagation of new information from assets for which data is available into others for which data may be limited. The conditional probabilities of the DBN are also derived using the structured expert judgment (SEJ) approach described above for the Markov chain.

BNs have been extensively used in reliability and civil engineering where high-dimensional probabilistic evaluation is necessary. For discrete BNs, the quantitative burden related to both the quantification of conditional probability assessments and the inference mechanism are known to be the main limitations. Castillo et al. [2015, 2016] introduce a high-dimensional probabilistic model using BNs for safety and risk anal-

ysis in the railway domain where 7,820 variables (on separate BNs) have been used. Špačková and Straub [2012] proposed a DBN model for probabilistic assessment of tunnel construction performance including a modified version of the Frontier algorithm to perform inference. One of the advantages shown in each of the three above-cited articles is that BNs can be a powerful tool to quantify the risk of extraordinary events. It is provided a global methodology through the so-called covariate-DBN model for asset management. Computationally-wise, it is shown that the inference combinations can significantly be reduced by advantageously exploiting results regarding the sensitivity of unexpected events. It should be noted that the Ferrándiz et al. [2005] have developed an aggregated method and algorithm for classes of directed acyclic graphs thus encompassing BNs, but not solely. Their purpose is to model spatio-temporal data and can be applied to every chain graph where an aggregation process is present. However, their model is not able to capture timely updated information by the integration of covariates, and thus also not measuring the impact of this data as we do. Our proposed model is not restricted to spatio-temporal data, even though we consider this example for the bridge network.

The use of embedded covariates in a DBN suggests an analogy with Markov switching models [Frühwirth-Schnatter, 2006] as they were introduced to model this type of stochastic process by adding conditionality through either observed or unobserved variables. These types of models were extensively developed in econometrics and finance whose main purpose is to capture switching regimes of time series data. The method's purpose here is, however, not to model changes in time series switching regimes but rather covariates are introduced with the twofold above-mentioned role. Secondly, modelling degradation through observable covariates also relates to the work of Singpurwalla [1995] and Bagdonavicius and Nikulin [2001] in survival analysis. Deterioration dynamics is driven by continuous stochastic processes and covariates in both approaches, however, they do not address multi-dimensional distributions as is done

through a DBN.

In a very recent paper by Trifonova et al. [2015], they develop a DBN approach including nodes representing spatial dependency across different location for revealing trophic dynamics in fisheries ecology. However, the proposed framework is specific to the application considered through spatial nodes and thus does not offer a general methodology to address classes of problems discussed above. Moreover, it is emphasized that the spatial characteristic may not be a systematic factor to generate the network. One could also think of other links found between multiple elements, such as common material properties, relationships between physics-based phenomena, etc.

5.2 Deterioration framework

A finite discrete-time Markov stochastic process $\{D_t^{(k)}, t \geq 0\}$ is used to model the degradation for element k. Whenever possible, it will be omitted superscript (k) for every stochastic process. The goal is simply to describe the probability that each of the elements can be in a particular state at time t conditionally on the previous state and some selected covariates. *covariates* are used to represent observable random variables that influence the degradation process $\{D_t\}$. To address the network-scale issue, an extension of the classic Dynamic Bayesian network (DBN) framework is presented. For the reader's convenience, notations can be found in Table 5.1

5.2.1 Markov Chain

Discrete-time Markov processes have been extensively used in the context of risk, reliability and maintenance management for civil infrastructures [Baik et al., 2006, Edirisinghe et al., 2015]. The Markov property mainly characterizes this class of stochastic processes. Recall that this property stipulates that it is only needed to know where the process D_t stands at present time t (first order), as opposed to rely on its complete

Table 5.1 – Notations

C_a	state space for covariate $\theta_{a,t}^{(k)}$	S	time horizon
$D_t^{(k)}$	Markov chain describing deterioration for element k at time t	$\boldsymbol{\omega}_\Theta$	matrix containing information for each covariate across time and element
f_X	probability density function of random variable X	$\omega_{\theta_{j,t}^{(k)}}$	entry of matrix $\boldsymbol{\omega}_\Theta$
$f_{X\|Y}$	conditional probability density function of X given Y	$\sigma_{i,\Theta}$	sensitivity metric for deterioration state i under information Θ
k	asset or element index	$\mu_\omega^{(k)}$	time at which a single piece of information is inserted
K	number of elements/assets	$\eta_\omega^{(k)}$	time up to which consecutive pieces of information are inserted starting at $t = 0$
n	number of covariates per element k and time t	$\theta_{a,t}^{(k)}$	covariate a for element k and time t
$p_{i,j}$	Markov transition probability from state i to j	$\Theta_t^{(k)}$	set of covariates for element k and time t
pa$(\cdot)$	set of parent variables	Ω	worst deterioration state of $\{D_t^{(k)}\}$
$\mathbf{P}$	Markov transition probability matrix		

history, to predict in a probabilistic sense how the process behaves in the future. It is denoted by $\{1, ..., \Omega\}$ the set in which D_t takes values. Conventionally, it is written the one time step transition probability $p_{i,j}$ from state i to j, $i, j \in \{1, ..., \Omega\}$, the probability $P(D_{t+1} = j | D_t = i)$. In the present case it is assumed a sequential degradation, meaning that only the $p_{i,i}$, $p_{i,i+1} > 0$ with $p_{i,i} + p_{i,i+1} = 1$. As it is assumed that bridges are in the best condition when newly constructed, $P(D_0 = 1) = 1$. The stochastic process $\{D_t, t \geq 0\}$ that models degradation is usually defined by the (Chapman-Kolmogorov) equation

$$P(D_t = j | D_0 = 1) = \mathbf{P}^t(1, j) \tag{5.1}$$

where $\mathbf{P}^t$ is the transition probability matrix (TPM) to the power t and $\mathbf{P}^t(1,j)$ refers to row 1 and column j of $\mathbf{P}^t$, with $1 \leq j \leq \Omega$ and for every $t \geq 0, \sum_j P(D_t = j|D_0 = 1) = 1$. A set of $n \geq 1$ so-called covariates is further introduced which designate random variables denoted by $\Theta_t = (\theta_{1,t}, ..., \theta_{n,t})$ for each time step t, with $(\theta_{1,t}, ..., \theta_{n,t}) \in C_1 \times \cdots \times C_n$, so that the process $\{D_t\}$ is dynamically influenced by such quantities. The transition probabilities are thus given by

$$\begin{aligned} p_{i,j} = \sum_{c_1,...,c_n} & P(D_t = j|D_{t-1} = i, \theta_{1,t} = c_1, ..., \theta_{n,t} = c_n) \\ & \times P(\theta_{1,t} = c_1, ..., \theta_{n,t} = c_n) \end{aligned} \tag{5.2}$$

Covariates may either directly or indirectly impact $\{D_t\}$. An indirect covariate would impact another covariate rather than directly D_t. This is precisely the reason why Bayesian networks are used as a suitable framework to handle the dependence structure and make transparent its visualization and quantification. The latter is introduced in the section 5.2.2 where the complete definition of the new DBN framework is presented. In the bridge engineering field, information can stem from inspection data, crack measurement testing or even monitoring systems collecting inputs regarding traffic as shown in section 5.4.

In a static discrete BN, nodes stand for discrete random variables which are the most common version that have been developed in risk and reliability modelling [Weber et al., 2012]. The BN displayed in Fig. 5.1 shows how the set Θ of four time-independent covariates, namely $\Theta = (\theta_1, \theta_2, \theta_3, \theta_4)$, and state node D can be linked when not accounting for any time nor network dimensions. In this example, nodes θ_2 and θ_4 are directly connected to D. Nonetheless, a more suitable version in the present case refers to dynamic BNs accounting for time dynamics through the process $\{D_t\}$ which is presented in the next section.

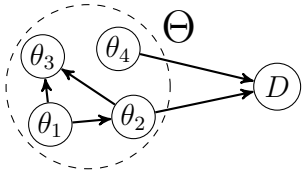

Figure 5.1 – Static covariate-BN structure

5.2.2 Covariate-DBN

While BNs are useful for modelling a dependence structure among random variables, they do not capture the evolution over time. For modelling dependencies between stochastic processes by direct or indirect covariates as described above in eq. (5.2), a convenient tool is *Dynamic Bayesian networks* (DBNs). Especially in degradation modelling, DBNs are a well suited [Straub, 2009]. Time is represented as a discrete time slices or steps which are connected by directed arcs from nodes in slice t to nodes in slice $t+1$. Note that the network structure is identical in each slice (i.e., does not change over time). A DBN that contains time-dependent conditional distributions is denoted a non-homogeneous DBN. Furthermore, the dependence between the deterioration nodes is in compliance with the Markovian property. Only time slice t is dependent on time slice $t+1$; thus, only current information is required to assess the probabilistic evolution (i.e, it is memoryless). Like the static version, the characterization of a DBN is defined by the graph structure at time t, between t and $t+1$., and the assessment of the conditional distributions for $t = 0$ and between slices t and $t+1$. Similar to the static BNs, inference may also be performed and there have been specific algorithms developed for DBN frameworks [Murphy, 2002].

It is proposed here an extension of the classic DBN formulation to a fleet- or network-level through the covariates introduced above. Network covariates make use of relationships between one or several elements composing the network. These could stand, for instance, for operating and environmental conditions, structure characteristics, material properties, etc. While data may be unavailable for the key metric of interest (i.e.,

D_t), information on various covariates may be obtained. These covariates can then be used as a means to insert information that will be propagated throughout the network due to their dependence structure with state of interest D_t. This extends the traditional DBN which contains only time dependence to additional dependence dimensions. In our model this second dimension is conveyed by the covariates.

Let $\Theta_t^{(k)} = (\theta_{1,t}^{(k)}, ..., \theta_{n,t}^{(k)})$ be the set of n covariates at time t for element k of the network. Note the addition of superscript k for the interdependent network case. A visual representation example of the extended DBN model is reported in Fig. 5.2. It contains $n = 4$ covariates per time slice t for a network composed of two elements $k = \{1, 2\}$. The set of covariates for each element $k = \{1, 2\}$, $\Theta_t^{(1)}$ and $\Theta_t^{(2)}$ is represented by the big dashed circles. It is assumed that in our proposed extended DBN the dependence structure does not change over time, but may change between elements k. Covariates may evolve independently or depend on other covariates and may or may not directly impact $\{D_t\}$. This is shown with $\theta_{4,t}^{(k)}$ being independent of $(\theta_{1,t}^{(k)}, \theta_{2,t}^{(k)}, \theta_{3,t}^{(k)})$ with $k = 1, 2$. Precisely, for element 1 the covariates $\theta_{2,t}^{(1)}$ and $\theta_{4,t}^{(1)}$ are directly impacting $\{D_t^1\}$ whereas for element 2, $\theta_{1,t}^{(2)}$ and $\theta_{4,t}^{(2)}$ are playing this role. Again, once this structure is set for each element it is kept over the whole time horizon. Although not shown in Fig 5.2, for a given element, covariates could also have a time-varying distribution. The latter has already been introduced in Straub [2009], but without incorporating a second dimension as is done. The connexions across the different elements are thus made through the set of covariates $\Theta_t^{(k)}$. It is also shown in Fig. 5.2 that $\theta_{1,t}^{(k)}$ and $\theta_{4,t}^{(k)}$ are the covariates performing the linking task. It is assumed that each element has the same set of covariates $\Theta_t^{(k)}$, although the dependence structure between covariates of different elements may vary according to the data. The DBN structure can be generalized similarly to what characterizes a classic DBN. For time epoch $0 \leq t \leq S$ and network element $1 \leq k \leq K$, there must be specified:

— the covariate dependence structure for each element k denoted by $\mathcal{G}_\Theta^{(k)} = (\mathcal{N}_\Theta^{(k)}, \mathcal{E}_\Theta^{(k)})$

with $\mathcal{N}_{\Theta}^{(k,t)} = \left\{\Theta_t^{(k)}\right\}$, $\mathcal{E}_{\Theta}^{(k)} = \left\{\left(pa\left(\theta_{i,t}^{(k)}\right); \theta_{i,t}^{(k)}\right), 1 \leq i \leq n\right\}$ and its set of conditional distribution functions $\mathcal{P}_{\Theta}^{(k)} = \left\{f_{\theta_{i,t}^{(k)}|pa\left(\theta_{i,t}^{(k)}\right)}, 1 \leq i \leq n\right\}$

— the covariate-to-element dependence structure denoted by $\mathcal{G}_{D^{\downarrow\Theta}}^{(k)} = (\mathcal{N}_{D^{\downarrow\Theta}}^{(k)}, \mathcal{E}_{D^{\downarrow\Theta}}^{(k)})$ with $\mathcal{N}_{D^{\downarrow\Theta}}^{(k)} = \left\{D_t^{(k)}\right\}$, $\mathcal{E}_{D^{\downarrow\Theta}}^{(k)} = \left\{\left(pa\left(D_t^{(k)}\right)^{\downarrow\Theta_t^{(k)}}; D_t^{(k)}\right)\right\}$ and set of conditional distribution functions $\mathcal{P}_{D^{\downarrow\Theta}}^{(k)} = \left\{f_{D_t^{(k)}|pa\left(D_t^{(k)}\right)^{\downarrow\Theta_t^{(k)}}}\right\}$ where $pa\,(X)^{\downarrow\mathbf{Y}}$ designate the set of parents for node X restricted to node set $\mathbf{Y}$.

— the element-to-element dependence structure denoted by $\mathcal{G}_{\Theta}^{(\rightarrow)} = (\mathcal{N}_{\Theta}^{(\rightarrow)}, \mathcal{E}_{\Theta}^{(\rightarrow)})$ with $\mathcal{N}_{\Theta}^{(\rightarrow)} = \left\{\Theta_t^{(k)} : 1 \leq k \leq K\right\}$, $\mathcal{E}_{\Theta}^{(\rightarrow)} = \left\{\left(pa\left(\theta_{i,t}^{(k)}\right); \theta_{i,t}^{(k)}\right) : pa(\theta_{i,t}^{(k)}) \not\subset \Theta_t^{(k)}, 1 \leq i \leq n\right\}$ and conditional probability set $\mathcal{P}_{\Theta}^{(\rightarrow,t)} = \left\{f_{\Theta_t^{(k)}|pa\left(\theta_{i,t}^{(k)}\right)} : pa\left(\theta_{i,t}^{(k)}\right) \not\subset \Theta_t^{(k)}, 1 \leq i \leq n\right\}$

The complete covariate-DBN can now be defined for time horizon S and bridges network size K as $\mathbf{B}^{K,S} = \{\mathcal{G}^{K,S}, \mathcal{P}^{K,S}\}$ where $\mathcal{G}^{K,S}, \mathcal{P}^{K,S}$ are summarized, respectively, through each of the graph and probabilistic sets introduced above.

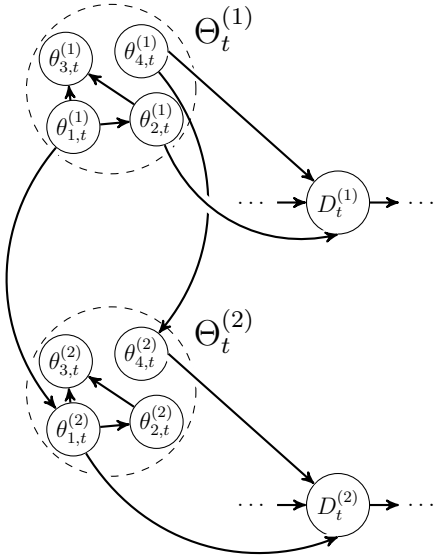

Figure 5.2 – A two-element Covariate-DBN with 4 covariates at time t

5.2.3 Network Sensitivity Analysis

It is proposed a methodology for evaluating the sensitivity of covariate information inserted into the network at different points in both time t and dimension k. This aids identifying the key elements of the network, the types of information with the greatest impact, and when and where to observe the network in order to obtain said information. Recall that the set of covariates $\Theta_t^{(k)} = (\theta_{1,t}^{(k)}, ..., \theta_{n,t}^{(k)})$ takes values in $C_1 \times \cdots \times C_n$. Let $\boldsymbol{\omega}_\Theta = \left(\omega_{\theta_{j,t}^{(k)}}\right)_{\substack{1\leq j\leq n \\ 0\leq t\leq S \\ 1\leq k\leq K}}$ be the n-by-S-by-K matrix of one possible combination where each $\omega_{\theta_{j,t}^{(k)}} \in C_j \cup NOI$, represents the possible information that can be inserted adding the "no information (NOI)" state. The unconditional case is simply the matrix $\boldsymbol{\omega}_\Theta$ with all entries being NOI. The total number of possible combinations of injecting evidence for the covariate-DBN model is given by all the permutations among the set $\{C_1, ..., C_n\}^{KS}$ given by

$$e_\Theta = ((|C_1| + 1) \times \cdots \times (|C_n| + 1))^{KS} - 1 \tag{5.3}$$

with T being the time horizon, K the total number of elements and $|C_j|$ the cardinality of each set $C_j, j = 1, ..., n$. One way to measure the value of the propagated information is to check how much it affects the posterior probability distribution. For bridge $0 \leq k \leq K$ and degradation state $i \in \{1, ..., \Omega\}$, the following sensitivity measure can therefore be computed

$$\sigma_{i,\Theta} = \frac{\left|P(D_t^{(k)} = i) - P(D_t^{(k)} = i|\boldsymbol{\omega}_\Theta)\right|}{P(D_t^{(k)} = i)} \tag{5.4}$$

From eq. (5.4) above, $\sigma_{i,\Theta} \in \mathbb{R}^+, \forall(i, \boldsymbol{\omega}_\Theta) \in \{1, ..., \Omega\} \times n \times S \times K$. Examples of the values obtained are depicted in section 5.5. This metric may provide insight on when and for what duration new information should be obtained as well as the quantity and location deployed across the network. Let $\tau = \inf\left\{t \geq 0 : \forall j, k, \omega_{\theta_{j,t}^{(k)}} \neq NOI\right\}$,

therefore

$$\sigma_{i,\Theta} \begin{cases} = 0 & \text{if } t < \tau \\ > 0 & \text{otherwise} \end{cases} \tag{5.5}$$

This means that the earliest piece of evidence being inserted only impacts the posterior probabilities of $P(D_t^{(k)} = i|\boldsymbol{\omega}_\Theta)$ for $t > \tau$.

To study how sensitive the network reacts, it is prohibitive to cover the list of all possibilities as e_Θ grows exponentially along K and S. Two different types of configurations are put forward to gain insight from a large covariate space: 1) the effect of information being inserted individually at different points in time and 2) the cumulative effect of inserting information at multiple points in time. The study is further restricted to the case where only the same type of information is entered over time.

For a fixed covariate $j \in \{1, ..., n\}$, covariate value $c \in C_j$, and element $k \in 1, ..., K$, let $\mu_\omega^{(k)} \in \{0, ..., S\}$ be the time a single piece of information $\left(\omega_{\theta_{j,t}^{(k)}}\right)_{0 \le t \le S}$ is inserted into the network. Furthermore, let $\eta_\omega^{(k)} \in \{0, ..., S\}$ be the time up to which consecutive pieces of information are inserted beginning at $t = 0$. Then the matrix $\boldsymbol{\omega}_\Theta = \left(\omega_{\theta_{j,t}^{(k)}}\right)_{\substack{0 \le t \le S \\ 1 \le k \le K}}$ can be a function of $\eta_\omega^{(k)}$ and the binomial coefficient $\binom{S}{\eta_\omega^{(k)}}$ which gives all possible orderings for a specific number of pieces of evidence. Thus we obtain

$$\frac{d\sigma_{i,\Theta}}{d\eta_\omega^{(k)}} \begin{cases} = 0 & \text{if } t \ge \tau \\ > 0 & \text{otherwise} \end{cases} \tag{5.6}$$

This shows that for a specific element k and a certain covariate $\theta_{j,t}$, regardless of the way pieces of information are incorporated, i.e. the various permutations among the set C_j, $\sigma_{i,\Theta}$ increases or is constant along $\eta_\omega^{(k)}$. This result holds for cumulative information incorporated across different elements. This results is particularly desirable in the reliability domain as it highlights the usefulness to obtain field data in a temporal cumulative manner from a specific element or several of them. Not only does it primar-

ily impact its own posterior distribution but it additionally affects the probability of the other elements. The sensitivity value (5.4) facilitates the quantitative identification of elements in the network with minor consequence on others and thus reduce the need of observation.

5.3 Parametrization through Structured Expert Judgment

The goal here is to parameterize the transition probabilities of the Markov chain D_t. The classical SEJ model developed by Cooke [1991] is used which is a performance-based weighted averaging model to aggregate individual experts' distributions into a single combined one. It is both a widely accepted [Cooke and Goossens, 2008] and appropriate method when quantitative data is missing, of dubious quality, or is insufficient for obtaining desired outcomes. The following briefly recalls what was presented in chapter 4 and further incorporates the corresponding results.

5.3.1 Cooke's model for eliciting expert opinions

The protocol of Cooke [1991] was followed which provides a clear statement of the questions to be answered, documents critical underlying assumptions, and establishes a logical structure for the elicitation interview. Experts are asked to specify their quantiles (e.g., 5th, 50th and 95th) of an uncertainty distribution regarding variables of interest and *seed variables* tailored to the problem considered. Seed variables are known quantities used to compute two measures of performance of the experts: the *calibration* and *information* scores. Loosely, calibration measures the statistical likelihood that a set of experimental results correspond, in a statistical sense, with the expert's assessments. Information measures the degree to which a distribution is concentrated. The weights are

derived from experts' calibration and information scores, as measured on seed variables. Seed variables serve a threefold purpose:

1. to quantify experts' performance as subjective probability assessors
2. to enable performance-optimized combinations of expert distributions
3. to evaluate and hopefully validate the combination of expert judgment.

5.3.2 Calibration of $p_{i,j}$

Several developments must be made in order to apply the Cooke's method to parametrize a Markov chain. Instead of explicitly eliciting $p_{i,j}$ expected transition time between consecutive states i to $i+1$ are asked. Cooke [Cooke, 1991] shows that directly estimating probabilities should be avoided as performing such a task is known to be challenging and generates greater uncertainty. Whenever possible, one can overcome this challenge by asking quantities which experts are more familiar with to derive the ones of interest. If not, relative frequencies are used as is done in this paper for *Q2*.

In order to quantify $p_{i,j}$ introduced in eq.(5.2), the expected time it takes for a bridge to transit between states i and j is given by

$$E[T_{i,j}] = 1 + \sum_{k \neq j} E[T_{k,j}]p_{i,k} \tag{5.7}$$

where $T_{i,j} = \inf\{M : D_M = j, D_{M-1} \neq j, ..., D_{m+1} \neq j | D_m = i\}$ is a strictly positive integer random variable and represents the first passage time from state i to state j, with $0 \leq m < M$. When $j = i$ one has $E[T_{i,i}] = 1/\pi_i$, where π_i is the limit distribution of the Markov chain for state i, $\lim_{t \to +\infty} P(D_t = i) = \pi_i$. Typically, as state $\{\Omega\}$ is the only absorbing state, $\pi = (\pi_1, ..., \pi_\Omega) = (0, ..., 0, 1)$ so $E[T_{i,j}] = \infty, \forall i \geq j$. In other words, we have a strictly degrading process that will eventually arrive in the failed state if no action is taken. In the very general case where **P** is complete, i.e., when

interventions improving the state of an element are allowed, the transition probability matrix is given by

$$\mathbf{P} = \begin{pmatrix} p_{1,1} & \dots & p_{1,\Omega} \\ \vdots & \ddots & \vdots \\ p_{\Omega,1} & \dots & p_{\Omega,\Omega} \end{pmatrix}$$

Moreover, matrix **E** of the expected first passage time transitions is given by

$$\mathbf{E} = \begin{pmatrix} E[T_{1,1}] & \dots & E[T_{1,\Omega}] \\ \vdots & \ddots & \vdots \\ E[T_{\Omega,1}] & \dots & E[T_{\Omega,\Omega}] \end{pmatrix}$$

From eq. (5.7), the following linear system of equations has to be solved

$$\mathbf{P}^*(\mathbf{E} - \text{diag}(\mathbf{E})) = \mathbf{E} - \mathbf{1} \tag{5.8}$$

where $*$ is the usual matrix product operator, diag(**E**) is the matrix having the values $E[T_{i,i}]$ and zeros in each of the other entries and **1** is the matrix having ones in every entry. Solving matrix equation (5.8), where the entries of matrix **P** are the unknowns, allows to indirectly quantify this matrix of interest given matrix **E** so that experts are spared from directly estimating transition probability values.

For matrix **E**, the entry (i, j) (with $i \neq j$) is non infinite if there exists $M > 0$ such that for any $m, 0 \leq m < M, P(X_M = j | X_m = i) > 0 \Leftrightarrow \mathbf{P}^{M-m}(i, j) > 0$. The latter simply translates quantitatively the fact there must exist a path starting from state i to reach state j in order to have a finite (expectation of) first passage time. Recall that $p_{i,i} + p_{i,i+1} = 1$ so only the $p_{i,i}$ or $p_{i,i+1}$ need be specified. The case of concern which features sequential degradation behaviour entails that from eq. (5.8), for each $i \in \{1, ..., \Omega\}$, we have

$$p_{i,i} = 1 - \frac{1}{E[T_{i,i+1}]} \tag{5.9}$$

so that $\Omega - 1$ expected transitions have to be elicited. Solving matrix equation (5.8), where the entries of matrix **P** are the unknowns, allows to indirectly quantify this matrix of interest given matrix **E** so that experts are spared from directly estimating transition probability values. From eq. (5.9), $E[T_{i,i+1}] \geq 1$ otherwise it yields $p_{i,i} < 0$. If an expert gives an estimate where $E[T_{i,i+1}] < 1$, one can simply rescale the time step to a smaller time unit. The time step should not exceed the minimum time for an asset to transition two states in order to maintain the sequential degradation property. A lower bound for the time step would be the minimum time necessary for the asset to transition from any given state.

Parametrizing the model amounts to calibrating the quantities $P(D_t = j|D_{t-1} = i, \theta_{1,t} = c_1, ..., \theta_{n,t} = c_n)$ (eq. (5.2)) and $E[T_{i,i+1}]$ (eq. (5.9)), as the joint distribution $P(\theta_{1,t} = c_1, ..., \theta_{n,t} = c_n)$ is assumed to be empirically obtained. The two main questions are then generated as follows

Q1 "Could you provide the $5^{th}, 50^{th}, 95^{th}$ quantiles of your uncertainty distribution about the expected years that it takes for each of the K elements considered to transit between each of the states in $\{1, ..., \Omega\}$?"

Q2 "Consider a sample of 100 000 data points each representing the following event. At time $t-1$ a certain element k was in a certain condition state $(1, ..., \Omega)$ and the covariates directly incident to the process $D_t^{(k)}$ were observed to be in each their possible states (i.e., cardinality of the state space of incident covariates). Recall that it is assumed elements can only deteriorate to their next worse state or remain in the same state at the next time step. Out of these 100 000 samples, what is the number of these assets transitioning to their next worse state at the next time step ?"

Note that **Q1** and **Q2** must be elicited for each element k, thus the number of questions to be asked is $2K$. More generally, for any number of questions q for each element k, the total number of questions becomes qK. However, the total network size may be

dramatically increased while limiting k, by considering different classes in which multiple elements belong to the same class. Thus, a very large network can be constructed without needing to elicit responses for each element if they are of the same class, hence the introduction of *similarly classified* assets. This will be detailed in the following sections of our bridge application in which hundreds of bridges may be present but only a few classes. In such a context, only questions on the classes need be elicited and not each individual bridge in the network. This further highlights the limited data framework application of this model.

The covariate-DBN methodology is summarized through the diagram displayed in Fig. 5.3. The arrows from the *SEJ (**Q2**)* node pointing to eq (5.2) is more precisely referring to member $P(D_t = j|D_{t-1} = i, \theta_{1,t} = c_1, ..., \theta_{n,t} = c_n)$ making the one-to-one correspondence link between the covariates $\Theta_t^{(1)}, ..., \Theta_t^{(K)}$ and the Markov processes $\{D_t^{(1)}\}, ..., \{D_t^{(K)}\}$. The latter are specified by the expectation of the random variable $T_{i,i+1}$ (eq. (5.9)) which is parametrize from SEJ by **Q1**. The dashed double-oriented arrow among the covariate sets refers to the possible dependence relationships between them. Note that the Fig. 5.3 only represents one slice in time, therefore the t subscript has been omitted. To represent the total time horizon, Fig. 5.3 would be repeated for all $t \in \{0, ..., S\}$.

5.4 Bridge Network Application

This section treats degradation modeling for a network of motorway steel bridges. Two different classes of motorway bridges are specifically considered with a steel (so-called *orthotropic*) bridge deck, namely moveable and fixed. On the network of motorways in the Netherlands there are approximately 100 steel bridges, divided into movable and fixed types [Jong, 2007]. These types should be quite representative of the category encompassing motorway steel bridges located in the Dutch bridge network. A key char-

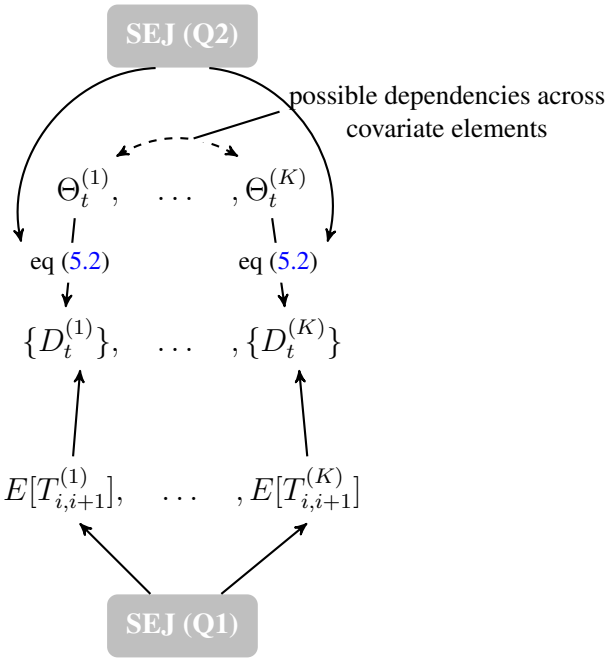

Figure 5.3 – Diagram of the covariate-DBN methodology

acteristic of a bridge is its deck plate thickness. The thickness of the bridges may vary throughout the network. It is assumed that the deck plate thickness for moveable and fixed bridge is chosen to be 12mm and 10mm, respectively. Furthermore, the thickness and type of deck plate overlay are assumed a 6 mm thick epoxy overlay and a 100 mm asphalt is applied for moveable and fixed bridges, respectively.

The underlying physical deteriorating process considered here is fatigue crack growth in the bridge deck which occurs due to repetitive loading by vehicles' axles. Fatigue is a degeneration process developing in time such that it can be detected before they grow so large that they obstruct the safe use or even integrity of the structure. It is assumed that the crack growth rate decreases for increasing deck plate thickness and surface finish. By consequence, the covariates chosen are traffic and loading as they are the main endogenous contributors in this mechanism. The covariate *traffic* is given by the number of axles per kilometre per lane averaged over the total number of lanes. In turn, loading is described as the kilo-Newtons (kN) per axle per kilometre per lane averaged over the

total number of lanes. Data coming from a monitoring system located in the Netherlands is available, presented subsequently and used to evaluate some of the conditional probability distribution sets.

5.4.1 Dependence structure

Traffic and loading covariates are denoted by $\{T_t^{(k)}\}$ and $\{L_t^{(k)}\}$, respectively. Thus, $\Theta_t^{(k)} = (T_t^{(k)}, L_t^{(k)})$, for any bridge k. The typical dynamic dependence structure for the deterioration of any bridge k is sequential, that is, $T_t^{(k)} \rightarrow L_t^{(k)} \rightarrow D_t^{(k)}$ for any time slice t. The edges connecting successively the degradation nodes $D_0^{(k)}, ..., D_S^{(k)}$ are translating the temporal aspect of the model. The traffic covariate is used serve as the dependence link connecting bridges. Traffic dynamics have been monitored and quantified in the Netherlands, for instance [Vervuurt, 2014]. The set of bridge-to-bridge edges $\mathcal{E}_\Theta^{(\rightarrow,t)}$ is specified through traffic dynamics. A possible layout is shown though in Fig. 5.4 which captures a distribution of K bridges across a highway section. In this case, for a any time step $t \geq 0$, nodes $\{T_t^{(k)}\}$ and $\{T_t^{(k+1)}\}$ are bonded in a consecutive manner. A pair of bridges are (un)conditionally independent given sets of covariates. This defines the dependence graph structure $\mathcal{G}^{K,S}$; only the conditional distribution set $\mathcal{P}^{K,S}$ has to be specified.

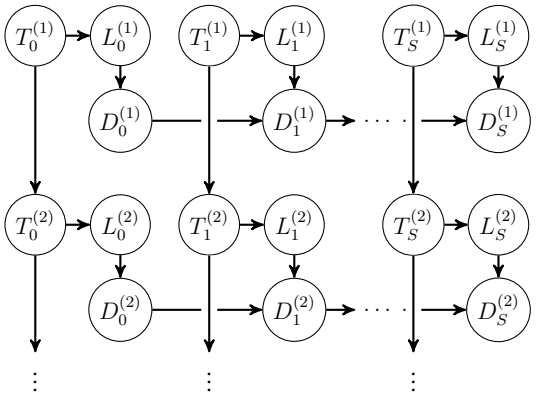

Figure 5.4 – Example layout of covariate-DBN structure $\mathbf{B}^{K,S}$

5.4.2 Traffic and load data

Data on traffic and loading is obtained from a Weigh-In-Motion (WIM) system. In Morales-Napoles and Steenbergen [2014] the same data coming from a WIM installation is input to model multidimensional distribution of axle loads together with other related quantities. A thorough investigation of dependencies between these quantities through a copula representation is presented. Here WIM data is used to derive a probability distribution on traffic density defined as the number of axles per time over a 100m bridge. In addition, the conditional probability distribution of loading given traffic density is derived assuming the covariate-DBN dependence structure presented in the previous subsection. This monitoring installation was set on a two-lane (fast and slow) motorway a few kilometres from a steel bridge in the Netherlands. As only the mechanism of fatigue for orthotropic steel bridges is investigated, loading coming from fluctuating stresses caused by vehicles is in general the most important factor and is seen as a random variable whose distribution is yearly stationary. The nature of traffic intensity influencing the loading behaviour is also stochastic [Morales-Napoles and Steenbergen, 2014]. Both distributions of loading and traffic are computed given sample distributions bootstrapped from WIM data. The data is first exploited so that kernel density estimators are computed for fast and slow lanes in a congested traffic configuration. Axles' positions and weights are further obtained by queuing all the vehicles the system recorded over a month. More precisely, a so-called 'train' of vehicles is created. By bootstrapping over a number of fixed vehicles among the total amount of recorded vehicles, a random distribution of vehicles is derived. The generated train provides each fast and slow lane vehicles' separation, axle position and weight, and the number of vehicles per lane. The loading moments are then computed using a finite element method whose discretization step is that of the triangular Bartlett window over the span of the bridge. In this case, the highest loading moment for a vehicle crossing the bridge occurs when it is located halfway through it.

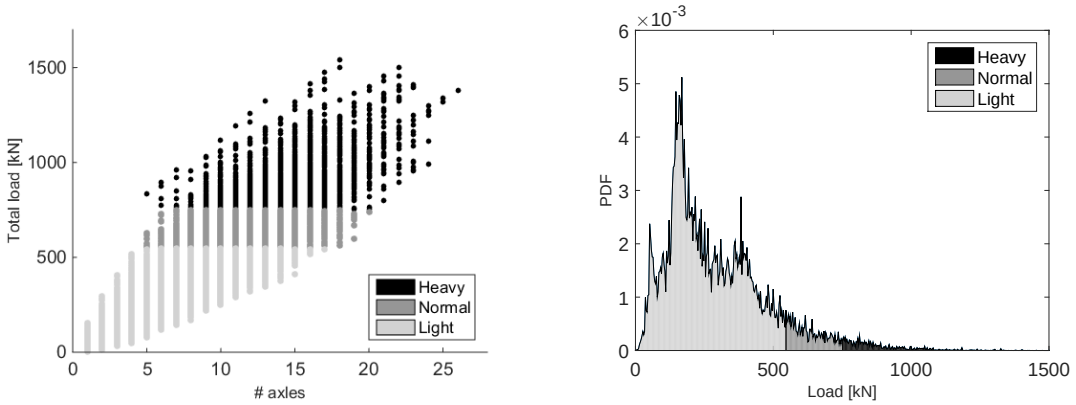

(a) Scatter plot of the number of axles against loading conditionally on $\{\#axles > 0\}$

(b) Probability distribution of the total load conditionally on $\{\#axles > 0\}$

Figure 5.5 – Load distribution conditionally on $\{\#axles > 0\}$

The scatter plot displaying the number of axles against loading and the marginal probability distribution function (PDF) of loading are illustrated in Fig. 5.5(a) and 5.5(b), respectively. Both distributions are plotted conditionally on the number of axles being strictly positive. Equivalently, this means there is always loading on the bridge. Many of the recordings refer to a no-loading scenario, namely $P(L_t^{(k)} = 0) = P(\#axles = 0) = 0.432$, for any k. In this configuration, the load variable is discretized by setting the following thresholds which are often used in probabilistic bridge design. A *Heavy* loaded situation is seen as all the recorded loads lying above the 97^{th} quantile bin of the load PDF conditioned on their being at least one axle. Numerically, this value represents 751.189 kN which can also be written as $P(L_t^{(k)} \leq 751.189\ kN | \#Axles > 0) = 0.97$. In Fig. 5.5(b) the *Heavy* load is represented by the shaded area below the PDF curve. Similarly, for *Normal* and *Light* loading states, values lying in between the 90^{th} and the 97^{th} quantile bins and below the 90^{th} quantile bin are chosen respectively. These are shown in Fig 5.5(a) through the dark and light grey scatter points for the Normal and Light loading cases. This way the probability distribution $f_{L_t^{(k)}|pa\left(L_t^{(k)}\right)}$ is fully determined. For every time slice t, the quantification of the conditional probability

distribution of traffic nodes $\left\{ f_{T_t^{(k)}|pa\left(T_t^{(k)}\right)} \right\}_{1\leq k\leq K}$ was in turn obtained from the National Data Warehouse for Traffic Information (NDW) measurements performed in 2013 from several Dutch highways [Vervuurt, 2014] and broken down into a 3-state space $\{High, Medium, Low\}$. It is further denoted by $\mathcal{L} = \{Heavy, Normal, Light\}$ and $\mathcal{T} = \{High, Medium, Low\}$ the sets that processes $L_t^{(k)}$ and $T_t^{(k)}$ take, respectively, value in.

5.4.3 Elicitation results

The complete SEJ experiment is presented in Chapter 4. The elicitation was carried out with three experts on steel bridge reliability and management. Particularly, the seed questions refer to historical data on crack length collected between 2006 and 2011 at a highway steel bridge in the Netherlands. A typical seed question asked to the experts is the following:

"An 80 mm crack was detected located in the deck plate 33 years after construction, what would be its length the following year?"

By varying the time gap between two crack measurements, the age of the bridge at the time of the first measurement, the crack measurement technique as well as the crack location, a total number of 12 seed questions were asked. The remainder of the questionnaire comprises the questions of interest **Q1** and **Q2** which were introduced in section 5.3.2. They must be asked for each element k (moveable of fixed bridge), loading configuration $\mathcal{L} = \{Heavy, Normal, Light\}$ and type of transition considered ($1 \rightarrow 2, 2 \rightarrow 3$ and $3 \rightarrow 4$), making a total of 24 items of interest. **Q1** allows fully calibrating the transition probability matrix as shown in eq. (5.9) while the second question provides the missing conditional probabilities of node D_t given D_{t-1} and L_t as the covariate-DBN structure introduced in section 5.4.2 suggests. From notation introduced

in section 5.2, we have $\left\{ f_{D_t^{(k)}|pa\left(D_t^{(k)}\right)} \right\}_{1\leq k\leq K}$. From the law of total probability, we get

$$f_{D_t^{(k)}}(x) = \begin{cases} \sum\limits_{l\in\mathcal{L}} P\left(D_t^{(k)} = x | L_t^{(k)} = l\right) P(L_t^{(k)} = l) & t = 0 \\ \sum\limits_{l\in\mathcal{L}} \sum\limits_{y\in\{x,x-1\}} P\left(D_t^{(k)} = x | D_{t-1}^{(k)} = y, L_t^{(k)} = l\right) & \\ \qquad \times P(L_t^{(k)} = l) P(D_{t-1}^{(k)} = y) & t > 0 \end{cases} \tag{5.10}$$

In particular, from eq. (5.10) the terms $P\left(D_t^{(k)} = x | L_t^{(k)} = l\right)$ (for $t = 0$) and $P\left(D_t^{(k)} = x | D_{t-1}^{(k)} = x-1, L_t^{(k)} = l\right)$ are the ones elicited from **Q2**. As a consequence, the burden for experts (i.e, the number of queries) increases in the number of states Ω for the Markov processes $D_t^{(k)}$, the number of edges that are incident to the Markov chain $\left(\mathcal{E}_{D^{\downarrow\Theta}}^{(k)}\right)$, and the number of states of the incident covariates.

Using the results in Table 5.2 by taking the median values (50^{th} percentile) together with eq. (5.9), the corresponding transition probability matrices for each class of bridge can be derived. Moreover, from eq. (5.7) and eq. (5.9), the complete matrix of expected duration of transition can be retrieved as well

$$\mathbf{P_M} = \begin{pmatrix} 0.954 & 0.046 & 0 & 0 \\ 0 & 0.905 & 0.095 & 0 \\ 0 & 0 & 0.834 & 0.166 \\ 0 & 0 & 0 & 1 \end{pmatrix}, \mathbf{P_F} = \begin{pmatrix} 0.976 & 0.024 & 0 & 0 \\ 0 & 0.797 & 0.203 & 0 \\ 0 & 0 & 0.824 & 0.176 \\ 0 & 0 & 0 & 1 \end{pmatrix}$$

$$\mathbf{E_M} = \begin{pmatrix} \infty & 21.62 & 32.14 & 38.16 \\ \infty & \infty & 10.52 & 16.54 \\ \infty & \infty & \infty & 6.02 \\ \infty & \infty & \infty & 1 \end{pmatrix}, \mathbf{E_F} = \begin{pmatrix} \infty & 41.14 & 46.08 & 51.77 \\ \infty & \infty & 4.94 & 10.63 \\ \infty & \infty & \infty & 5.69 \\ \infty & \infty & \infty & 1 \end{pmatrix}$$

where subscripts **M** and **F** denote the moveable and fixed classes, respectively. Back-

Table 5.2 – Assessments obtained from the performance based combination scheme (IT) for expected transitions (Yrs) between sequential degradation conditions defined in Table 5.3 after removing one seed question

Bridge type	Transition	5^{th}	50^{th}	95^{th}
Moveable	$1 \rightarrow 2$	3.09	21.62	49.45
	$2 \rightarrow 3$	5.04	10.52	24.59
	$3 \rightarrow 4$	3.30	6.02	28.18
Fixed	$1 \rightarrow 2$	4.73	41.14	54.60
	$2 \rightarrow 3$	3.81	4.94	20.25
	$3 \rightarrow 4$	1.15	5.69	34.56

ward reasoning also applies, that is, conditioning on one or more states of the covariates, the conditional transition probability matrix can be computed as well as the conditional expectation matrix using eq. (5.7). Upon this basis, the annual probability distribution of process D_t to reach the worst state, $P(D_t = 4|D_0 = 1)$ (eq. (5.10)), using the IT DM combined distribution are displayed in Fig. 5.6 for both moveable and fixed bridge categories. For each distribution the median (50^{th} quantile) is presented. The differences in sensitiveness through inserted information highlighted by the posterior distributions are quite sharp. Unlike the case featuring a *Normal* load, observe that distributions conditioned on a heavy load do not differ much between the two classes of bridge considered.

5.5 Numerical experiment

Various experiments are presented to show the sensitivity of the posterior degradation distribution to inserting various types of information at different points in time. As an illustrative example, a subset network of bridges is constructed using the new covariate-DBN model introduced in section 5.2.2. This network is illustrated in Fig 5.9.

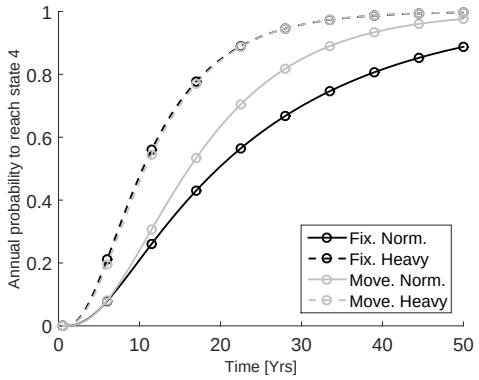

Figure 5.6 – Performance based combination of the median estimate for annual probability distribution to reach worst state (see Table 5.3) for both *Moveable* and *Fixed* bridges classes.

The quantification methods used for the conditional probability sets are those introduced in sections 5.4.2 and 5.4.3. The network is comprised of four bridges, three moveable and one fixed, whose layout is similar to that of Fig. 5.4 having the same set of covariates $\Theta_t^{(k)} = \{T_t^{(k)}, L_t^{(k)}\}$ standing for traffic density and loading. The example relates to bridges located at the intersection highways A2 and A15 in the Netherlands. A15 has one of the most dense yearly traffic while A2 is more average [Vervuurt, 2014]. Such a configuration is supposed to be representative for many real-world cases. For the example, bridges 1 (fixed) and 2 belong to A15 and bridges 3 and 4 to A2.

The PPTC algoritm (*probability propagation in trees of clusters*) for inference first developed by Lauritzen and Spiegelhalter [1988] is used in our study. More specifically, the PPTC extended by Huang and Darwiche [1996] as a more efficient approach for dynamic BNs is implemented through the Bayesian network framework *Smile* application programming interface (API). It is shown how much the network beliefs are modified when information is obtained from various covariates and elements at different points in time. As previously discussed, this can lead to prohibitive number of combinations. Scenarios leading to changing traffic conditions are numerous as well as their loading characteristics. Examples affecting traffic conditions include maintenance for

one or more bridges in the surrounding network area, traffic accidents or environmental disasters.

Consider a single 4-state condition space for both bridge categories (fixed and moveable) whose conditions are defined in Table 5.3.

A first example of inference is illustrated in Fig. 5.7 where the (conditional) CDF of the condition states for Bridges 1 and 3 are plotted at each time step for a time horizon $S = 50$ years. Left figures (Fig. 5.7(a)) stand for the unconditional (NOI) case while right figures (Fig. 5.7(b)) show updated distributions conditionally on consecutively inserting evidence of "high traffic" between year 5 and year 10 for Bridge 1. Observations that can be drawn are:

— While Bridge 1 is the only one of fixed type, its degradation curve shows very little difference compared to Bridge 3. Moreover, they also belong to motorways having different traffic characteristics

— In the right-hand column, the probability area for state 4 has increased for both bridges with respect to the no information case. This demonstrates that the distribution of Bridge 3 is slightly sensitive to information obtained from Bridge 1.

In general, inserting information that deviates more significantly from the expected

Table 5.3 – Bridge condition states

State	Definition
1 - Excellent	Almost no damage/cracks are present. A new bridge is assumed to start from this state.
2 - Fair	At least one crack in the deck plate that can be detected ultrasonically [30mm, 100mm]
3 - Mediocre	Multiple cracks are present [30mm, 500mm]; at least one crack requires repair
4 - Poor	Multiple significant fatigue cracks with at least one >500mm in the deck plate that needs urgent repair; this condition does not mean a collapse but a threat to safety and/or functionality.

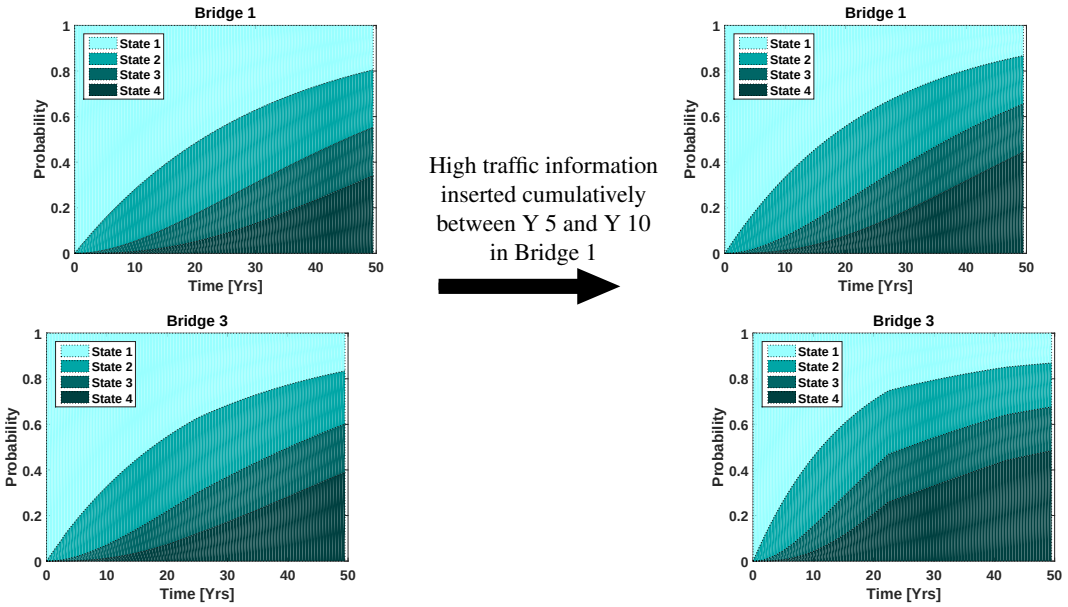

(a) *NOI* case

(b) Distribution conditional on High Traffic Information inserted between *Y5* and *Y10*

Figure 5.7 – Impact of High Traffic Information on the Network

should have a greater impact on the sensitivity. The propogation of information is mainly governed by the conditional probability distributions across traffic nodes obtained from Vervuurt [2014]. For instance, the conditional distribution $T_t^{(3)}|T_t^{(2)}$ is given in Table 5.4. The same tests were carried out using *Low* and *Medium* states individually in the same context and updated distributions showed minor modification. Similar observations were also drawn with respect to Bridges 2 and 4.

Fig. 5.7 showed the cumulative effects of inserting hight traffic information into

Table 5.4 – Conditional probability distribution of traffic process $T_t^{(3)}$ given $T_t^{(2)}$

$T_t^{(3)}\|T_t^{(2)}$	Low	Medium	High
Low	0.934	0.0448	0.0385
Medium	0.0492	0.879	0.0651
High	0.0168	0.0762	0.8964

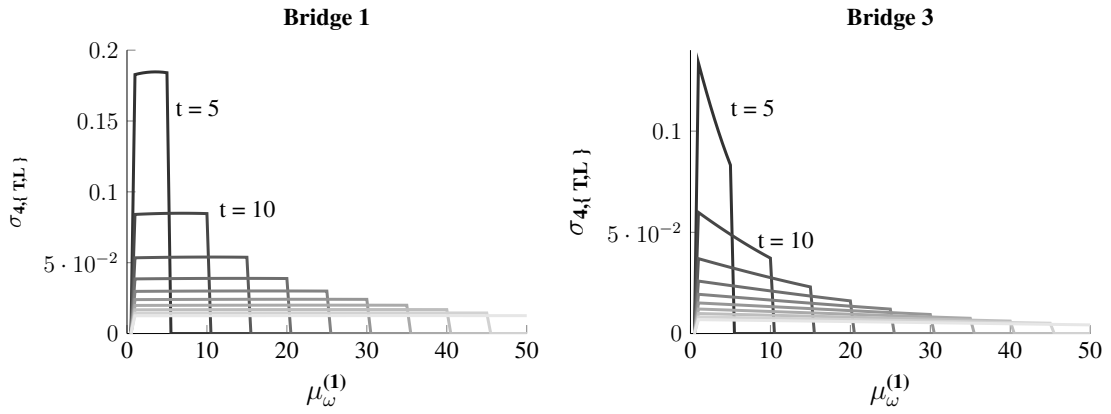

Figure 5.8 – Sensitivity curves for $\sigma_{4,\Theta}$ plotted against $m_\omega^{(1)}$ where the colour gradient from dark to light grey for each curve indicates fixed time epochs for each plot spaced by 5 years for bridge 1 (left) and bridge 3 (right).

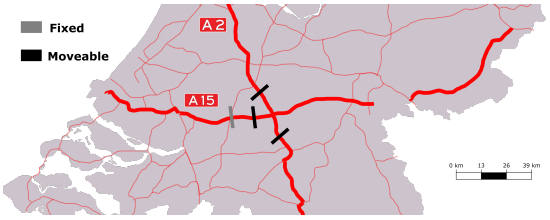

Figure 5.9 – Map of a fictitious bridge network in the Netherlands at the intersection of highways A15 and A2

the network. The effect of inserting high traffic information individually as shown in Fig 5.8 are examined. The horizontal axis denotes ($\mu_\omega^{(k)}$) the vertical axis the sensitivity measure $\sigma_{i,\Theta}$ computed as defined in eq. (5.4) for state $i = 4$. Each plot represents a fixed time slice $t \in \{5, 10, ..., S = 50\}$, the boldest curve represents $t = 5$ and lightest curve refers to $t = 50$. Thus [MV], the "$t = 5$" curve represents the sensitivity at $t = 5$ of inserting hight traffic information individually over the time horizon. Notice that once information has been inserted posteriorly to the fixed time epoch ($\mu_\omega^{(k)} > t$), the sensitivity drops to zero as previously detailed in eq (5.5). The sensitiveness dramatically decreases both as information is inserted later in time and evaluated later in time. Thus, the figure shows that it is most relevant to insert information as early

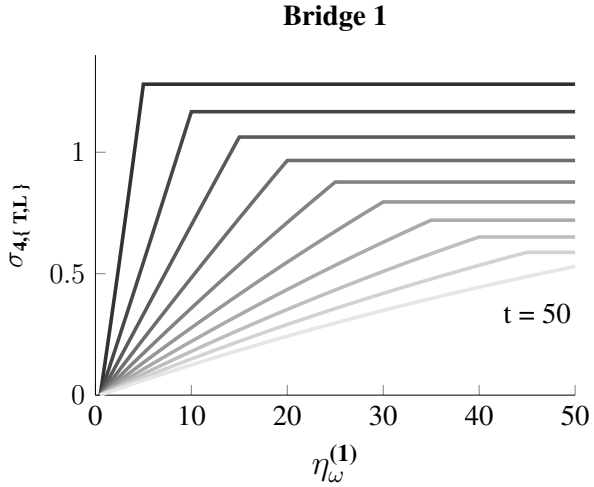

Figure 5.10 – Sensitivity curves for $\sigma_{4,\Theta}$ (left) where the colour gradient from dark to light grey for each curve indicates fixed time epochs for each plot spaced by 5 years. The type of information inserted is state *High* for node $T_t^{(1)}$

as possible and the return on information dramatically decreases over time. The same comments can be made for Bridge 3 and more generally shows a lesser amplitude for the $\sigma_{4,\Theta}$ curves. For example, $\mu_\omega^{(k)}$ peaks at $\sim 18\%$ for Bridge 1, while the maximum does not reach 14% for Bridge 3. This reduced sensitivity is to be expected as it has a downstream impact from where the information was directly obtained Bridge 1. Similar tests were performed for the remainder of the network, namely Bridges 2 and 4, which showed similar behavior.

Likewise, analyses on $\eta_\omega^{(k)}$ were performed as defined in section 5.2.3 for cumulative information. Sensitivity curves for $\eta_\omega^{(k)}$ are displayed Fig. 5.10. The various grey gradient curves read in similar fashion to those of the plots displayed in Fig 5.8. Compared to the single insertion case (Fig. 5.7), the sensitivity increases dramatically for every fixed time epoch. This is evidenced by comparing the 't = 5' curves; the sensitivity for Fig. 5.10 peaks above 120% whereas Fig. 5.7 (Bridge 1) does not pass 20%. Most importantly, the figure demonstrates that more information is always better and information loses its value over time. The latter can be explained by the distribution of

each state being bounded asymptotically by some upper and lower conditional distributions as shown in Fig. 5.6. In the case of most or least expected information being inserted consecutively from $t = 0$ throughout the network, the degradation distribution will correspond to respective bounding distribution. In this numerical experiment, the upper bound corresponds to the least expected information (i.e., high traffic/heavy loading) being inserted. Although, not demonstrated from the experiment, we believe that regardless of the manner information is inserted (i.e., consecutive or not), more information will always have a greater impact on sensitivity.

5.6 Conclusion

An extension to the classic dynamic Bayesian network framework which is termed the covariate-DBN is proposed. a second dimension for K elements is added as well as method for indirectly linking them through a set of covariates. It is further proposed a Markov chain as the underlying stochastic process for the covariate-DBN. In the case where limited data is available, a formal mathematical framework is developed making use of Cooke's method for structured expert judgement to parametrize a Markov chain and the covariate relationships between elements in the covariate-DBN. Some metrics are also presented for evaluating the sensitivity of information inserted into the covariate-DBN.

The proposal is then applied to a real-world bridge network application based on steel bridges in the Netherlands. It is shown how traffic and load information may serve as covariates to link bridge elements in the covariate-DBN. An actual expert judgment elicitation was carried out to parametrize the model using the prescribed methods. Numerical experiments show that information is most valuable as early as possible, and the value of information decreases over time.

While the model is applied to a specific bridge network scenario, different sets of

covariates could be envisioned in the same framework. Furthermore, we believe the model could be expanded to other bridge types and civil infrastructure. Applications are not only limited to degradation modelling but could include other fields and contexts such as financial asset modelling and epidemiology.

In sections 5.2.3 and 5.5, it is shown how one could reduce the computational intractability referring to running through all the possible combinations of inference. In particular, from figures 5.8 and 5.10 it is observed that :

— cumulative inserted pieces of information dominate over individual piece of information; in other words, any inference combination having a lower number of inserted pieces of information than its cumulative counterpart will show a less sensitive change in the posterior distribution. Practically speaking, continuous monitoring should prevail as opposed to condition-based (by also taking into account cost constraints)

— the sensitiveness of the inserted information decreases in time so that pieces of evidence inserted at early epochs should be preferred over later ones. This means that if significant and unexpected event are observed (represented by the type of inserted information), the sensitivity metric is also able to capture those.

Thus, by advantageously combining the two above observations, one could selectively opts for the most sensitive combinations of inference. This further results in substantially decreasing the inference choices.

As for any Markov-based model, our approach can be validated through classic statistics test, e.g. Fisher's contingency table for verifying Markovian order if data is available. However, one of the main purposes here is in particular to represent a large-scale network with the simplifying assumption that assets are grouped into similarly classified types. By consequence, one can mainly quantify those categories in a general and subjective fashion, hence the need of experts. The classical BN validation methods Cowell et al. [1999] may also be applied to our model.

For discrete BNs the main limitation of the proposed methodology refers to dimensionality. Our model further increases this complexity through the added k dimension. Other classes of BNs dealing with continuous distributions could facilitate the parametrization procedure. For example, a dynamic non-parametric class recently developed [Hanea et al., 2015] could be a useful tool to overcome this. An extension to influence diagrams would provide a decision making framework for the underlying covariate-DBN to facilitate managers applying model forecasts.

Chapter 6

Representing k-th order Markov processes as a dynamic non-parametric Bayesian network

Contents

6.1 Introduction

Stochastic processes have been extensively used to model numerous types of applications from stock prices in finance to systems degradation in engineering, or epidemi-

ological patterns in biology, to only name a few. Their popularity mainly comes from their ability to capture certain observed patterns to then give predictions. In many areas, problems can be impacted by a great number of variables thus requiring models of high-dimension random systems. By consequence, this can become a very complex task in constructing models where dependence is involved and must be further evaluated.

In multivariate statistics or multivariate analysis, recent attractive approaches refer to copula-based graphical models. A copula captures the dependence between multiple random variables. Their attractiveness is largely due to the flexibility that copula models provide, whereby the marginal distributions can be modelled arbitrarily, and any dependence captured by the copula. Copula have been extensively developed over the years; see Joe [2014] for a recent overview. For data-driven time series modelling, there can be a wide variety of copulae from which to choose and only a few are readily applicable to high-dimensional problems. Copula built from elliptical distributions, such as the Gaussian or the t-copula are most popular in this case. However, these can prove restrictive [Kurowicka and Cooke, 2006], and in the recent graphical models literature, alternative approaches have been proposed that construct series of bivariate copulae as opposed to a one or more large multivariate copula(e).

The merging of stochastic process and statistical copula approaches, to the best of our knowledge, have not been examined in the literature. The main reason lies in the purpose of each. The former assumes a priori an evolution governed through the collection of time-based probabilistic distributions. On the other hand, the latter uses observations of data to describe the dependence of a certain events involving various variables. Nevertheless, both exhibit dependence characteristics, and both have proven efficient in domains where the ability to model high-dimensional problems is required. Our objective is thus to advantageously combine the two frameworks in order to provide a Markov process representation as a dynamic copula-based graph. Among these advantages the parametrization of the model would be drastically diminished as only the stochastic

process parameters would be needed. Moreover, conditioning may be analytically performed upon the nature of the conditional densities. Conditioning for Markov processes can sometimes be difficult, especially in cases where the conditioning set cannot be broken down in order to make use of conditional independencies. Furthermore, the need to recalibrate the whole process can be tedious whenever continuous information is available. The pair-copula construction approach is able to directly generate the conditional pair-copula and marginal densities appear straightforward integral form. The conditional expectation of any time epoch can be thus be obtained using this formulation in a more clean way without requiring a complete recalculation of the parameters at each update. The ability to dynamically recognize non-stationary characteristics through the pair-copula representation is also a benefit that our combined approach provides.

Most of the research on copulae has been devoted to spatial dependence due to great interest in practice for new spatial dependence models [Kurowicka and Joe, 2011], but the analysis of temporal dependence is also possible by the copula approach. In order to account for the time component inherent in the definition of stochastic processes, so-called *time-copula* have been developed. The first paper dealing exclusively with copulae and stochastic processes was presented by Darsow et al. [1992] who established the connection between copulae and Markov processes by providing a copula representation for the Chapman-Kolmorgorov equation. Këllezi et al. [2003] derive some results on the time-copula of time-changed Brownian motions and discuss the time-copula of a Lévy process, showing how the dependency evolution of a Lévy process can be modelled with a copula.

Bedford and Cooke [2002] organize the different decompositions of multivariate distributions in a systematic way. They label the resulting pairwise copulae *vines*, while Aas et al. [2009] label the component bivariate copulae *pair-copula*. Henceforth in this chapter, we will refer to them as pair-copula. When considering a d-variate vine copula model, this requires the specification of $\binom{d}{2} = d(d-1)/2$ pair-copula, and

the marginal densities evaluated at each time point. Nevertheless, this number could be reduced upon the nature of the data in which conditional independences may be found. In this case, the corresponding pair-copula are set to be independence copulae, i.e. $C(u_1, u_2) = u_1 u_2$. Instead of leaving the detection of conditional independences to chance, one may, however, consider modelling these independences a priori to obtain more efficient models. Unfortunately, the construction of vine copula models satisfying pre-specified conditional independence restrictions is a hard problem in general. A class of models suited for this task are so-called non-parametric Bayesian networks (NPBN) as they are directed graphs to capture dependence as opposed to the undirected vine framework. NPBN are comprised of pair-copula and rank correlations and will be formally defined in the next section.

Among these relative recent developments in the copula-based graph field, models accounting for time dynamic systems generated in a systematic way are lacking. For example, a data-driven dynamic NPBN was developed by Morales-Nápoles and Steenbergen [2015] to model traffic behaviour through vehicle loads. The dependence metrics which are essentially given by conditional time-copula and conditional rank correlations turn out to be time-varying through data parametrization. Overall, research in multivariate dependence modelling using copulae is focused mostly on the case of time-homogeneous [Brechmann and Czado, 2014] dependence structures. However, promising approaches for allowing time variation in dependence have been put forth [Manner and Reznikova, 2012]. The dependence among variables can be rendered time-varying by allowing either the dependence parameter or the copula function to vary over time. However, those dynamic dependence metrics have never been combined thus far within probabilistic graph frameworks. By doing so, this would dynamically highlight the ability to capture characteristics such as tail or non stationary dependencies. For the latter, the classic stochastic process modelling approach does not facilitate its identification as, for instance, Levy processes possess independent and stationary increments.

Time-copula were specifically studied for Markov processes since there is a close relationship between the time-copula and the conditional distribution of two different times. Darsow et al. [1992] define a product of copulae that corresponds in a natural way to the operation on transition probabilities contained in the Chapman-Kolmogorov equations. For non-Markovian processes, the expression of conditional distributions for two time steps may be more complicated to evaluate as the past up to a certain time step influences the future. This could even become harder if non-stationarity or non-homogeneity features come into play. Theoretically, a time-copula could be derived from any stochastic process. This existence and uniqueness of copula was answered by Sklar [Sklar, 1959]. Moreover, compared to the statistics-based approach, the time copula makes the model less flexible but on the other hand reduces the parametrization burden. The rank correlation component of an NBPN may be directly derived from the chosen stochastic process and no additional parameters need to be determined.

Our goal is to combine the NPBN framework with k-th order Markov processes in order to model univariate time series. In fact, we prove that any k-th order Markov process may be represented as a dynamic NBPN. In doing so, the resulting framework desirably allows the generation of dynamic pair-copula-based models in a structured manner. We also explicitly provide the exact necessary and sufficient dependence metrics borrowed from the NPBN framework to represent any k-th order Markov process.

When it comes to Bayesian network (BN) modelling, one of the main challenges refers to inference. For discrete BN, it is widely known that inference grows exponentially across the number of states and degree of vertices. In the original NPBN framework, conditioning can be analytically undertaken provided that the copula is chosen to be Gaussian [Hanea et al., 2006]. If any other copula is assumed, the inference problem reverts to the discrete case due to the numerical evaluation of the integrals. Following the pioneering work of Kurowicka and Cooke [2005], who introduced NBPN and inference methods for them, the authors of Bauer and Czado [2016] recently derived the

expressions of joint and conditional distributions in terms of pair-copula decomposition similar to that of the vine-copula approach. The pair-copula decomposition allows better understanding of the role of blocks of pair-copula into joint and conditional distributions as well as the impact of the copula itself regarding conditioning. With respect to the framework of the k-th order Markov representation, we extend the findings of Bauer and Czado [2016] on conditional and marginal distributions to fit our approach. It is found that analytical conditioning can be performed if the k-th order Markov process is a Gaussian process as well. Therefore, we extend the Gaussian copula requirement to encompass other types of copulae, i.e. time-copula, that comply with the Gaussian process requisite. Additionally, the computational complexity of the Bauer and Czado [2016] algorithm is reduced for deriving the marginal densities of a k-th order Markov process necessary for analytical conditioning

The remainder of this chapter is organized as follows. The next section presents the original framework of non-parametric Bayesian networks. Section 6.3 details the dependence metrics borrowed from the NPBN specific to the Markov process framework. Section 6.4 shows the k-th order Markov process representation as dynamic NPBN. It is further explicitly provided the requirements to perform conditioning using the NPBN characteristics in section 6.5. An example using Brownian motion is finally presented in order to illustrate our findings.

6.2 Non-parametric Bayesian networks

Non-parametric Bayesian networks (NPBN) are probabilistic graphical objects that capture an n-dimensional distribution (n referring to the number of vertices) where to each edge is associated a conditional pair-copula and a conditional rank correlation. In practice, such BN have been developed in various fields (see Hanea et al. [2015]) because dependence is handled in a very flexible way, i.e., copula and rank correlations

allow a great deal of ways to capture a specific dependence structure.

Nodes are associated with arbitrary, continuous, invertible distributions, influences are associated with conditional rank correlations and are realized by conditional copulae. A copula C is a distribution on the unit square with uniform margins. Random variables X and Y are joined by copula C if their joint distribution can be written

$$F_{XY}(x, y) = C(F_X(x), F_Y(y)) \tag{6.1}$$

Sklar's theorem stipulates that this copula exists for any X and Y and is unique if F_X and F_Y are continuous. Let us consider a BN on n variables. Then the factorization of the joint density in the standard way (following the sampling order $1, ..., n$) is

$$f_{1,...,n}(x_1, ..., x_n) = f_1(x_1) \prod_{i=2}^{n} f_{i|pa(i)}(x_i|x_{pa(i)}) \tag{6.2}$$

where $f_{1,...,n}$ denotes the joint density of the n variables, f_i denotes their marginal densities, and $f_{i|j}$ denotes conditional densities. Each variable X_i is represented by the node i. The parent nodes of i form the set $pa(i)$. Conversely, for node i the set of the children nodes is denoted as $ch(i)$. Recall that the set of parents including the node itself is called the *family*: $fa(i) = pa(i) \cup \{i\}$ and for a subset A of nodes we let fa$(A) = \cup_{a \in A} fa(a)$.

Assume $pa(i) = \{i_1, ..., i_{|pa(i)|}\}$. We associate the arcs $i_{|pa(i)|-k} \to i$ with the conditional rank correlations:

$$\begin{cases} r(i, i_{|pa(i)|}) & s = 0 \\ r(i, i_{|pa(i)|-s}|i_{|pa(i)|}, ..., i_{|pa(i)|-s+1}) & 1 \leq s \leq |pa(i)| - 1 \end{cases} \tag{6.3}$$

The assignment is vacuous if $\{i_1, ..., i_{|pa(i)|}\} = \emptyset$. Assigning conditional rank correlations for $i = 1, ..., n$, as the above results in associating every arc of the NPBN with a conditional rank correlation between parent and child.

Our objective is to give the necessary and sufficient conditions to represent for any k-th order Markov process as a dynamic NPBN. To do so, we make use of the conditional rank correlation assignment given in eq.(6.3) as well as the following theorem in order to complete the characterization.

Theorem 6.2.1 (Bauer [2013]). *Let $\mathcal{D} = (V, E)$ be a directed acyclic graph on $d = |V|$ vertices. Let P be a probability measure on $\mathbb{R}^d$ translating the conditional independent statements corresponding to the directional separation criterion (also called the $\mathcal{D}$-Markov probability measure). Then P is uniquely determined by the margins of each node $i \in V$ and its conditional pair-copula $c_{i,i_{|pa(i)|-s}|i_{|pa(i)|},\dots,i_{|pa(i)|-s+1}}, 1 \leq s \leq |pa(i)| - 1$.*

6.3 Dependence framework for a k-th order Markov process

Little focus has been given for these classic NPBN to fit within a full probabilistic framework, even less for dynamic modelling, e.g. with stochastic processes. In order to do so, one may extract from any Markov process the dependence metrics NPBN use, i.e. conditional copulae, conditional rank correlations and their specific dependence structure. The idea is then to make use of the conditional rank correlation assignment eq.(6.3) and Theorem 6.2.1 to represent any Markov process by

1. vertices standing for the margins at each time step
2. constructing the exact dependence structure corresponding to the Markov process
3. assigning to each edge the related conditional time-copula and conditional rank correlation

While the first item should remain unchanged regardless of the Markov process considered, the second and third items should be closely examined according to the choice of the Markov process. Without loss of generality, we first propose that copulae are chosen to be exactly the time-copula any stochastic process exhibits. Let $\boldsymbol{X} = \{X_t, t \geq 0\}$ be an $\mathbb{R}$-valued stochastic process and let the time interval $[0, \tau]$ with lattice $0 = t_0 < t_1 < t_2 < \cdots < t_{n-1} < t_n = \tau$. One may consider the joint distributions $F_{t_i,t_j}(x, y)$,

$$F_{t_i,t_j}(x, y) = \mathbb{P}[X_{t_i} < x, X_{t_j} < y] \tag{6.4}$$

of the process at times t_i and $t_j, i \neq j$. The copula $C_{t_i,t_j}(u, v)$ defined as

$$F_{t_i,t_j}(x, y) = C_{t_i,t_j}(F_{X_{t_i}}(x), F_{X_{t_j}}(y)) \tag{6.5}$$

is called the *time-copula* for the process $\boldsymbol{X}$, where $F_t(x)$ is the marginal distribution function of X_t at time t. Notice that eq. (6.5) is similar to eq. (6.1) but applied to process $\boldsymbol{X}$. Compared to the data-oriented approach, the time-copula is parameter-free since the complete dependence is determined by time epochs t_i and t_j. The main downside here lies in the loss of flexibility in terms of dependence modelling which trades off with the reduction of the estimation of copula parameter(s). In practice, the derivation of such a copula is carried out using the relationship between the copulae and conditional

probabilities as follows :

$$\begin{aligned}
\mathbb{P}(X_{t_i} \leq x | X_{t_j} = y) &= \lim_{h \searrow 0} \mathbb{P}(X_{t_i} \leq x | y \leq X_{t_j} \leq y + h) \\
&= \lim_{h \searrow 0} \frac{F_{X_{t_i} X_{t_j}}(x, y+h) - F_{X_{t_i} X_{t_j}}(x, y)}{F_{X_{t_j}}(y+h) - F_{X_{t_j}}(y)} \\
&= \lim_{h \searrow 0} \frac{C(F_{X_{t_i}}(x), F_{X_{t_j}}(y+h)) - C(F_{X_{t_i}}(x), F_{X_{t_j}}(y))}{F_{X_{t_j}}(y+h) - F_{X_{t_j}}(y)} \\
&= \lim_{h \searrow 0} \frac{C(F_{X_{t_i}}(x), F_{X_{t_j}}(y) + \Delta(h)) - C(F_{X_{t_i}}(x), F_{X_{t_j}}(y))}{\Delta(h)} \\
&= \frac{\partial}{\partial v} C(u, v) \Big|_{\left(F_{X_{t_i}}(x), F_{X_{t_j}}(y)\right)}
\end{aligned} \tag{6.6}$$

with $\Delta(h) := F_{X_{t_j}}(y+h) - F_{X_{t_j}}(y)$ wherever the derivative exists. Conversely, one can check that

$$\mathbb{P}(X_{t_j} \leq y | X_{t_i} = x) = \frac{\partial}{\partial u} C(u, v) \Big|_{\left(F_{X_{t_i}}(x), F_{X_{t_j}}(y)\right)} \tag{6.7}$$

The partial derivatives of the copula distributions in Eq. (6.6) and eq. (6.7) are also known as h-functions in the copula literature [Aas et al., 2009].

Likewise, additional to the time-copula associated to each of the edges, we use the rank correlation specification given in (6.3). As we force the distribution to follow a particular stochastic process, the complete rank correlation structure can as well be computed first using Pearson's autocorrelation function

$$\rho(i, j) = \frac{Cov(i, j)}{\sigma_i \sigma_j} \tag{6.8}$$

where $Cov(i, j) = \mathbb{E}(X_{t_i} X_{t_j}) - \mu_i \mu_j$, with $\mu_i = \mathbb{E}(X_{t_i})$, and $\sigma_i^2 = \text{Var}(X_{t_i})$. The relationship between conditional rank correlation and Pearson's correlation is then given

by

$$r(i,j) = \rho(F_i(i), F_j(j)) \tag{6.9}$$

Note that the rank correlation can be expressed in terms of the copula as well as

$$r(i,j) = 12 \int_{[0,1]^2} C_{i,j}(u,v)\, du\, dv - 3 \tag{6.10}$$

We mention that eq. (6.10) can be used only for one-parameter copulae. To simplify notation, we use the bijection $X_{t_i} \to i$ to refer to vertex X_{t_i}. For the time interval $[0, \tau]$, the complete autocorrelation/autocovariance matrix is thus provided with indices i and j denoting the rows and columns, respectively. For the reader's convenience we refer to Kurowicka and Cooke [2006] for the definition of the dependence metrics introduced thus far. To investigate points two and three of the requirements cited earlier, we present the case addressing Markov processes next.

6.4 Representing Markov processes as a dynamic NPBN

We are now able to formulate the representation of any k-th order Markov process as a dynamic NPBN. Note that due to the so-called directional Markov property, we believe that this class of stochastic process are the only class applicable to the NPBN framework. Let $\mathcal{G} = (V, E)$ be an directed acyclic graph (DAG) over vertices V where elements are connected by directed edges $E \subseteq V \times V$. Then let us introduce a total order $<_v$ on $pa(v)$ for every $v \in V$. For every $v \in V$ and $w \in pa(v)$, set

$$pa(v; w) = \{u \in pa(v) : u <_v w\}$$

Then the joint distribution function f can hence be written as [Bauer and Czado, 2016]

$$f(\boldsymbol{x}) = \prod_{v \in V} f_v(x_v) \prod_{w \in pa(v)} c_{v,w|pa(v;w)}(F_{v|pa(v;w)}(x_v|\boldsymbol{x}_{pa(v;w)}), F_{w|pa(v;w)}(x_w|\boldsymbol{x}_{pa(v;w)})) \tag{6.11}$$

where $\boldsymbol{x} = (x_v)_{v \in V} \in \mathbb{R}^{|V|}$. We are now able to formulate any k-th order Markov process as a non-parametric BN.

Theorem 6.4.1. *Let $(\Omega, \mathcal{F}, (\mathcal{F}_t)_{t \in T}, \mathbb{P})$ be a filtered probability space with $T = [0, \tau] \subset \mathbb{R}^+$ for any $\tau \in (0, \infty)$. Take time lattice $0 = t_0 < t_1 < t_2 < \cdots < t_{n-1} < t_n = \tau$ with $n \in \mathbb{N}^*$. Let $\boldsymbol{X} = (X_t)_{t \in T}$ be an adapted k-th order Markov process, $k \in \mathbb{N}^*$. Then, $\boldsymbol{X}$ has the NPBN specification as the couple $\mathcal{B} = (\mathcal{G}, \mathcal{P})$ where*

- *$\mathcal{G} = (V, E)$ and $V = \{X_{t_i} : i \in \mathbb{N}^*\}$, $E = \left\{\bigcup_{i=0}^{n-k} E_i\right\} \cup \left\{\bigcup_{j=n-k+1}^{n} E_j\right\}$, where $E_i = \{(i, l), \forall l \in \{1, ..., n\} : l - i \leq k\}$ and $E_j = \{(j, m) : m \in \{n - k + 2, ..., n\}\}$.*
- *$\mathcal{P} = (\mathcal{P}_{\boldsymbol{X}}, \mathcal{C}_E, \mathcal{R}_E)$, where $\mathcal{P}_{\boldsymbol{X}}$ is the set of all marginal distributions of $\boldsymbol{X}$, $\mathcal{C}_E$ and $\mathcal{R}_E$ denote the set of conditional time-copula and conditional rank correlations, respectively, associated to each of the edges.*

Proof. The main idea is to show that the joint density $f_{X_{t_0}, ..., X_{t_n}}$, for any $n \in \mathbb{N}^*$, of any k-th order Markov process and corresponding one using eq. (6.11) are equal in both cases. For the sake of simplicity, we will use the abbreviation F_i to denote distribution $F_{X_{t_i}}$. The same applies to conditional distributions ($F_{i|j}$ to denote $F_{X_{t_i}|X_{t_j}}$) and density functions (f_i to denote $f_{X_{t_i}}$). For any $(x_0, ..., x_n) \in \mathbb{R}^{n+1}$, the joint cdf $F_{0,...,n}(x_0, ..., x_n)$ of a k-th order Markov process $\boldsymbol{X} = (X_t)_{t \in T}$ is given by

$$F_{0,...,n}(x_0, ..., x_n) = F_0(x_0) F_{1|0}(x_1|x_0) \cdots F_{n|n-1,...,n-k}(x_n|x_{n-1}, ..., x_{n-k}) \tag{6.12}$$

Eq. (6.12) is obtained using the simple chain rule and the k-th order Markov property. The marginal conditional densities $f_{X_{t_i}}(x_i) = \dfrac{\partial}{\partial x_i} F_{X_{t_i}}(x_i)$ are assumed to exist so the

density is straightforwardly given as

$$f_{0,\dots,n}(x_0,\dots,x_n) = f_0(x_0) f_{1|0}(x_1|x_0)\cdots f_{n|n-1,\dots,n-k}(x_n|x_{n-1},\dots,x_{n-k}) \tag{6.13}$$

Next, we use the pair copula construction of joint distributions originally proposed by Joe [1996]. For the reader's convenience we omit the function arguments. The conditional density $f_{n|n-1,\dots,n-k}$ can be written as

$$\begin{aligned} f_{n|n-1,\dots,n-k} &= \frac{f_{n-k,n|n-1,\dots,n-k+1}}{f_{n-k|n-1,\dots,n-k+1}} \\ &= \frac{c_{n-k,n|n-1,\dots,n-k+1}(F_{n-k|n-1,\dots,n-k+1}, F_{n|n-1,\dots,n-k+1})}{f_{n-k|n-1,\dots,n-k+1}} \\ f_{n-k|n-1,\dots,n-k+1} & f_{n|n-1,\dots,n-k+1} \\ &= c_{n-k,n|n-1,\dots,n-k+1}(F_{n-k|n-1,\dots,n-k+1}, F_{n|n-1,\dots,n-k+1}) f_{n|n-1,\dots,n-k+1} \end{aligned}$$

where $c_{i,j|w}$ denotes the conditional pair-copula density of variables X_{t_i} and X_{t_j} given X_{t_w} By iterating k times on the conditioning set $\{n-1,\dots,n-k\}$ we obtain

$$\begin{aligned} f_{n|n-1,\dots,n-k} = f_n & c_{n-1,n}(F_{n-1}, F_n) \\ & \prod_{i=0}^{k-2} c_{n-k+i,n|n-1,\dots,n-k+i+1}(F_{n-k+i|n-1,\dots,n-k+i+1}, F_{n|n-1,\dots,n-k+i+1}) \end{aligned} \tag{6.14}$$

Again iterating over every density in (6.13) the same way to that of (6.14) we finally get

$$\begin{aligned} f_{0,\dots,n} = & \prod_{i=0}^{n} f_i \prod_{i=1}^{k} \prod_{j=1}^{i} c_{j-1,i|i-1,\dots,j}(F_{j-1|i-1,\dots,j}, F_{i|i-1,\dots,j}) \\ & \prod_{i=k+1}^{n} c_{i-1,i}(F_{i-1}, F_i) \prod_{j=0}^{k-2} c_{i-k+j,i|i-1,\dots,i-k+j+1}(F_{i-k+j|i-1,\dots,i-k+j+1}, F_{i|i-1,\dots,i-k+j+1}) \end{aligned} \tag{6.15}$$

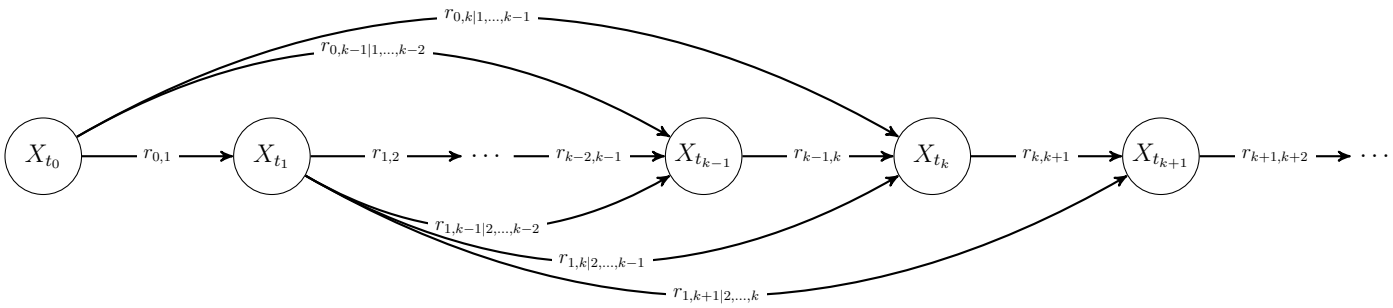

Figure 6.1 – NPBN representation of k-th order Markov process

For the NPBN density, according to its specification, we simply use the decomposition given in (6.11) to formulate the joint density $f_{0,\ldots,n}$. Suffice to consider the parent orderings $i-1 <_i i-2 <_i \cdots <_i i-k$ and $j-1 <_j j-2 <_j \cdots <_j 0$ for each vertex $i \in \{k, ..., n\}$ and $j \in \{0, ..., k\}$, respectively. By doing so, we obtain the same density to that of eq. (6.15). □

An NPBN representation of the k-th order Markov process is given in Fig. 6.1. The total ordering is chosen as is in the conclusion of the proof of Theorem 6.4.1. The NPBN representation thus provides that any k-th order Markov process can be jointly characterised by its dependence structure, i.e. the graph set $\mathcal{G}$, and its probabilistic part given by the marginal distributions, conditional time-copula and rank correlations. In order to provide more guidance on how to use Theorem 6.4.1, we summarize below the step-by-step procedure that provides the NPBN representation of any k-th order Markov process.

— for the graph part $\mathcal{G}$

1. The elements composing the set of vertices V are obtained by taking the corresponding random variable X_{t_i} given the time lattice $0 = t_0 < t_1 < \cdots < t_n$.

2. The set of edges E is directly derived from the exact dependence structure

any k-th order Markov process exhibits; in other words, it is known that

$$\left\{X_{t_0},\ldots,X_{t_{n-k-1}}\right\} \perp X_{t_n} | \left\{X_{t_{n-k}},\ldots,X_{t_{n-1}}\right\} \Leftrightarrow \left\{X_{t_0},\ldots,X_{t_{n-k-1}}\right\} \perp X_{t_n} | pa\left(X_{t_n}\right)$$

— for the probabilistic part $\mathcal{P}$

3. The marginal distributions for each X_{t_i} are obtained for each element of the sets $\mathcal{P}_{\boldsymbol{X}}$ or V which have a one-to-one correspondence

4. The set of time copula $\mathcal{C}_E$ is obtained using, for each conditional copula associated to an edge in E, eq. 6.5 details provided by Theorem 3.1 from Darsow et al. [1992]

5. The rank correlation set $\mathcal{R}_E$ is obtained using eq. (6.9) or eq. (6.10) for every conditional rank correlation associated to an edge in E

6.5 Conditioning

Conditioning is known to be one of the major advantages BN possess. Recall that compared to discrete BN framework, where conditioning can rapidly become intractable, for the NPBN methodology it has been proven that whenever the Gaussian copula is assumed conditioning can be done analytically [Hanea et al., 2006]. If the Gaussian copula is not assumed, the NPBN can be sampled and a discrete version is obtained so that traditional updating methods are summoned. As part of eq. (6.15), one of the challenges is to estimate conditional distributions $F_{v|J}$, for $v \in V$ and $J \subseteq V \setminus \{v\}$. Notice that using conditional independence provided by the k-th order Markov property, if, for any $v \in V$, $pa(v) \subseteq J$, then

$$f_{v|J} = \frac{f_{\{v\}\cup J}}{f_J} = \frac{f_{\{v\}\cup pa(v)\cup(J\setminus pa(v))}}{f_J} = \frac{f_{v|pa(v)}f_J}{f_J} = f_{v|pa(v)}$$

where $pa(v) = \{v-1, ..., v-k\}$. More generally, we seek to determine the following

$$F_{v|J}(y|\boldsymbol{x}_J) = \frac{\int_{-\infty}^{y} f_{\{v\}\cup J}(\boldsymbol{x}_{\{v\}\cup J})dx_v}{f_J(\boldsymbol{x}_J)} \tag{6.16}$$

It is worth noting that a more general conditioning case was investigated, that is, for any $I, J \subseteq V$, with $I \subseteq V \setminus J$ such that we sought to determine the conditional distribution $F_{I|J}$. However, the conditional independence may not desirably be used upon the nature of the sets I and J and thus does not further facilitate the factorization. We borrow from Bauer and Czado [2016] the main thread, that is, to provide pair-copula decomposition for marginal distributions. Let us first recall their development.

Theorem 6.5.1 (**Theorem 4.3 Bauer and Czado [2016]**). *Let $I \subseteq V$, $I_{-v} = I \setminus \{v\}$ and v_{max} the maximal vertex in I by the well ordering of the BN. Moreover, define $S_{v_{max}} := \{u \in pa(v_{max}) | \{u\} \perp I_{-v_{max}}\}$ and*

$$W_{v_{max}} := \begin{cases} \emptyset & \text{if } I_{-v_{max}} = \emptyset \\ \{w_1\} \cup pa(v_{max}; w_1) & \text{if } I_{-v_{max}} \subseteq pa(v_{max}) \text{ and } I_{-v_{max}} \neq \emptyset \\ \{w_2\} \cup pa(v_{max}; w_2) & \text{otherwise} \end{cases}$$

where w_1 and w_2 denote the maximal vertex in $I_{-v_{max}}$ and $pa(v_{max}) \setminus S_{v_{max}}$, respectively, according to the parent ordering $<_{v_{max}}$. Further let J denote the set of vertices corresponding to the iterative procedure whose purpose is to obtain the pair-copula decomposition for pdf $f_{W_{v_{max}} \cup I_{-v_{max}}}$ (and including $W_{v_{max}} \setminus I$). Then

$$f_I(\boldsymbol{x}_I) = \int_{\mathbb{R}^{|J|}} \prod_{v \in I^+} f_v(x_v) \prod_{w \in W_v} c_{v,w|pa(v;w)}(F_{v|pa(v;w)}(x_v|\boldsymbol{x}_{pa(v;w)}), F_{w|pa(v;w)}(x_w|\boldsymbol{x}_{pa(v;w)}))d\boldsymbol{x}_J \tag{6.17}$$

We are thus interested in formulating f_I for the NPBN representation given in Theorem 6.4.1. In order to do so, we exploit the k-th order Markov property and the corre-

sponding conditional independence property. For the reader's convenience, we will use as short-hand notation i to interchangeably refer to either vertex or random variable X_{t_i}. Now define $M = \{(i,j) \in I^2 : |i-j| > k\}$. Depending on whether M is empty, we have the the following lemmas.

Lemma 6.5.1. *Let I^+ be the well-ordered set I augmented with every missing vertex between the minimal and maximal vertices in I and let $J = I^+ \setminus I$. If $M = \emptyset$ then*

$$f_I(\boldsymbol{x}_I) = \int_{\mathbb{R}^{|J|}} \prod_{v \in I^+} f_v(x_v) \prod_{w \in T_v} c_{v,w|pa(v;w)}(F_{v|pa(v;w)}(x_v|\boldsymbol{x}_{pa(v;w)}), F_{w|pa(v;w)}(x_w|\boldsymbol{x}_{pa(v;w)}))d\boldsymbol{x}_J \tag{6.18}$$

where $T_v := \{w \in I^+ : w < v\}$.

Proof. In the present case, the set M indicates whether there are vertices in I separated by more than k other vertices. If this set is empty, when applying Theorem 4.3 in Bauer and Czado [2016] the marginalization set J appears immediately. □

For the more general case where $M \neq \emptyset$, we have the following lemma.

Lemma 6.5.2. *Let the notation be in as in Lemma 6.5.1. Let $K = v_{max} - (v_{min} + k)$ and partition I^+ as $\bigcup_{m \geq 0}^{K} I_m^+$ where $I_m^+ = \{m + v_{min}, ..., m + v_{min} + k\}$ with v_{min} and v_{max} the minimal and maximal vertices in I, respectively. Likewise, let $J = \bigcup_{m \geq 0}^{K} J_m$ with $J_m = I_m^+ \setminus I_m$ and $I_m = I_m^+ \cap I$. Then*

$$\begin{aligned} f_I(\boldsymbol{x}_I) = \int_{\mathbb{R}^{|J|}} \prod_{v \in I^+ \setminus I_0^+} f_v(x_v) \prod_{m=1}^{K} \\ c_{v_{max}^m, pa(v_{max}^m)|pa(v_{max}^m;pa(v_{max}^m))}(F_{v_{max}^m|pa(v_{max}^m;pa(v_{max}^m))}(x_{v_{max}^m}|\boldsymbol{x}_{pa(v_{max}^m;pa(v_{max}^m))}), \\ F_{pa(v_{max}^m)|pa(v_{max}^m;pa(v_{max}^m))}(\boldsymbol{x}_{pa(v_{max}^m)}|\boldsymbol{x}_{pa(v_{max}^m;pa(v_{max}^m))})) \\ \times f_{I_0^+}(\boldsymbol{x}_{I_0^+})d\boldsymbol{x}_J \end{aligned} \tag{6.19}$$

with

$$c_{v,pa(v)|pa(v;pa(v))}(F_{v|pa(v;pa(v))}(x_v|\boldsymbol{x}_{pa(v;pa(v))}), F_{pa(v)|pa(v;pa(v))}(\boldsymbol{x}_{pa(v)}|\boldsymbol{x}_{pa(v;pa(v))})) = \prod_{w\in pa(v)} c_{v,w|pa(v;w)}(F_{v|pa(v;w)}(x_v|\boldsymbol{x}_{pa(v;w)}), F_{w|pa(v;w)}(x_w|\boldsymbol{x}_{pa(v;w)}))$$

and $\{v^m_{max}\}$ *is the maximal vertex of* I^+_m*, i.e.* $\{v^m_{max}\} = \{m + v_{min} + k\}$.

Proof. The main body of the proof uses again Theorem 4.3 from Bauer and Czado [2016]. For the case $|I| = 1$ the proof is trivial. Thus, assume $I_{-v_{max}} \neq \emptyset$. Observe from the definition of W_v, the condition $I_{-v_{max}} \subseteq pa(v_{max})$ is the main driving factor to either obtain $\{w_1\} \cup pa(v_{max}; w_1)$ or $\{w_2\} \cup pa(v_{max}; w_2)$. Since we assume $M \neq \emptyset$, then necessarily $K > 0$. The partition of I into sets I_m each of length k facilitates the use of the k-th order Markov property. The procedure proceeds backwards taking vertex $\{v^m_{max}\}$ and testing condition $I_{-v_{max}} \subseteq pa(v^m_{max})$, where I^+ gets shrunk of $\{v^m_{max}\}$ at each iteration. First, by noticing that $I^+_m = pa(m + v_{min} + k) \cup \{m + v_{min} + k\} = fa(v^m_{max})$, where $fa(v)$ is the family of v, and since $M \neq \emptyset$, $I_{-v_{max}} \nsubseteq pa(v^m_{max})$. Thus, $W_{v_{max}}$ is essentially determined by the third condition up to the last iteration when I^+ reduces to I^+_0. When reaching I^+_0, $W_{v_{max}}$ is determined by the second condition as $M = \emptyset$ the term $f_{I^+_0}$ remains as last and is decomposed using Lemma 6.5.1 as the set $\{I^+_0\}$ is of length equal to k. Fig. 6.2 provides an illustration of the dynamics between the sets that come into play which determine the factorization of I.

For each I_m, with $1 \leq m \leq K$, we thus compute

$$f_{I_m}(\boldsymbol{x}_{I_m}) = \int_{\mathbb{R}^{|J_m|}} f_{v^m_{max}}(x_{v^m_{max}}) \prod_{w\in pa(v^m_{max})} c_{v^m_{max},w|pa(v^m_{max};w)}(F_{v^m_{max}|pa(v^m_{max};w)}(x_{v^m_{max}}|\boldsymbol{x}_{pa(v^m_{max};w)}), F_{w|pa(v^m_{max};w)}(x_w|\boldsymbol{x}_{pa(v^m_{max};w)}))d\boldsymbol{x}_{J_m}$$

Whenever $I_m = \emptyset$, then we assume by convention that $f_{I_m} = 1$. By iterating over m, it

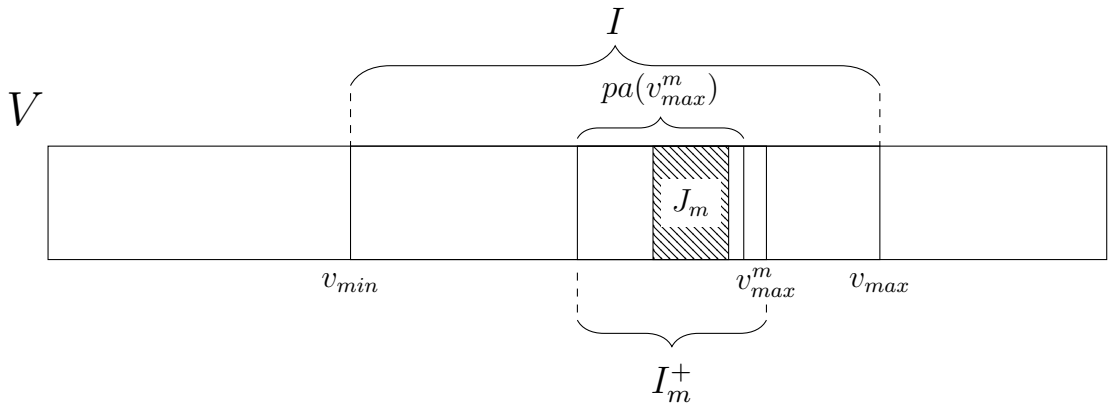

Figure 6.2 – Sets illustration at iteration m

finally yields

$$f_I(\boldsymbol{x}_I) = f_{I_0^+}(\boldsymbol{x}_{I_0^+}) \prod_{m=0}^{K} f_{I_m}(\boldsymbol{x}_{I_m})$$

□

In terms of efficiency, the algorithm summarizing Theorem 6.5.1 developed in Bauer and Czado [2016] could be said to have a weak lower bound of $|I|$ iterations to complete. We believe that this lower bound can be improved to $|I^+|$ if the algorithm is fed with any $|I|$ from k-th order Markov NPBN framework. We also conjecture that Algorithm 18 summarizing Lemma 6.5.2 should have lower bound $K \leq |I^+|$, thus performing at worse equally. We leave the proofs of these claims as future work. This reduction is mostly due to the deletion of the unnecessary conditions meant to determine the set W_v. In fact, it was pointed out in the proof of Lemma 6.5.2 that in the k-th order Markov process framework, the set W_v is known mainly because the dependence structure is known as well. This is a dramatic computation reduction compared to Bauer and Czado [2016] who must construct the set in each iteration.

As an immediate consequence of Lemma 6.5.2, one can check that for Gaussian k-th order Markov processes conditioning can be performed analytically on Gaussian densities.

Algorithme 1 : Factorization of the marginal density f_I for any set $I \subseteq V$

input : Well ordered NPBN; set of parent ordering for each node; non-empty set $I \subseteq V$; order k of the Markov process

output : Factorisation f_I

$f \leftarrow 1$;
$K \leftarrow v_{max} - (v_{min} + k)$;
$I^+ \leftarrow \{v_{min}, \dots, v_{max}\}$; // I populated with all missing nodes between v_{min} and v_{max}
$J \leftarrow \emptyset$; // indices of integration variables
for $m \in \{1, \dots, K\}$ **do**
  $I_m^+ \leftarrow \{m + v_{min}, \dots, m + v_{min} + k\}$;
  $v_{max}^m \leftarrow m + v_{min} + k$;
  $f \leftarrow f \cdot f_{v_{max}^m}$;
  $I_m \leftarrow I \cap I_m^+$;
  $J_m \leftarrow I_m^+ \setminus I_m$;
  $J \leftarrow J \cup J_m$;
  if $I_m \neq \emptyset$ **then**
    for $w \in pa(v_{max}^m)$ **do**
      $f \leftarrow f \cdot c_{w,v_{max}^m|pa(w;v_{max}^m)}(F_{w|pa(w;v_{max}^m)}(x_w|\boldsymbol{x}_{pa(w;v_{max}^m)}), F_{v_{max}^m|pa(w;v_{max}^m)}(x_{v_{max}^m}|\boldsymbol{x}_{pa(w;v_{max}^m)}))$
    end
  end
end
/* Terminate by using Lemma 6.5.1 applied to the set I_0^+ */
$f \leftarrow \int_{\mathbb{R}^{|J|}} f d\boldsymbol{x}_J$;

Corollary 6.5.1. *Let $\boldsymbol{X} = (X_t)_{t \in T}$ be an adapted k-th order Gaussian Markov process and consider its dynamic NPBN representation. Then for any $v \in V$ and any $J \subseteq V_{-v}$, the conditional density $f_{v|J} = \dfrac{f_{\{v\} \cup J}}{f_J}$ reduces to the division of Gaussian integrals.*

Proof. Using Lemma 6.5.2 on both the numerator and the denominator, the marginal

density of any set I_m can be written as

$$f_{I_m} = \int_{\mathbb{R}^{|J_m|}} f_{v^m_{max}} \prod_{w \in pa(v^m_{max})} c_{v^m_{max}, w|pa(v^m_{max};w)}(F_{v^m_{max}|pa(v^m_{max};w)}, F_{w|pa(v^m_{max};w)}) d\boldsymbol{x}_{J_m}$$

$$= \int_{\mathbb{R}^{|J_m|}} f_{v^m_{max}} c_{v^m_{max}-1, v^m_{max}}(F_{v^m_{max}-1}, F_{v^m_{max}}) \prod_{i=0}^{k-2}$$

$$c_{m+v_{min}+i, v^m_{max}|v^m_{max}-1,\dots,m+v_{min}+i+1}(F_{m+v_{min}+i|v^m_{max}-1,\dots,m+v_{min}+i+1}, F_{v^m_{max}|v^m_{max}-1,\dots,m+v_{min}+i+1}) d\boldsymbol{x}_{J_m}$$

$$\overset{\text{eq. (6.14)}}{=} \int_{\mathbb{R}^{|J_m|}} f_{m+v_{min}+k} \frac{f_{m+v_{min}+k|m+v_{min},\dots,m+v_{min}+k-1}}{f_{m+v_{min}+k|m+v_{min}+1,\dots,m+v_{min}+k-1}} \frac{f_{m+v_{min}+k|m+v_{min}+1,\dots,m+v_{min}+k-1}}{f_{m+v_{min}+k|m+v_{min}+2,\dots,m+v_{min}+k-1}}$$

$$\times \cdots \times \frac{f_{m+v_{min}+k|m+v_{min}+k-2,m+v_{min}+k-1}}{f_{m+v_{min}+k|m+v_{min}+k-1}} \frac{f_{m+v_{min}+k|m+v_{min}+k-1}}{f_{m+v_{min}+k}} d\boldsymbol{x}_{J_m}$$

$$= \int_{\mathbb{R}^{|J_m|}} f_{m+v_{min}+k|m+v_{min},\dots,m+v_{min}+k-1} d\boldsymbol{x}_{J_m}$$

By definition, the density $f_{m+v_{min}+k|m+v_{min},\dots,m+v_{min}+k-1}$ is a Gaussian density and when iterating over index m, f_I is a multivariate Gaussian density as a product of Gaussian density. The integral can always be analytically solved with the solution varying on the nature of the set J_m. This finally proves the claim. □

We proceed by illustrating our findings through the example of the Brownian motion.

Example 6.5.1 (Brownian motion)**.** *In this example we illustrate the framework developed above through the example of the Brownian motion denoted as* $\boldsymbol{B} = \{B_t, t \geq 0\}$. *The Brownian motion is a first-order Markov process usually characterised by the following:*

- $\mathbb{P}(B_0 = 0) = 1$ *a.s.*
- $\boldsymbol{B}$ *has independent Gaussian increments, with* $B_{s+t} - B_s \sim \mathcal{N}(0, t)$
- $\boldsymbol{B}$ *has continuous path*

Moreover, it is known to follow a multivariate Gaussian distribution with mean 0 and autocorrelation $\rho(B_{t_i}, B_{t_j}) = \sqrt{\frac{t_i}{t_j}}$, *for* $t_j > t_i$. *Applying Theorem 6.4.1 and the corre-*

sponding procedure, we are able to give the following NPBN representation $\mathcal{B} = (\mathcal{G}, \mathcal{P})$ *where*

— $\mathcal{G} = (V, E)$ *with (step 1. of the procedure at the conclusion of section 6.4)* $V = \{B_{t_i} : i \in \mathbb{N}^*\}$ *and (step 2.)* $E = \{(i, i+1) : i \in \{0, ..., n-1\}\}$ *(see Fig. 6.4 for dependence structure)*

— $\mathcal{P} = (\mathcal{P}_{\boldsymbol{B}}, \mathcal{C}_E, \mathcal{R}_E)$, *where* $\mathcal{P}_{\boldsymbol{X}} = \{\forall i, B_{t_i} \sim \mathcal{N}(0, t_i)\}$ *is the set of all marginal distributions of* $\boldsymbol{B}$ *(step 3.),* $\mathcal{C}_E$ *(step 4.) denotes the set of time-copula density given by [Darsow et al., 1992]*

$$c^B_{t_i,t_j}(u,v) = \sqrt{\frac{t_j}{t_j - t_i}} \frac{\varphi\left((\sqrt{t_j}\,\Phi^{-1}(v) - \sqrt{t_i}\,\Phi^{-1}(u))/\sqrt{t_j - t_i}\right)}{\varphi(\Phi^{-1}(v))} \qquad \text{for } t_j > t_i \tag{6.20}$$

where Φ *denotes the distribution function of a standard normal random variable and* φ *is the density function of a standard normal random variable.* $\mathcal{R}_E$ *(step 5.) denotes the set of rank correlations associated to each of the edges. We therefore observe that the copula is non stationary for pair-wise time steps as both* t_i *and* t_j *are parameters influencing the distribution of* $c^B_{t_i,t_j}$. *This fact is not obvious from the stochastic process formulation. Note that the copula (6.20) could be more specifically written as*

$$c^B_{t_i,t_{i+1}}(u,v) = \sqrt{\frac{t_{i+1}}{t_1}} \frac{\varphi\left((\sqrt{t_{i+1}}\,\Phi^{-1}(v) - \sqrt{t_i}\,\Phi^{-1}(u))/\sqrt{t_1}\right)}{\varphi(\Phi^{-1}(v))} \tag{6.21}$$

since the NPBN representation reduces to only consider sequential time steps in the case of first order Markov processes. Plots of the Brownian copula densities and their corresponding contours may be found in Fig. 6.3. The non-stationarity can easily be observed through both the densities and their corresponding contours. The distributions resemble in many ways that of the Gaussian copula with different correlation values. For the rank correlation set $\mathcal{R}_E$ *and since the Brow-*

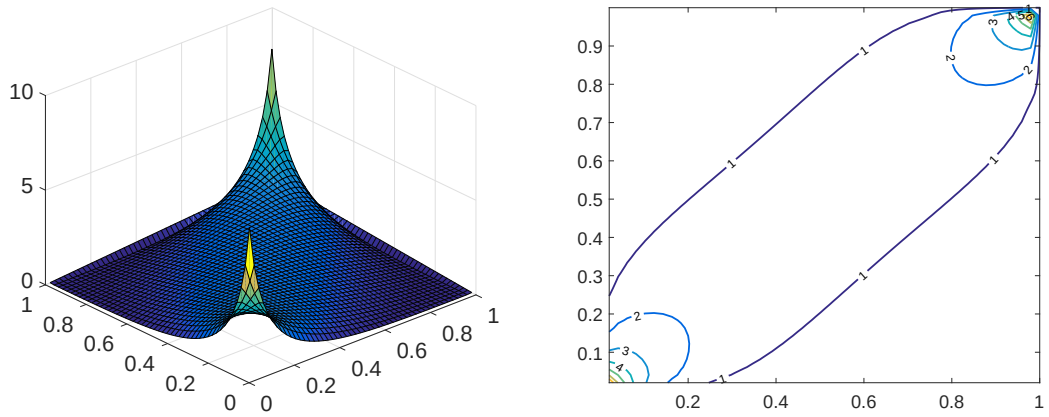

(a) $t_i = 0.1, t_{i+1} = 0.2$

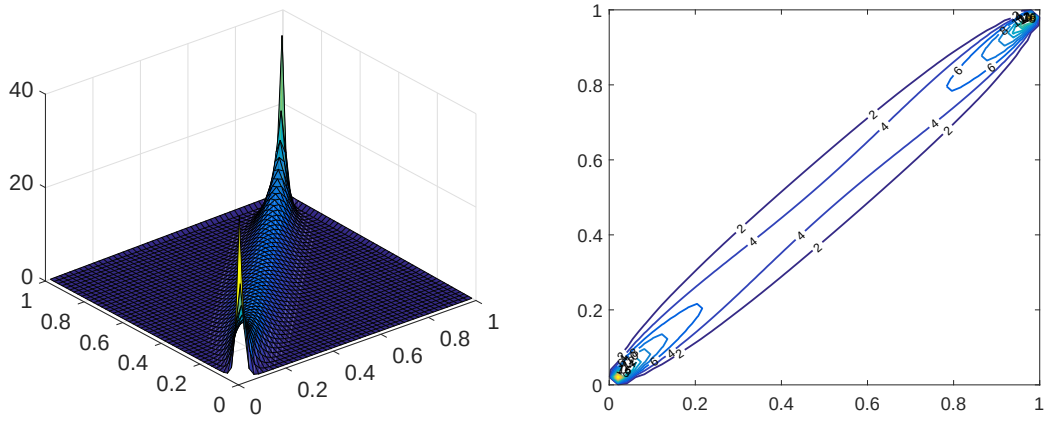

(b) $t_i = 1.9, t_{i+1} = 2$

Figure 6.3 – Brownian copula density (left) and corresponding contour (right) for two different time steps.

nian motion is a Gaussian first order Markov process, ranks of autocorrelation can be given as [Kurowicka and Cooke, 2006]

$$r(B_{t_i}, B_{t_j}) = \frac{6}{\pi} \arcsin\left(\frac{1}{2}\rho(B_{t_i}, B_{t_j})\right)$$

Fig. 6.4 provides a graphical visualization of Brownian motion as dynamic NPBN.

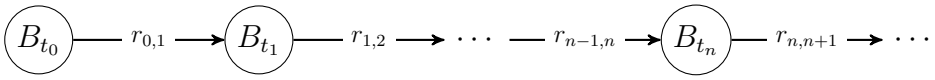

Figure 6.4 – NPBN representation of the Brownian motion

6.6 Conclusion

We proved in this chapter that a k-th order Markov process has a dynamic NPBN representation. Guidance is given on how to obtain the various dependence metrics that are sufficient and necessary. We additionally derive the conditions required to perform conditioning which can be analytically done for the Gaussian case.

One of the advantages consists in having a clear vision on the dependence dynamics expressed through the time copula and rank correlation. Compared to classic stochastic process based modelling, this may shed the light on non-stationarity concerning dependence. It thus enhances the description/characterization of dependencies. More precisely, for Levy processes whose increments are independent and stationary, the associated time-copula may thus be non-stationary as is shown taking the example of the Brownian motion.

The applicability of the Markov process representation may find interest in various fields ranging from finance, where Markov processes such as the geometric Brownian motion is key for stock pricing, to deterioration modelling, speech recognition, etc. Basically, these are the areas into which Markovian features have been successfully tested and validated. In this regard, one may investigate whether the corresponding time-copula possesses an analytical inverse. In fact, validating the Markovian property may be done through classic statistical tests, e.g. Fisher's. However, validation may not be sufficient for the whole model, especially concerning dependence aspects. Copula-based models require the copula inversion as means for dependence validation through sampling.

Chapter 7

Conclusions

This thesis has primarily investigated high-dimension deterioration problems using Bayesian networks. The approach advocated in this manuscript is of both statistical and probabilistic nature. The reason for choosing such a combination is twofold. First, as systems get more and more sophisticated, uncertainty surrounding their reliability and safety grows with it. Furthermore, the task of identifying and quantifying their causes, which often happens to be uncertain as well, also increases in difficulty. Models exclusively leaning on physics-based approaches fail to fully encompass the dynamics of high-dimensional issues. Secondly, the availability of large data sets coming from monitoring and sensors would steer one towards statistical approaches. We shed light on the fact that Bayesian networks can be a versatile framework in which both statistical and probabilistic modelling are smartly intertwined. Their efficiency in the field of bridge deterioration modelling has been adequately addressed through Chapters 3, 4 and 5. Although no reliability-oriented application was presented in Chapter 6, we can assert that the developed approaches are in line with the previous ones for degradation-related discussions on their effectiveness. A straightforward argument would be that regardless of the class considered, the Markov property symbolized through conditional independence has been, and continues being an attractive method in degradation modelling. For

completeness, we reiterate the most important contributions each Chapter provides.

In Chapter 3, a crack growth model for cracks in welded details of the orthotropic deck structure of steel bridges has been developed. Monitoring a complete bridge is known to be expensive and might be unnecessary because crack growth developments in different sections of the bridge are correlated. The Bayesian network model shows a sharp advantage over other modelling choices in order to cope with this optimization issue. Through the BN approach, a new conditioned failure year distribution is obtained not only for the monitored detail, but also for other details of the bridge. The updated, more accurate prediction of the failure year of the details considered causes a reduction of unnecessary maintenance and helps preventing unplanned closures of the bridge due to ad hoc repairs. Also, the BN makes possible the application of monitoring results in order to make more accurate predictions about the non-monitored details. Finally it enables a root cause analysis to underline the governing variables having the most influence in the crack growth model.

Chapter 4 proposed a structured expert judgment method to quantify the degradation model presented in Chapter 5. The aim of this study is to provide parametrization and insight on degradation models via uncertainty assessments. In this sense, it was possible to highlight the limited knowledge as well as attempting to give another viewpoint that current practice has. Furthermore, although substantial material is available in various fields, including in the domain of infrastructure reliability, no records were found for this particular class of structures. Addressing the quantification problem demonstrates a rather great uncertainty interval proving how challenging this task is, especially when using discrete BN whose probabilistic quantification can be very demanding.

An extension to the classic, dynamic Bayesian network framework termed the covariate-DBN is proposed in Chapter 5. A second dimension is added element-wise as well as a method for indirectly linking them through a set of covariates. In the case where limited data is available, a formal mathematical framework is developed for making use of

Cooke's method for structured expert judgement to parametrize a Markov chain and the covariate relationships between elements in the covariate-DBN. Sensitivity metrics that allow measuring the change in amplitude between conditional and conditional distributions are also presented.

A real-world bridge network application was presented which emphasizes how traffic and load information may serve as the relevant covariates to link bridge elements in the covariate-DBN. While the model is applied to a specific bridge network scenario, different sets of covariates could yet be envisioned in the same framework.

We were able to show that using the sensitivity metrics gave insightful information such as posterior distributions that showed a difference as large as two order of magnitude at some points in time compared to the unconditional case. In particular, it was observed that continuous monitoring should prevail as opposed to condition-based (by also taking into account cost constraints). Moreover, the sensitiveness of the inserted information decreases in time so that pieces of evidence inserted at early epochs should be preferred over later ones. In summary, numerical experiments show that information is most valuable as early as possible, and the value of information decreases over time. Thus, by advantageously combining the two above observations, one could selectively opt for the most sensitive combinations of inference. This further results in substantially decreasing the inference combinations.

In Chapter 6, it was proved that a k-th order Markov process has a dynamic NPBN representation. Guidance is given on how to obtain the various dependence features that are borrowed from the NPBN framework. We additionally derive the required conditions to perform conditioning which can be analytically done for the Gaussian case. One of the advantages consists in having a clear vision on the dependence dynamics expressed through the time copula and rank correlation. Compared to classic stochastic process based modelling, this may shed light on non-stationarity concerning dependence. It thus enhances the description/characterization of dependencies. More pre-

cisely, for Levy processes whose increments are independent and stationary, the associated time-copula may be non-stationary as is shown taking the example of the Brownian motion.

Overall, the specific profile of degradation from which can be undertaken leads us to explore two classes of BN having different probabilistic representations of dependence. On the one hand, when 'classic' Markov modelling can be chosen for deterioration of civil infrastructure, dynamic BN appear to be well-suited. Despite the possible intractability of quantification, the dependence translated by conditional probability tables can be generically assessed, unless assuming homogeneity constraints. It was successfully shown and tested in Chapter 5 that taking a 4-state space deterioration having a parent node featuring a 3-state space was not an obstacle for quantification purposes using expert judgment.

The ability for the two classes of BN to handle continuous, discrete or mixture is also a crucial aspect. Theoretically, discretizing continuous variables can almost always be performed. However, this is often at the cost of losing information that may be substantial at the modelling stage and also computationally intensive. NPBN have proven efficient primarily to achieve this objective. Probabilistic dependence is expressed through (conditional) copulae and (conditional) rank correlation. As briefly discussed in Chapter 3, these two dependence characteristics allow capturing a great variety of dependence patterns. This latter ability can be particularly desirable for structures' reliability where dependence may not be always of the same "random" nature across a stock of assets. Chapter 6 showed that dependence could also be handled dynamically when using NPBN. However, the probabilistic dependence metrics as well as the marginal distributions are derived from the chosen Markov process which implicitly assumes how the dependence and the marginal distributions are interacting. In the context of reliability, random changes that may temporally impact both the uncertainty and the corresponding dependence dynamics could also be captured.

7.1 Perspectives

In Chapter 3, the next steps constitute further calibration of distributions and correlations between parameters using field measurements and information from fatigue tests. In addition, further validation of the outcomes of the model by comparing it to reported cracks in actual bridges is suggested.

For the 2-dimension, dynamic BN model presented in Chapter 5, the main limitation of the proposed methodology is the curse of dimensionality. Our model further increases this complexity through the added spatial aspect. The theoretical requirements to elicit expert opinion would become prohibitive as the number of states grows. As an extension, the possibility of jumping by more than one state when deteriorating could be taken into account, hence allowing for transitions probabilities $p_{1,3}, p_{1,4},$, etc., or even considering spontaneous actions improving the state of the bridge. This would entail for instance the $p_{i,j}$ with $i > j$, to be non-null. From the parametrization perspective and, in particular, regarding expert judgment, this would increase the number of items to add to the current elicitation making it even more tedious for experts.

If one wants to keep discrete dynamic BN as the driving framework for large-scale modelling, one of the few solutions to overcome the combinatorial quantification issue would be to sample synthetic data from empirical distributions constructed from available data sets. A more viable option would be to investigate other classes of BN like the one proposed in Chapter 6 to deal with continuous distributions where parametrization requires significantly less inputs. Moreover, even in the absence of data, eliciting conditional rank correlation from experts is gaining interest Morales et al. [2008], Werner et al. [2017].

Chapter 6 essentially treats theoretical aspects of the NPBN, namely that it can characterize any Markov process through its associated dependence characteristics and structure. Mainly because of time constraints, the applicability of the model was only briefly addressed. However, we believe that fields where Markov-based models prove

effective could be of substantial interest. Reliability could be one of these domains using, for example, the geometric Brownian motion to model deterioration. Validating the Markovian property may be done through classic statistical tests, e.g. Fisher's. However, validating the whole model should not reduce to the validation of the Markov property as dependence aspects. In this regard, one may investigate whether the corresponding time-copula possesses an analytical inverse. In fact, Copula-based models require the conditional copula inversion as means for dependence validation through sampling.

An important observation that is common to the models presented in Chapter 3, Chapter 4 and Chapter 5 is the flexibility in terms of the application. While studying degradation for steel bridges was the main thread, one could potentially apply these models to other bridge types and even other civil infrastructures. However, applications are not only limited to degradation modelling but could include other fields than that of reliability into which Markovian features have been successfully tested and validated. The applicability of Markov process-based models finds interest in various other fields ranging from speech recognition, finance, where the geometric Brownian motion is key for stock pricing, to only name a few.

An extension to influence diagrams [Howard and Matheson, 1984] would provide a decision making framework for all three models. For the approaches presented in Chapter 3 and Chapter 5, this extension would not be hard as the discrete, dynamic BN framework is readily applicable for this extension, especially in a Markovian context [Lauritzen and Nilsson, 2001]. For the NPBN approaches depicted in Chapter 3 and Chapter 6, literature lacks an extension that accounts for a decision-making framework. More generally, for continuous BN, only the Gaussian case was extended to address decision analysis through influence diagrams [Shachter and Kenley, 1989]. More research in this direction would thus be advised.

The underlining Markovian assumption due to the D-separation property of BN used

throughout this whole thesis may be restrictive in some cases. Relaxing this assumption to account for a broader spectrum of probabilistic graphs may thus be a direction to take. As a matter of fact, more advanced BN-based models are emerging which, for instance, allow for more freedom on the sojourn time distribution [Foulliaron et al., 2015].

Appendices

Appendix A

Structured Expert Judgment

We provide next the typical elicitation questionnaire each of the experts underwent and from which data was obtained and further processed to calibrate eq. (5.9) and eq. (5.10).

Elicitation of uncertainty over steel bridges condition in time in the Netherlands

1. Introduction

This questionnaire is concerned with the elicitation of uncertainty distributions over duration of transition between bridges' condition states. More precisely, we are interested of different classes of bridges whose characteristics can be found in the next sections. The type of data that this questionnaire refers to is presented in section Data of interest. The bridges resemble real bridges in the Netherlands in the sense that we could retrieve straightforwardly most of this data.

Your personal details will not be used in the open literature to associate individual answers to individual experts. They are necessary however to warranty the accountability and reproducibility of this workshop as a scientific exercise. We therefore will be attaching your name and profession to this questionnaire.

Name:

Profession:

2. Definition of the states

This section describes the different condition states that will be considered as well as the various loading configurations. We first provide the definitions of the various degradation states bridges can be subject to. Note that condition scales used represent the general or overall condition of a bridge. Moreover the scale is not necessarily equidistant, which means that the difference between consecutive states might not be the same. We thus define the following condition states.

Bridge condition states

Green (denoted further G)

This state corresponds to a perfect condition where no damage/problems are present; it is always considered that a newly constructed bridge is in this state.

Yellow(denoted further as Y)

This state corresponds to a bridge having at least one crack in the deck plate that can be detected by the UT measurements technique, namely that it can be greater or equal than 30mm up to 100mm.

Orange(denoted further as O)

This state corresponds to deterioration such that multiple cracks are present whose minimum length is greater or than 30mm and largest crack can be up to 500mm. In terms of maintenance, at least one crack needs repair.

Red(denoted further as R)

This state corresponds to multiple important fatigue cracks among which at least one crack is larger than 500mm in the deck plate and need imminent repair. Note that this condition does not mean a failed state but it requires urgent intervention and is synonym of threat to safety/functionality.

Loading condition states

We will refer to loading classes being either *Heavy*, *Normal* or *Low.* For *Heavy* the loading is to be associated with loading conditions that can be observed in the Randstad area, e.g. in highways A15 or A16. A *Normal* loading is to be associated with loading conditions that resemble to those observed in the South area of the Netherlands, such as in highways A2 or A59. Finally, a *Light* loading refers to conditions observed in the North area of the Netherlands, e.g. highways A32 or A7.

3. Crack measurement techniques

As assumed previously, techniques are performed to detect cracks only in the deck plate.

The first method is called the '**Ultrasonic Testing'** (UT) which works with a scanner. This inspection technique works from the underside of the deck plate and it inspects the deck plate between the two crossbeams. The inspection can only start at approximately 30 mm from the crossbeam web. The probes are able to inspect through the paint on the steel parts.

The second method considered is the '**Crack Pulsed Eddy Current**' (Crack-PEC) which allows detecting cracks in the steel deck plate from the top side of the bridge without having to remove asphalt surfacing on fixed bridges. The technique uses pulsed magnetic fields to generate eddy currents in the steel. A measurement car with 8 PEC probes installed on it performs the inspection. Four probes are available for both wheel tracks. For an inspection of a bridge deck a measurement grid is defined on the deck. The measurement grid is likely to focus on the locations of the

crossbeams and gives the locations where the inspection will be carried out. At each measurement point on the grid the inspected area per trough web is approximately the diameter of the probe, 100 mm.

Third method focuses on **Visual Observation (VO)** which is carried out by specialists. The purpose is to visually inspect the top layer in order to detect a crack at the surface. Additionally, a method denoted by *craquelé* can be considered.

4. Data of interest

The data of interest that this questionnaire addresses is over expected duration of transition between hypothetical bridges' condition states. When degrading, at each time step bridges transit successively from one state to its next (worsened) state or remain in the same condition. We are interested in eliciting the uncertainty distribution over the expected duration that each bridge takes to perform these transitions in time. We could also name these quantities "expected first passage time" between these states. We would further like to assess transition dependencies in terms of loading.

We consider two different classes of bridges, namely **Moveable** and **Fixed**. The deck plate thickness for moveable and fixed bridge is 12mm and 10mm respectively. The thickness and type of deck plate overlay are assumed as follows:

- For moveable bridges a 6 mm thick epoxy overlay is assumed.
- For fixed bridges a 100 mm asphalt (i.e. ZOAB) is applied.

5. Questions

You are asked to elicit the 5th, 50th and 95th quantiles of your uncertainty distribution over the quantities this elicitation is concerned with. The 5th quantile means that you think with probability 95% the quantity will be greater than your estimate and conversely with probability 5% it will be smaller than the value you are providing. Same reasoning applies for the 50th and 95th quantiles.

If you are to fill out the following answer

5th quantile: a 50th quantile: b 95th quantile: c

the interpretation is:

- with 95% probability the realization (or best estimate) will be greater than a
- with 50% probability it will be greater than b
- with 5% probability it will be greater than c

with $a < b < c$.

Only questions 1 – 5 are related to crack measurements for a steel bridge performed between **30 up to 35 years** after the bridge was constructed. It is a 1km long steel box girder bridge containing 5 traffic lanes. Figure 1 below shows the type of cracks considered as well as the geometry of the steel bridge.

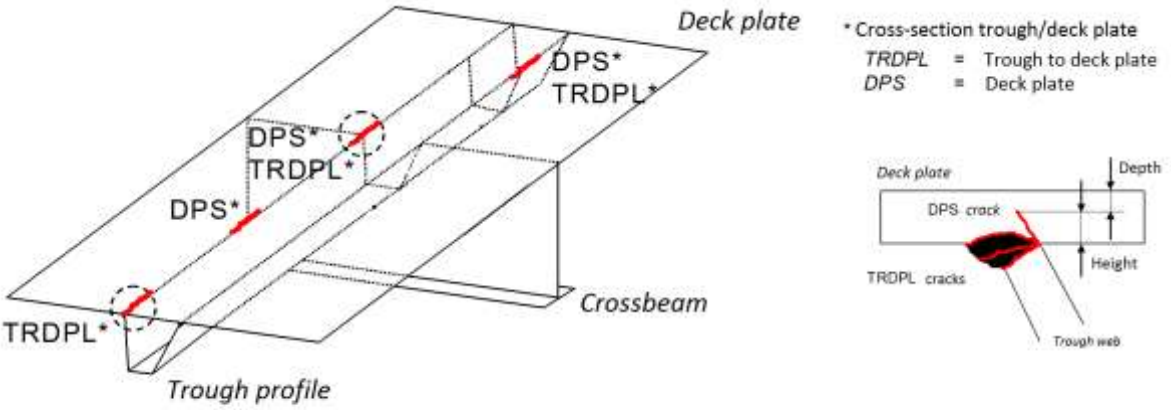

Figure 1: 3d view of the bridge considered cracks' location (left); longitudinal cross-section with 'trough to deck plate' crack location (right);

Questions 1 to 5 are considering a ***Normal*** loading condition through the time span between 2 measurements. Unless explicitly mentioned, we are considering cracks **only in the deck plate** (referred to as *DPS* in Figure 1). Questions 6 - 8 are questions of interest regarding expected transitions and proportion of transitions accounting with loading dependencies.

1. A crack was detected by the **Crack-PEC** technique to be a certain length **32 years** after construction, what would be its length (in mm) **the following year** using the same measurement technique?

	Crack length using 'Crack-PEC' 32 years after construction (mm)	5^{th}	50^{th}	95^{th}
Crack length using 'Crack-PEC' the following year (mm) ?	200	mm	mm	mm
	250	mm	mm	mm

Comments/reasoning behind answer:

2. A crack was detected by **the Crack-PEC** technique to be a certain length **30 years** after construction, what would be its length (in mm) **3 years** after using the same measurement technique?

	Crack length using 'Crack-PEC' (mm) at age 30 years	5^{th}	50^{th}	95^{th}
Crack length using 'Crack-PEC' 3 years later (mm) ?	100	mm	mm	mm
	200	mm	mm	mm
	300	mm	mm	mm

Comments/reasoning behind answer:

3. A crack was detected by the **'Ultrasonic Testing'** technique to be a certain length **33 years** after construction, what would be its length **the following year** using the same measurement technique?

	Crack length using 'UT' 33 years after construction (mm)	5^{th}	50^{th}	95^{th}
Crack length using 'UT' the following year (mm) ?	30	mm	mm	mm
	80	mm	mm	mm
	100	mm	mm	mm
	550	mm	mm	mm

Comments/reasoning behind answer:

4. In this question we are focusing on cracks **in the 'TRDPL' location** of the bridge (see Figure 1). A crack was detected by the **VO technique** to be a certain length **32 years** after construction. What would be its detected length the **following year** and **two years later** using the same measurement technique?

	Crack length using 'VO' 32 years after construction (mm)	5^{th}	50^{th}	95^{th}
Crack detected length using 'VO' the following year (mm) ?	100	mm	mm	mm
Crack detected length using 'VO' two years later (mm) ?	100	mm	mm	mm

Comments/reasoning behind answer:

5. A crack was measured by the **Crack-PEC** technique to be a certain length **34 years** after construction. What would be its length using the technique **the following year**?

	Crack length using **'Crack-PEC' 34 years** after construction (mm)	5^{th}	50^{th}	95^{th}
Crack length using 'Crack-PEC' the following year (mm) ?	400	mm	mm	mm

Comments/reasoning behind answer:

Questions 6, 7 and 8 address expected duration and conditionality in terms of loading on transitions between bridges' condition states. Notice that we now refer to the two classes of bridges described in section Data of Interest, namely **Moveable** and **Fixed**.

6. Could you provide with the 5^{th}, 50^{th} and 95^{th} quantiles of your uncertainty distribution about the expected years that it takes for the bridges considered to transit between the conditions defined in section 2 ? In this question, it is considered that the load configuration is ***Normal***.

	Transitions/Quantiles	5^{th}	50^{th}	95^{th}
Moveable	Green to Yellow	years	years	years
	Yellow to Orange	years	years	years
	Orange to Red	years	years	years
Fixed	Green to Yellow	years	years	years
	Yellow to Orange	years	years	years
	Orange to Red	years	years	years

Comments/reasoning behind answer:

7. Same as previous, now considering a ***Heavy*** load configuration.

	Transitions/Quantiles	5^{th}	50^{th}	95^{th}
Moveable	Green to Yellow	years	years	years
	Yellow to Orange	years	years	years
	Orange to Red	years	years	years
Fixed	Green to Yellow	years	years	years
	Yellow to Orange	years	years	years
	Orange to Red	years	years	years

Comments/reasoning behind answer:

8. Consider a sample of 100 000 data points each representing the following event:
"At time *t-1* a bridge of interest (left column) was in a certain condition state and annual load solicitation observed to be either $Heavy$ or $Normal$" as defined in section 2. Recall that we assume bridges can only deteriorate to their next worse state or remain in the same state at the next time step. Out of these 100 000 samples, what is the number of bridges transiting to their next worse state ?
. This translated into more compact writing reads:

$$\#bridge_t = transit\ to\ next\ worse\ state\ |100\ 000\ samples\ with\ Load_{t-1} = Heavy, bridge_{t-1} = previous\ better\ state$$

We take here a time step of **5 years.**

	Probabilities/Quantiles	5th	50th	95th
Moveable	$\# B_t = Y \mid Load_{t-1} = Heavy, B_{t-1} = G$			
	$\# B_t = O \mid Load_{t-1} = Heavy, B_{t-1} = Y$			
	$\# B_t = R \mid Load_{t-1} = Heavy, B_{t-1} = O$			
	$\# B_t = Y \mid Load_{t-1} = Normal, B_{t-1} = G$			
	$\# B_t = O \mid Load_{t-1} = Normal, B_{t-1} = Y$			
	$\# B_t = R \mid Load_{t-1} = Normal, B_{t-1} = O$			
Fixed	$\# B_t = Y \mid Load_{t-1} = Heavy, B_{t-1} = G$			
	$\# B_t = O \mid Load_{t-1} = Heavy, B_{t-1} = Y$			
	$\# B_t = R \mid Load_{t-1} = Heavy, B_{t-1} = O$			
	$\# B_t = Y \mid Load_{t-1} = Normal, B_{t-1} = G$			
	$\# B_t = O \mid Load_{t-1} = Normal, B_{t-1} = Y$			
	$\# B_t = R \mid Load_{t-1} = Normal, B_{t-1} = O$			

Comments/reasoning behind answer:

List of Tables

List of Figures

Bibliography

Kjersti Aas, Claudia Czado, Arnoldo Frigessi, and Henrik Bakken. Pair-copula constructions of multiple dependence. *Insurance: Mathematics and Economics*, 44 (2):182–198, apr 2009. doi: 10.1016/j.insmatheco.2007.02.001. URL http://dx.doi.org/10.1016/j.insmatheco.2007.02.001. 97, 104

Mohamed Abdel-Hameed. A gamma wear process. *IEEE Transactions on Reliability*, R-24(2):152–153, jun 1975. doi: 10.1109/tr.1975.5215123. 2, 14

Thomas Attema, Alex Kosgodagan Acharige, Oswaldo Morales-Nápoles, and Johan Maljaars. Maintenance decision model for steel bridges: a case in the netherlands. *Structure and Infrastructure Engineering*, 13(2):242–253, apr 2016. doi: 10.1080/15732479.2016.1158194. 5, 23, 29, 34

Vilijandas Bagdonavicius and Mikhail S. Nikulin. Estimation in degradation models with explanatory variables. *Lifetime Data Analysis*, 7(1):85–103, 2001. doi: 10.1023/a:1009629311100. URL http://dx.doi.org/10.1023/A:1009629311100. 65

Hyeon-Shik Baik, Hyung Seok Jeong, and Dulcy M. Abraham. Estimating transition probabilities in Markov chain-based deterioration models for management of wastewater systems. *J. Water Resour. Plann. Manage.*, 132(1):15–24, jan 2006.

doi: 10.1061/(asce)0733-9496(2006)132:1(15). URL http://dx.doi.org/10.1061/(ASCE)0733-9496(2006)132:1(15). 66

Alexander Bauer and Claudia Czado. Pair-copula Bayesian networks. *Journal of Computational and Graphical Statistics*, 25(4):1248–1271, oct 2016. doi: 10.1080/10618600.2015.1086355. URL http://dx.doi.org/10.1080/10618600.2015.1086355. 8, 9, 26, 99, 100, 106, 110, 111, 112, 113

Alexander Xaver Bauer. *Pair-copula constructions for non-Gaussian Bayesian networks*. PhD thesis, Technische Universität München, 2013. 102

Tim Bedford and Roger M. Cooke. Vines–a new graphical model for dependent random variables. *The Annals of Statistics*, 30(4):1031–1068, aug 2002. doi: 10.1214/aos/1031689016. URL http://dx.doi.org/10.1214/aos/1031689016. 97

Pierre Boutet, François Hild, and Fabien Lefebvre. Probabilistic prediction of fatigue life of cracked parts: Linear elastic fracture mechanics based approach. *Procedia Engineering*, 66:343–353, 2013. 31

Eike Christian Brechmann and Claudia Czado. COPAR-multivariate time series modeling using the copula autoregressive model. *Applied Stochastic Models in Business and Industry*, 31(4):495–514, jun 2014. doi: 10.1002/asmb.2043. URL http://dx.doi.org/10.1002/asmb.2043. 98

Enrique Castillo, Aida Calviño, Zacarías Grande, Santos Sánchez-Cambronero, Inmaculada Gallego, Ana Rivas, and José María Menéndez. A Markovian-Bayesian network for risk analysis of high speed and conventional railway lines integrating human errors. *Computer-Aided Civil and Infrastructure Engineering*, 31(3):193–218, jun 2015. doi: 10.1111/mice.12153. URL http://dx.doi.org/10.1111/mice.12153. 64

Enrique Castillo, Zacarías Grande, and Aida Calviño. Bayesian networks-based probabilistic safety analysis for railway lines. *Computer-Aided Civil and Infrastructure Engineering*, 31(9):681–700, apr 2016. doi: 10.1111/mice.12195. URL http://dx.doi.org/10.1111/mice.12195. 64

Roger M. Cooke. *Experts in uncertainty: opinion and subjective probability in science*. Environmental Ethics and Science Policy Series. Oxford University Press, New York, 1991. 4, 16, 46, 50, 64, 74, 75

Roger M. Cooke and Louis L.H.J. Goossens. TU delft expert judgment data base. *Reliability Engineering & System Safety*, 93(5):657–674, may 2008. doi: 10.1016/j.ress.2007.03.005. URL http://dx.doi.org/10.1016/j.ress.2007.03.005. 50, 59, 74

Roger M. Cooke and Dimitri Solomatine. *EXCALIBR Integrated System for Processing Expert Judgements version 3.0*. Delft University of Technology and SoLogic Delft, Delft, 1992. 54

R. Cowell, A. Dawid, S. L. Lauritzen, and D. J. Spiegelhalter. *Probabilistic networks and expert systems*. Statistics for Engineering and Information Science. Springer, New York, 1999. 19, 92

Paul Dagum, Adam Galper, and Eric Horvitz. Dynamic network models for forecasting. In *Uncertainty in Artificial Intelligence*, pages 41–48. Elsevier, 1992. doi: 10.1016/b978-1-4832-8287-9.50010-4. 3, 15

William Frank Darsow, Bao Nguyen, and Elwood T. Olsen. Copulas and markov processes. *Illinois Journal of Mathematics*, 36(4):600–642, Winter 1992. 97, 99, 109, 116

Yang Deng, Ai qun Li, and You liang Ding. Analysis of monitored mass strain data

and fatigue assessment for steel-box-girder bridges. *Gongcheng Lixue/Engineering Mechanics*, 31(7):69–77, 2014. doi: 10.6052/j.issn.1000-4750.2013.01.0008. 31

Ruwini Edirisinghe, Sujeeva Setunge, and Guomin Zhang. Markov model—based building deterioration prediction and ISO factor analysis for building management. *Journal of Management in Engineering*, 31(6):04015009, nov 2015. doi: 10.1061/(asce)me.1943-5479.0000359. URL http://dx.doi.org/10.1061/(ASCE)ME.1943-5479.0000359. 66

J. Ferrándiz, E. Castillo, and P. Sanmartín. Temporal aggregation in chain graph models. *Journal of Statistical Planning and Inference*, 133(1):69–93, jul 2005. doi: 10.1016/j.jspi.2004.03.012. 65

Josquin Foulliaron, Laurent Bouillaut, Anne Barros, and Patrice Aknin. Dynamic bayesian networks for reliability analysis: from a markovian point of view to semi-markovian approaches. *IFAC-PapersOnLine*, 48(21):694–700, 2015. doi: 10.1016/j.ifacol.2015.09.608. 125

Dan M. Frangopol and Paolo Bocchini. Bridge network performance, maintenance and optimisation under uncertainty: accomplishments and challenges. *Structure and Infrastructure Engineering*, 8(4):341–356, apr 2012. doi: 10.1080/15732479.2011.563089. URL http://dx.doi.org/10.1080/15732479.2011.563089. 62

Sylvia Frühwirth-Schnatter. *Finite Mixture and Markov Switching Models*. Springer-Verlag GmbH, 2006. ISBN 0387329099. 65

Jonathan L. Gross, Jay Yellen, and Ping Zhang. *Handbook of Graph Theory*. Chapman and Hall/CRC, 2013. ISBN 1439880182. URL http://www.ebook.de/de/product/20520301/handbook_of_graph_theory_second_edition.html. 14

A. M. Hanea, D. Kurowicka, and R. M. Cooke. Hybrid method for quantifying and analyzing Bayesian belief nets. *Qual. Reliab. Engng. Int.*, 22(6):709–729, 2006. doi: 10.1002/qre.808. URL http://dx.doi.org/10.1002/qre.808. 99, 109

Anca Hanea, Oswaldo Morales Napoles, and Dan Ababei. Non-parametric Bayesian networks: Improving theory and reviewing applications. *Reliability Engineering & System Safety*, 144:265–284, dec 2015. doi: 10.1016/j.ress.2015.07.027. URL http://dx.doi.org/10.1016/j.ress.2015.07.027. 16, 19, 31, 93, 100

Frank Harary. *Graph Theory*. WESTVIEW PR, 1994. ISBN 0201410338. URL http://www.ebook.de/de/product/3596767/frank_harary_graph_theory_on_demand_printing_of_02787.html. 14

Ronald A. Howard and James E. Matheson. Influence diagrams. *Decision Analysis*, 2 (3):127–143, sep 1984. doi: 10.1287/deca.1050.0020. 124

Cecil Huang and Adnan Darwiche. Inference in belief networks: A procedural guide. *International Journal of Approximate Reasoning*, 15(3):225–263, oct 1996. doi: 10.1016/s0888-613x(96)00069-2. URL http://dx.doi.org/10.1016/S0888-613X(96)00069-2. 86

Mohsen A Issa, Hameed I Shabila, and Mohammad Alhassan. Structural health monitoring systems for bridge decks and rehabilitated precast prestress concrete beams. In *Sensing Issues in Civil Structural Health Monitoring*, pages 363–372. Springer, 2005. 30

Yi Jiang, Mitsuru Saito, and Kumares C Sinha. Bridge performance prediction model using the markov chain. *Transportation Research Record*, 1180:25–32, 1988. 63

Harry Joe. Families of m-variate distributions with given margins and $m(m-1)/2$ bivariate dependence parameters. In *Institute of Mathematical Statistics Lecture Notes*

- *Monograph Series*, pages 120–141. Institute of Mathematical Statistics, 1996. doi: 10.1214/lnms/1215452614. 8, 26, 107

Harry Joe. *Dependence Modeling with Copulas*. CRC Press, 2014. 96

FBP de Jong. *Renovation techniques for fatigue cracked orthotropic steel bridge decks*. PhD thesis, Delft University of Technology, 2007. 53, 78

Michael I. Jordan. *Learning in Graphical Models*. MIT PR, 1999. ISBN 0262600323. 48

M. J. Kallen. *Markov processes for maintenance optimization of civil infrastructure in the Netherlands*. PhD thesis, Delft University of Technology, Delft, Netherlands, 2007. 2, 15

Evis Këllezi, Nick Webber, and Coventry Cv Al. Numerical methods for lévy processes: Lattice methods and the density, the subordinator and the time copula, 2003. 97

Kiyoshi Kobayashi, Myungsik Do, and Daeseok Han. Estimation of Markovian transition probabilities for pavement deterioration forecasting. *KSCE Journal of Civil Engineering*, 14(3):343–351, may 2010. doi: 10.1007/s12205-010-0343-x. URL http://dx.doi.org/10.1007/s12205-010-0343-x. 63

Alex Kosgodagan, Oswaldo Morales-Napoles, Johan Maljaars, and Wim Courage. Expert judgment in life-cycle degradation and maintenance modelling for steel bridges. *Proceedings of the Fifth International Symposium on Life -Cycle Civil Engineering (IALCCE2016)*, 2016. 5, 24

Alex Kosgodagan, Oswaldo Morales-Nápoles, Thomas G. Yeung, Wim Courage, Johan Maljaars, and Bruno Castanier. A two-dimension dynamic bayesian network for large-scale degradation modelling with an application to a bridges network. *Accepted in Computer-Aided Civil And Infrastructure Engineering*, 2017. 6, 25

D. Kurowicka and R. M. Cooke. Distribution-Free Continuous Bayesian Belief Nets. In *Series on Quality, Reliability and Engineering Statistics*, pages 309–322. World Scientific Pub Co Pte Lt, oct 2005. doi: 10.1142/9789812703378_0022. URL http://dx.doi.org/10.1142/9789812703378_0022. 3, 15, 99

Dorota Kurowicka and Roger M. Cooke. *Uncertainty Analysis with High Dimensional Dependence Modelling*. John Wiley & Sons Inc., 2006. ISBN 0470863064. 96, 105, 117

Dorota Kurowicka and Harry Joe. *Dependence Modeling: Vine Copula Handbook*. World Scientific Publishing Co. Pte. Ltd., 2011. ISBN 9814299871. 97

S. L. Lauritzen and D. J. Spiegelhalter. Local computations with probabilities on graphical structures and their application to expert system. *Journal of the Royal Statistical Society. Series B (Methodological)*, 50(2):157–224, 1988. 86

Steffen L. Lauritzen. *Graphical Models*. Oxford Statistical Science Series. OXFORD UNIV PR, 1996. ISBN 0198522193. URL http://www.ebook.de/de/product/3256393/steffen_l_lauritzen_graphical_models.html. 19

Steffen L. Lauritzen and Dennis Nilsson. Representing and solving decision problems with limited information. *Management Science*, 47(9):1235–1251, sep 2001. doi: 10.1287/mnsc.47.9.1235.9779. URL http://dx.doi.org/10.1287/mnsc.47.9.1235.9779. 124

Ming Liu, Dan M. Frangopol, and Kihyon Kwon. Fatigue reliability assessment of retrofitted steel bridges integrating monitored data. *Structural Safety*, 32(1):77–89, jan 2010. doi: 10.1016/j.strusafe.2009.08.003. 31

Samer M. Madanat, Matthew G. Karlaftis, and Patrick S. McCarthy. Probabilistic infrastructure deterioration models with panel data. *J. Infrastruct. Syst.*, 3(1):4–9, mar

1997. doi: 10.1061/(asce)1076-0342(1997)3:1(4). URL http://dx.doi.org/10.1061/(ASCE)1076-0342(1997)3:1(4). 63

J. Maljaars and A.C.W.M. Vrouwenvelder. Probabilistic fatigue life updating accounting for inspections of multiple critical locations. *International Journal of Fatigue*, 68:24–37, nov 2014. doi: 10.1016/j.ijfatigue.2014.06.011. 33, 34

Johan Maljaars, Frank van Dooren, and Henk Kolstein. Fatigue assessment for deck plates in orthotropic bridge decks. *Steel Construction*, 5(2):93–100, 2012. 30

Hans Manner and Olga Reznikova. A survey on time-varying copulas: Specification, simulations, and application. *Econometric Reviews*, 31(6):654–687, nov 2012. doi: 10.1080/07474938.2011.608042. URL http://dx.doi.org/10.1080/07474938.2011.608042. 98

Snežana Mašović and Rade Hajdin. Modelling of bridge elements deterioration for Serbian bridge inventory. *Structure and Infrastructure Engineering*, 10(8):976–987, mar 2013. doi: 10.1080/15732479.2013.774426. URL http://dx.doi.org/10.1080/15732479.2013.774426. 63

Tom Micevski, George Kuczera, and Peter Coombes. Markov model for storm water pipe deterioration. *J. Infrastruct. Syst.*, 8(2):49–56, jun 2002. doi: 10.1061/(asce)1076-0342(2002)8:2(49). URL http://dx.doi.org/10.1061/(ASCE)1076-0342(2002)8:2(49). 63

Z. Mirzaei, B. T. Adey, P. Thompson, and L. Klatter. The IABMAS bridge management committee overview of existing bridge management systems. Technical report, Institute for Construction and Infrastructure Management, Swiss Federal Institute of Technology, Zürich, Switzerland, 2014. 45, 63

O. Morales, D. Kurowicka, and A. Roelen. Eliciting conditional and unconditional rank correlations from conditional probabilities. *Reliability Engineering & System*

Safety, 93(5):699–710, may 2008. doi: 10.1016/j.ress.2007.03.020. URL http://dx.doi.org/10.1016/j.ress.2007.03.020. 123

O. Morales-Napoles and R. D. J. M. Steenbergen. Analysis of axle and vehicle load properties through bayesian networks based on weigh-in-motion data. *Reliability Engineering and System Safety*, 125:153–164, 2014. 4, 47, 81

Oswaldo Morales-Nápoles and Raphaël D. J. M. Steenbergen. Large-scale hybrid Bayesian network for traffic load modeling from weigh-in-motion system data. *J. Bridge Eng.*, 20(1):04014059, jan 2015. doi: 10.1061/(asce)be.1943-5592.0000636. URL http://dx.doi.org/10.1061/(ASCE)BE.1943-5592.0000636. 98

George Morcous and Afshin Hatami. Developing deterioration models for nebraska bridges. Technical report, University of Nebraska at Lincoln, 2011. 45

Kevin Patrick Murphy. *Dynamic bayesian networks: representation, inference and learning*. PhD thesis, University of California, Berkeley, 2002. 3, 15, 69

Mark Newman, Albert-László Barabási, and Duncan J. Watts. *The Structure and Dynamics of Networks:*. Princeton University Press, 2011. URL http://www.ebook.de/de/product/16564567/mark_newman_albert_laszlo_barabasi_duncan_j_watts_the_structure_and_dynamics_of_networks.html. 14

Judea Pearl. *Probabilistic Reasoning in Intelligent Systems*. Morgan Kauffman Publishers, San Francisco, 1988. 4, 15, 17, 20, 48

Tara Reale and Alan O'Connor. Cross-entropy as an optimization method for bridge condition transition probability determination. *Journal of Transportation Engineering*, 138(6):741–750, jun 2012. doi: 10.1061/(asce)te.1943-5436.0000379. URL http://dx.doi.org/10.1061/(ASCE)TE.1943-5436.0000379. 63

Guillermo A. Riveros and Elias Arredondo. Predicting future deterioration of hydraulic steel structures with Markov chain and multivariate samples of statistical distributions. *Journal of Applied Mathematics*, 2014:1–8, 2014. doi: 10.1155/2014/360532. URL http://dx.doi.org/10.1155/2014/360532. 63

Ross D. Shachter and C. Robert Kenley. Gaussian influence diagrams. *Management Science*, 35(5):527–550, may 1989. doi: 10.1287/mnsc.35.5.527. 15, 124

Nozer D. Singpurwalla. Survival in dynamic environments. *Statistical Science*, 10(1): 86–103, feb 1995. doi: 10.1214/ss/1177010132. URL http://dx.doi.org/10.1214/ss/1177010132. 65

Abe Sklar. Fonctions de répartition à n dimensions et leurs marges. *Publications de l'Institut de statistique de l'Université de Paris*, 8:229–231, 1959. 99

Olga Špačková and Daniel Straub. Dynamic Bayesian network for probabilistic modeling of tunnel excavation processes. *Computer-Aided Civil and Infrastructure Engineering*, 28(1):1–21, apr 2012. doi: 10.1111/j.1467-8667.2012.00759.x. URL http://dx.doi.org/10.1111/j.1467-8667.2012.00759.x. 65

Daniel Straub. Stochastic modeling of deterioration processes through dynamic bayesian networks. *Journal of Engineering Mechanics*, 135:1089–1099, October 2009. 48, 69, 70

Henrik Stensgaard Toft, John Dalsgaard Sørensen, T. Yalamas, and Julien Baussaron. *Reliability assessment of welded steel details in bridges using inspection*, pages 3803–3810. C R C Press LLC, 2014. ISBN 978-1-13800-086-5 (Book+CD). 31

Neda Trifonova, Andrew Kenny, David Maxwell, Daniel Duplisea, Jose Fernandes, and Allan Tucker. Spatio-temporal Bayesian network models with latent variables for revealing trophic dynamics and functional networks in fisheries ecology. *Ecological*

Informatics, 30:142–158, nov 2015. doi: 10.1016/j.ecoinf.2015.10.003. URL http://dx.doi.org/10.1016/j.ecoinf.2015.10.003. 66

A. H. J. M. Vervuurt. Percentage file op rijkswegen analyse ndw-meetgegevens april 2013 (IQ-2014-33b). Technical report, TNO, November 2014. 80, 83, 86, 88

P. Weber, G. Medina-Oliva, C. Simon, and B. Iung. Overview on Bayesian networks applications for dependability, risk analysis and maintenance areas. *Engineering Applications of Artificial Intelligence*, 25(4):671–682, jun 2012. doi: 10.1016/j.engappai.2010.06.002. URL http://dx.doi.org/10.1016/j.engappai.2010.06.002. 2, 15, 68

Christoph Werner, Tim Bedford, Roger M. Cooke, Anca M. Hanea, and Oswaldo Morales-Nápoles. Expert judgement for dependence in probabilistic modelling: A systematic literature review and future research directions. *European Journal of Operational Research*, 258(3):801–819, 2017. 4, 123

UNIVERSITE BRETAGNE LOIRE

IMT Atlantique
Bretagne-Pays de la Loire
École Mines-Télécom

Thèse de Doctorat

Alex KOSGODAGAN - DALLA TORRE

Modélisation de dépendance en grandes dimensions par les réseaux Bayésiens pour la détérioration d'infrastructures et autres applications

High-dimensional dependence modelling using Bayesian networks for the degradation of civil infrastructures and other applications

Résumé

Cette thèse explore l'utilisation des réseaux Bayésiens (RB) afin de répondre à des problématiques de dégradation en grandes dimensions concernant des infrastructures du génie civil. Alors que les approches traditionnelles basées l'évolution physique déterministe de détérioration sont déficientes pour des problèmes à grande échelle, les gestionnaires d'ouvrages ont développé une connaissance de modèles nécessitant la gestion de l'incertain. L'utilisation de la dépendance probabiliste se révèle être une approche adéquate dans ce contexte tandis que la possibilité de modéliser l'incertain est une composante attrayante.

Le concept de dépendance au sein des RB s'exprime principalement de deux façons. D'une part, les probabilités conditionnelles classiques s'appuyant le théorème de Bayes et d'autre part, une classe de RB faisant l'usage de copules et corrélation de rang comme mesures de dépendance. Nous présentons à la fois des contributions théoriques et pratiques dans le cadre de ces deux classes de RB ; les RB dynamiques discrets et les RB non paramétriques, respectivement. Des problématiques concernant la paramétrisation de chacune des classes sont également abordées. Dans un contexte théorique, nous montrons que les RBNP permet de caractériser n'importe quel processus de Markov.

Mots clés

Réseaux Bayésiens, Modèle de dégradation probabiliste, Modélisation de copules, Jugement structuré d'expert

Abstract

This thesis explores high-dimensional deterioration-related problems using Bayesian networks (BN). Asset managers become more and more familiar on how to reason with uncertainty as traditional physics-based models fail to fully encompass the dynamics of large-scale degradation issues. Probabilistic dependence is able to achieve this while the ability to incorporate randomness is enticing.

In fact, dependence in BN is mainly expressed in two ways. On the one hand, classic conditional probabilities that lean on the well-known Bayes rule and, on the other hand, a more recent class of BN featuring copulae and rank correlation as dependence metrics. Both theoretical and practical contributions are presented for the two classes of BN referred to as discrete dynamic and non-parametric BN, respectively. Issues related to the parametrization for each class of BN are addressed.

For the discrete dynamic class, we extend the current framework by incorporating an additional dimension. We observed that this dimension allows to have more control on the deterioration mechanism through the main endogenous governing variables impacting it. For the non-parametric class, we demonstrate its remarkable capacity to handle a high-dimension crack growth issue for a steel bridge. We further show that this type of BN can characterize any Markov process.

Key Words

Bayesian networks, Deterioration modelling, Copula modelling, Bridge reliability, Stochastic modelling, Structured expert judgment